ANALYSIS OF CONTIGUOUS PILE WALL AS DEEP EXCAVATION SUPPORT SYSTEM IN SILTY SOILS INCASE OF ADAMA TOWN.

A Thesis Submitted to
School of Graduate Studies of Adama science and Technology University
In Partial Fulfillment of the Requirement for the Degree of
Master of Science in Civil Engineering

By
BIRHANE GEBRU
Advisor
HENOK FIKRE (DR. ING)

MARCH 2016
Adama, Ethiopia.

ADAMA SCIENCE AND TECHNOLOGY UNIVERSITY
SCHOOL OF GRADUATE STUDIES

ANALYSIS OF CONTIGUOUS PILE WALL AS DEEP EXCAVATION SUPPORT SYSTEM IN SILTY SOILS INCASE OF ADAMA TOWN.

By BIRHANE GEBRU

MARCH 2016

Approved by Board of Examiners

Dr. Henok Fikre ____________________ ____________________
Advisor **Signature** **Date**

Dr. Addisalem Zeleke ____________________ ____________________
External Examiner **Signature** **Date**

Dr. Argaw Asha ____________________ ____________________
Internal Examiner **Signature** **Date**

Solomon Abebe (MSc) ____________________
____
Chairperson **Signature** **Date**

DECLARATION

I, the undersigned, declare that this thesis is the result of my own work performed under the supervision of my research advisor Henok Fikre (Dr.Ing) except where specific reference is made to the works of others, the contents of this thesis are original and have never been submitted, in part or as a whole, to any other university for any degree or other qualifications. All sources of materials used for this thesis have also been duly acknowledged.

Name Birhane Gebru

Signature ______________

Place School of Civil Engineering and Architecture,

Adama Science and Technology University,

Adama.

Date March 2016

Acknowledgements

First, I would like to thank the almighty GOD for all the blessings I have received and the strength he gave me through my life time and during my research work.

Secondly, I would like to express my deepest gratitude to my advisor Henok Fikre (Dr. Ing) for his continued support, inspiration, provision of necessary relevant information, his guidance and encouragement throughout my work. Working with him has offered me an opportunity to learn a lot as an academician.

Thirdly, I would like to use this opportunity to express my thankfulness to ADDIS GEOSYSTEMS PLC., for providing me the necessary data's. They were very cooperative and helpful whenever I need any materials.

Lastly but most importantly, I would like to thank my family and my friends for their support. This would have not been possible without their vision, support and sacrifice under very difficult circumstances and also to my colleagues who contribute a lot in their positive advice during this research.

.

TABLE OF CONTENTS

CONTENTS **PAGE**

LIST OF SYMBOLS AND ABBREVIATIONS

ASTM	American Society for Testing Materials standard;
BBM	Barcelona Basic Model;
BSC	Bangkok Soft Clay;
C	Cohesion;
CBP	Contiguous bored pile;
CFA	Contiguous Flight Auger;
C increment	Increment in cohesion;
CS	Clayey Sand;
D_{ex}	Excavation Depth;
DS	Dense Sand;
D-wall	Diaphragm wall;
E	Elastic modulus;
e_0	Void ratio;
EA	Normal stiffness;
EI	Flexural rigidity;
E increment	Increment in Elastic modulus;
EPB	Earth Pressure Balance;
erfc	error function;
FE	Finite Element;
FEM	Finite Element Model;

HC	Hard Clay;
He	Final excavation depth;
HS	Hardening soil model;
I	Moment of inertia;
Ka	Active earth pressure ratio;
K	Soil modulus;
K0	initial earth pressure ratio;
Lb	Bond length;
L*s*	horizontal anchor spacing;
M	wall bending moment;
MC	Medium Clay;
MCC	Modified Cam Clay;
MCM	Mohr Coulomb Model;
MG	Made Ground;
MRT	Mass Rapid Transit;
P	Load intensity;
PIZ	Primary Influence Zone;
P*v*	Pressure;
Q	Axial load in the wall;
qs	Distributed surface load;
R*d*	Design resistant force;

RL	Reduced level;
SC	Stiff Clay;
SIZ	Secondary Influence Zone;
SPT	Standard Penetration Test;
SPW	Sheet pile wall;
Sr	relative wall stiffness;
SSM	Soft Soil Model;
t	Thickness;
TBM	Tunnel Boring Machines;
TSA	Total Stress Automatic;
w	Weight;
X	Distance;
y	Wall horizontal deflection at depth z;
yref	Reference depth;
Z1	Start depth;
Z2	End depth;
ϕ	Angle of internal friction;
ɣ	Unit weight;
δhm	maximum lateral wall deflection;
δvm	maximum ground settlement;
Ψ	Dilatancy angle;

γ_{bulk}	Bulk unit weight;
γ_r	Partial factor ;
τ	Shear stress;
σ	Compressive stress;
$\Delta\sigma_h$	Increase in lateral earth pressure;
υ	poisons ratio;
γ_{sat}	saturated unit weight;

LIST OF TABLES

LIST OF FIGURES

LIST OF TABLES AND FIGURES IN APPENDIXES

Abstract

Development in urban areas around the world has rapidly increased in recent years. This rapid development has not been matched by the ever decreasing open space commonly associated with urban centers. Providing space for parking, public amenities, etc in multi-storey buildings at town centers has created a need to go deep excavations into ground. Deep excavation is often required for urban construction. Unfortunately, the ground movements associated with deep excavation can result in damage to adjacent buildings. Thus, it is critically important to accurately predict the damage potential of nearby deep excavations and designing adequate support systems. This thesis describes the analysis of contiguous pile walls as deep excavation support system in silty soils. A detailed analysis of deep excavation support system using PLAXIS 2D in silty soils at Adama town is furnished in this study with an objective to realistically simulates the deep excavation behavior. Some difficulties of not quite precise regulative have been encountered. Nevertheless, the proposed model has been able to describe the effects in the process of excavation in the selected material and loading conditions.

This study presents details of problems with deep excavation, Analysis and design approaches of deep excavation support systems, Numerical and Analytical studies of deep excavations, laboratory and field performance measurements. Besides literatures on wall deformation, Ground movement, Earth and pore water pressure, Prop loads and wall bending moments, Deformation and damage of adjacent infrastructures are discussed to understand the design and construction trends of excavation support system. Numerical modeling and field studies are also discussed to predict the effect of model selection and precisely choose the best model that suits the selected soil type and area of study. Parametric study has been conducted to analyze the effects of surcharge and its location and pile diameter on horizontal displacement, vertical deformation and bending moment of the support system. Analysis results and discussion from the study are also presented with details of constitutive soil model used during analysis to analyze the suitability of contiguous walls as deep excavation support system during deep excavation and provide helpful first estimate of probable damages caused on adjacent structures due to excessive excavation. Limitations in the analyses and recommendations for future work are also presented at last.

Key Words: - Deep excavation, Contiguous pile wall, support system, Ground deformation.

CHAPTER 1
INTRODUCTION

1.1 General Retaining Systems

Urbanization made cost of land high and it necessitated to go deeper into the ground for construction of subway stations, basements for high-rise buildings, underground car parks and shopping centers and also towering vertically towards the sky. A deep excavation into the ground is indispensible to create additional floor space to meet increasing space requirements for parking and for multi-storey buildings at the town centers. Numbers of deep excavation pits in city centers are increasing every year. Structures in the immediate vicinity of excavations, dense traffic scenario, presence of underground obstructions and utilities have made excavations a difficult task to execute because the excavation process inevitably alters the stress states in the ground and may cause significant wall deformations and ground movements. Especially when the excavation is close to adjacent infrastructure, e.g. buildings, tunnels, buried pipelines, piled foundations, the excavation induced ground movements must be carefully monitored and controlled within an acceptable amount, to avoid any potential damage to these classes of infrastructure.

Therefore, analysis and design of proper deep excavations and their supporting systems (such as secant pile walls, diaphragm walls, or tangent pile walls) are essential to limit ground movement-induced damages. Even in complicated urban settings, deep retaining systems have been deployed successfully by overcoming construction challenges. Several case histories exist for the use of stiff excavation support systems; examples such as the use of secant pile walls for the construction of a subway station (Finno and Bryson, 2002), cut-and-cover tunnel excavation (Koutsoftas et al., 2000), and deep basement excavations (Ou et al., 2000; Ng, 1992); inter alios. The problem of excessive excavation-induced damage associated with underground construction in urban areas is a major concern, especially in soft clays and adjacent buildings with shallow foundation. Excessive ground movements can lead to significant displacements and rotations in adjacent structures, thereby causing damages ranging from cosmetic to structural. Hence, an accurate prediction of the ground movements related to deep excavation is a critical step in the design and analysis of excavation support systems (Sekyi K. Intsiful, 2015).

The structural elements that are designed to retain soils and rock slopes during deep excavations are called retaining systems. They connect two different earth elevations to hold on the lateral earth pressure. Various types of retaining systems are classified according to construction methodologies and applications. Ergun (2008) provides a comprehensive review of various types of retaining systems such as braced walls, sheet walls, diaphragm walls, contiguous walls and others.

Contiguous pile walls are piled retaining walls constructed with small gaps between adjacent piles. The use of low-cost augers and, more particularly, Contiguous Flight Auger (CFA) rigs to drill successive unconnected piles provide an economical wall. Diameter and spacing of the piles are decided based on soil type, ground water level and magnitude of design pressures. Large spacing is avoided as it can result in caving of soil through gaps. Pile diameters range from 300mm to 1000mm. CFA piles are considered more economical than diaphragm wall in small to medium scale excavations due to reduction in cost and time of site operations. Besides, no Bentonite mud is needed for the excavation. Contiguous piles are suitable where the groundwater table is below excavation level. It is normally the most economic and rapid option. The wall consists of discrete piles typically installed at centers 150mm greater than their diameter, leaving gaps where soil is exposed during excavation.

1.2 The Present Problems of Deep Excavation

Unsupported deep excavations pose hazard to workers and equipments. Prevention and minimizing damages to surrounding is of at most concern to the design and construction engineers for any excavation work. A variety of excavation methods and lateral supporting systems are to be practiced based on local soil, ground water and environmental conditions, allowable construction period, money and machinery. Excavation methods include full open cut methods, braced excavation methods, anchored excavation methods, island excavation (partial excavation) methods, and top-down construction methods and zoned excavation methods. The most common types of deep vertical soil support systems are Conventional retaining walls, Soldier pile with wooden lagging walls, Sheet pile walls, Diaphragm walls and Pile walls- Contiguous, Secant or Tangent. During construction of excavation supporting system, the adjacent facilities may be damaged. Vibration due to adjacent machinery, vehicles, rail-roads, blasting and other sources require that additional bracing precautions have to be taken. This can be avoided by taking some ground improvement measures such as grouting the ground between the excavation site and adjacent building. Dewatering should be done if the soil at the site is relatively impervious like clayey soil. In this research analysis and parametric study of contiguous pile walls as deep excavation support system will be introduced. The contiguous wall can only be used where ground water is not a hazard or where grouting or jet grouting can be used to render leakage between the piles. Applying maximum verticality tolerances quoted for augers and Continuous Flight Auger (CFA) pile installation, typically 1 in 100 with depth and allowing this maximum tolerance to adjacent piles in opposite directions can assess the risk of 'windows' between adjacent piles. Where soil and ground water conditions are favorable, bored piles can be installed as anchored piles with the spaces between them are shot-creted to provide soil support as excavation proceeds.

Adama is one of the fastest growing cities in the country and there is a big volume of construction works. Since it is the transit way on the road from Addis Ababa to Djibouti, the growth of trade and commerce is very high in the city. Due to its location and near distance which is around 100km from Addis Ababa, investors are attracted to construct in Adama town and the nearby areas. However, Analysis of deep excavation support system in the city has not yet studied. This research is therefore deals with Analysis of contiguous pile walls as a deep excavation support system in silty soils**.**

1.3 Objective of the Study

The objective of this study is to analyze the suitability of contiguous walls as deep excavation support system during deep excavation**.**

The specific objectives of this work include:

- ✓ Analysis and parametric study of contiguous walls as a deep excavation support system in silty soils.
- ✓ Provide helpful first estimate of probable damages caused on adjacent structures due to excessive excavation.

1.4 Scope of the Investigation.

The scope of this study is limited to the analysis and parametric study of contiguous pile wall as deep excavation support system in silty soils incase of Adama town using PLAXIS 2D finite element software. The data and parameters which are obtained from the field studies will be evaluated in all manner of how they affect the ground deformation. Thus by using the field data and study results the probable and predictable ground deformations can be estimated. The results from this research can be used in estimating the possible damage that will be caused during and after excavation. Hence possible measures can be taken to reduce the problems arising to the new structures and existing structures during and after construction. Adama town is chosen because it is one of the towns that shows rapid development in infrastructure next to Addis Ababa.

1.5 Methodology

To achieve the aforementioned purpose different soil data's are collected and interpreted to use as an input during analysis using finite element software and any related researches and journals accomplished on analysis and design of deep excavation support system are reviewed.

Suitable finite element software is then used to determine the effect of those parameters in the design of contiguous pile wall and their significance are discussed.

1.6 Organization of the Thesis

The thesis is organized into six Chapters.
The first Chapter is about the current problems associated with deep excavations, objectives of the study and scope of the thesis and methodology.

Literature review on analysis and design approaches of deep excavation support systems, numerical and analytical studies of deep excavations and laboratory and field performance measurements are presented in Chapter two.

Chapter Three presents study area description, parameter identification for base model, lateral earth pressure, calculation of ground anchor loads, base model generation and Soil, Pile, Diaphragm Wall and Anchor Parameters for base model.

In Chapter four analysis and parametric study of contiguous pile wall is presented. The effect of Change in location and amount of surcharge and Change in pile diameter of the pile on horizontal and vertical deformation and bending moment of the wall is also furnished.

The last chapter, Chapter Five, discusses the conclusions derived from this study and limitations in the analyses and recommendations for future work. Relevant figures and constitutive models of PLAXIS is presented in the appendices.

CHAPTER II
LITERATURE REVIEW

2.1 INTRODUCTION

Currently limiting movements and deformations that result from constructing deep excavations is becoming a significant design issue, especially in urban environments. Because failure to control deformations and movements can cause significant damage to adjacent structures and utilities. And this makes design more challenging due to increasing requirements for deeper excavations on poorer sites, tighter limits on allowable displacements for adjacent structures and new methods of construction that extend beyond the experience base used to develop historical design methods. Increasingly designs are controlled by the need to limit movements, which goes beyond the traditional approach of focusing on required support loads and avoiding collapse.

Designing to control movements became possible with the development of nonlinear finite element analysis in the early 1970's. However, it was not a practical design tool in its early versions. In recent years, finite element software has greatly improved. There are more realistic stress-strain models, more stable numerical methods, tools to ease the creation of the geometric model, and especially tools to provide powerful and useful graphical output for quick interpretation and presentation of results. Some products also compute a factor of safety against soil failure at any stage of the excavation.

Ground movements adjacent to deep excavations occur in response to lateral deflections of the excavation support system. These movements are influenced by wall installation, soil ground conditions, support system stiffness, and methods of support system installation and interaction between the soil and the support. Hence, parameters have to be identified accordingly.

In this chapter analysis of deep excavation support system, literature review, numerical and analytical study and laboratory and field performance measurements are assessed and presented.

2.2 Analysis of deep excavation support systems.

The common approaches in analysis and design of deep excavation support systems are the Analytical model, Spring model and the Finite element model. The analytical model is based on the most famous and widely used theories that determine the stresses on a retaining structure for the cases of active and passive earth pressure among which are Rankine and Coulomb earth pressure theories. The main drawbacks of this theory is that the Coulomb and Rankine passive earth pressure theory do not consider the construction process and give no indications on the wall deformations and ground movements in the more complex braced deep excavations methods and consistently overestimates the passive pressure developed in field and model tests for ϕ greater than 35°.

The spring model focuses on the bending of a beam resting on an elastic foundation. It assumes that the reaction offered by the support at any point is directly proportional to the displacement of that point along the vertical direction, and is in a direction opposite to the displacement. This model uses Winkler's model for simulation of series of springs. In this model the retaining structure is simulated as a vertical beam on elastic foundation with springs on both sides of retaining wall. The main drawbacks of this model are that analysis is based on the plane strain condition. But in reality, the excavation on the short side of the building pit will be affected by the corner effect, and result in smaller deformation compared to plane strain condition. Besides, it is hard to determine the appropriate spring stiffness constants of the soil, as these constants are not fundamental properties of soil. And the spring model isn't suitable to estimate the surface settlement behind the retaining structure, which is crucial if the excavation is taken place in city centre.

The finite element method is the dominant discretization technique that subdivides the mathematical model into non-overlapping disjoint components of simple geometry called elements. The response of each is expressed in terms of a finite number of degrees of freedom at a set of nodal points. It is then approximated by connecting and assembling all elements. Unlike finite difference models, finite elements do not overlap in space. PLAXIS is special purpose finite element software designed for deformation and stability analysis. It is widely used for analyzing geotechnical problems. Especially the PLAXIS, it gives a more realistic approximation for soil structure interaction compared to analytical model and spring model, without sacrificing too much calculation time. It is widely used for analyzing geotechnical problems. Application of this model requires constitutive models for the simulation of the non-linear, time dependent and anisotropic behaviour of soils and rocks, which are provided as special features. In order to approximate the real case in a two dimensional domain, PLAXIS 2D uses either a plane strain or axisymmetric model. A plane strain model is used for geometries with a uniform cross section and corresponding stress state and loading scheme over a certain length perpendicular to the cross section. An axisymmetric model is used for a circular structure with a uniform radial cross section and loading scheme around the central axis, where the deformation and stress state are assumed identical in any radial direction. The main advantage of this model is that it considers the construction process and gives a precise result on the wall deformations and ground movements even for more complex braced deep excavations. In this study analysis is made using the finite element approach.

In this chapter, previous works done on deep excavations will be assessed and presented.

Johansson et al (2014) presented and compared the forces and deformations measured at a multi-anchored sheet pile wall, installed during the construction of Götatunneln with similar conditions, to the results of different calculation methods. The calculation methods were hand calculations, the one-dimensional finite element software Novapoint GS Supported Excavation and the Mohr-Coulomb, Hardening Soil and Hardening Soil with small strain stiffness constitutive models in the two-dimensional finite element software PLAXIS 2D. A parametric study was also performed for the PLAXIS models to see how the different models reacted when varying certain parameters and assessing the importance of investigating these parameters. The sheet pil wall (SPW) used in this analysis was an anchored Z-section AZ36 SPW. The SPW was installed down to and attached to the bedrock, at 23.5 m depth, and the base of the SPW was sealed for groundwater flow to prevent hydraulic uplift. Three rows of anchors were used at depths 3.5, 7.5 and 10.5 meters which were installed with an angle of 45° and anchored in bedrock.

Based on the analysis made by this model Johansson et al (2014) using NOVAPOINT GS SUPPORTED EXCAVATION, the maximum displacement was approximately 8 mm and occurred 1.5-2 m below shaft bottom. During analysis the constitutive model used for the soil was Total Stress Automatic (TSA), which gives only the horizontal deformation.

For PLAXIS – MOHR-COULOMB model Johansson et al (2014) found the maximum horizontal displacement as 27mm and the total principal strains span from $-4.1*10^{-3}$ to $6.5*10^{-3}$.

In PLAXIS – HARDENING SOIL model the drainage conditions were set to Undrained since effective parameters were required for the soil stiffness stress dependency. From the results found the maximum horizontal displacement were 46 mm and the total principal strains span from $-6.3*10^{-3}$ to $9.8*10^{-3}$.

In this study PLAXIS – HARDENING SOIL WITH SMALL STRAIN model were also used. The input for the HSS model was the same as for the HS model, except for Effective initial shear modulus, G'^{0} and Shear strain level where $G/ G'^{0} = 0.7$. Based on this model the maximum horizontal displacement was found to be 28 mm and the total principal strains span from $-4.4*10^{-3}$ to $9.1*10^{-3}$.

Based on the analysis made by Johansson et al (2014) using the four above mentioned models the following conclusions were withdrawn.

a) When comparing the resulting deformations from the different models they all gave results of the same magnitude, varying between approximately 7-46 mm, see Figure 2.1. The model that gave the most different results compared to the measured deformations was the GSS model and it also failed to capture the shape of the real deformation curve.

b) From the bending moment diagram the HSS model gave the lowest bending moments of the PLAXIS models. The maximum bending moment was rather similar for all PLAXIS models, while it was a bit lower in the GSS model.

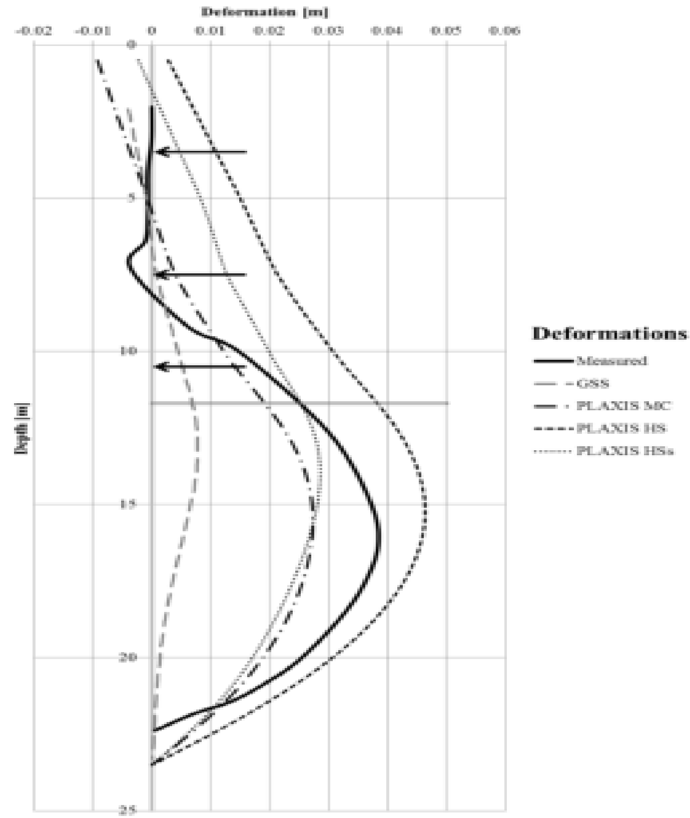

Figure 2.1: Comparison of calculated deformations in the SPW from different models to measured deformations E. Johansson et al.(2014)

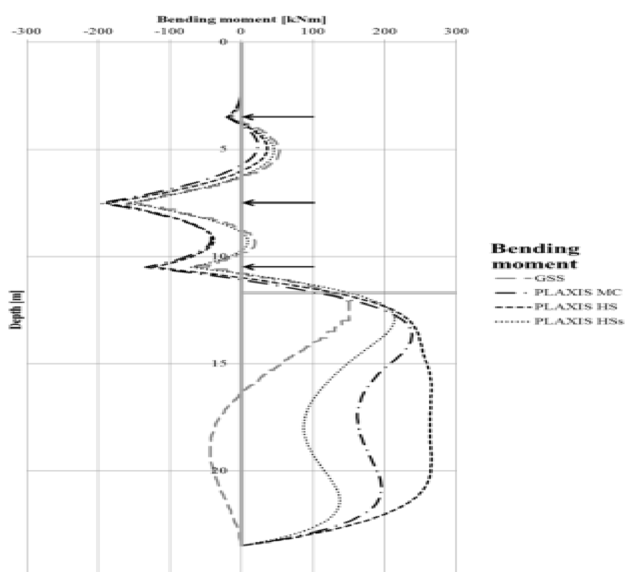

Figure 2.2: Comparison of calculated bending moments in the SPW from different models**.** E. Johansson et al.(2014)

c) The earth pressure distribution comparison also showed that the results from the PLAXIS models were more similar to each other than to other models, see Figure 2.3. The pressure distributions behind the SPW were very similar to each other down to 9 m depth, except for the hand calculations. Below that, the results from the PLAXIS models were fairly similar to each other, with the MC model giving slightly lower earth pressures than the other two, and the GSS model and hand calculations giving higher pressures. In front of the SPW the GSS model and the hand calculations gave very similar results while the PLAXIS models generally gave lower pressures. At 15 m depth, the earth pressures from the HS and HSS models decreased instantly. Below that the results from the PLAXIS models were quite similar, with HSS giving slightly higher earth pressures than the other two.

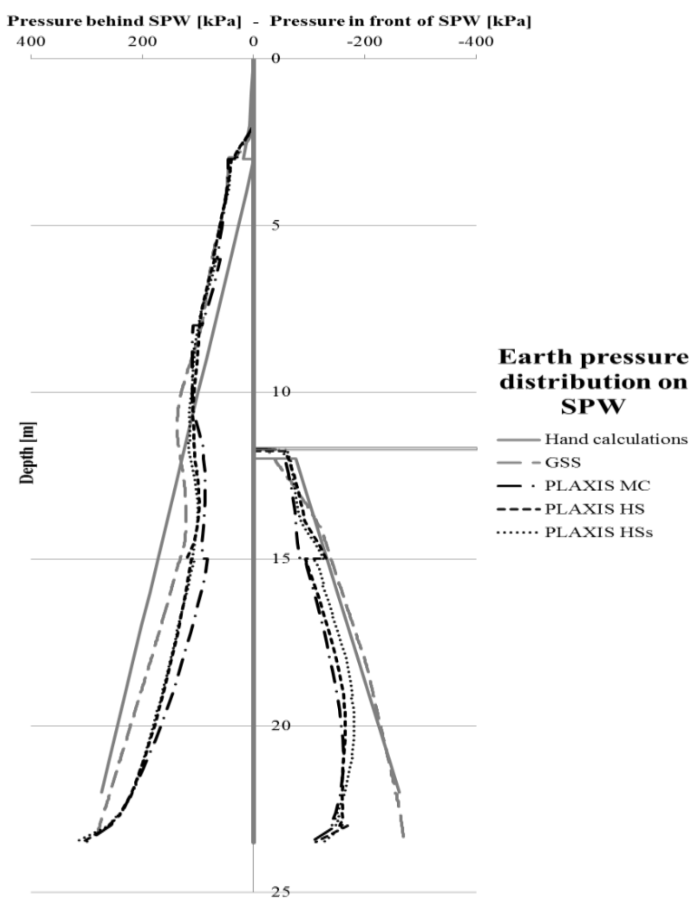

Figure 2.3: Comparison of earth pressures acting on the SPW calculated using different models. E. Johansson et al.(2014)

d) The measured subsidence that eventually occurred behind the SPW after the final excavation stage can be seen in Figure 2.4, together with the resulting subsidence calculated using the different PLAXIS models. Neither GSS nor the hand calculations are sophisticated enough to provide such information and are thus not included. The comparison shows that all three constitutive models underestimate the maximum measured subsidence. None of the models capture the shape of the deformation curve for the first 20 meters behind the wall, but after that the HS model seems to give quite realistic results. All three models also show that heave occurs just behind the SPW, which is not something that has been measured.

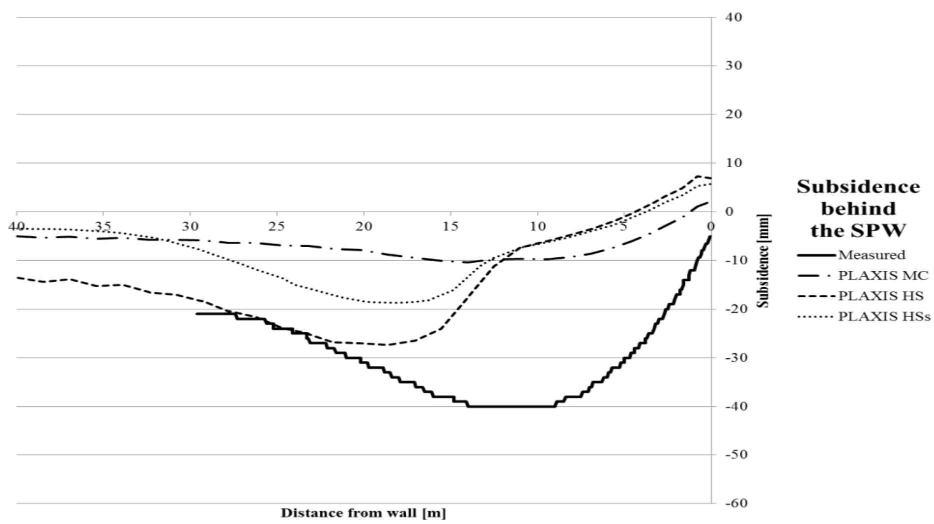

Figure 2.4: Comparison of subsidence behind the SPW calculated from the PLAXIS models and measured result E. Johansson et al.(2014)

Godavarthi et al, (2011) presented details of various deep excavation supporting systems and comprehensive design philosophy of an excavation supporting systems. They also presented details of a case study on the analysis and design of a Contiguous pile wall for supporting deep excavation at a town centre. They discussed the advantages and disadvantages of each type of support system and came up with the conclusion that Contiguous pile wall is better than the others due to the following reasons.

- ✓ Contiguous pile walls are constructed with small gaps between adjacent piles. The use of low-cost augers and, more particularly, Contiguous Flight Auger (CFA) rigs to drill successive unconnected piles provide an economical wall.

- ✓ They are economical than diaphragm wall in small to medium scale excavations due to reduction in cost and time of site operations. Besides no Bentonite mud is needed for the excavation.
- ✓ Contiguous piles are suitable in crowded urban areas, where traditional retaining methods would otherwise encroach the adjoining properties, these piles restricts ground movements on the backfill side.
- ✓ Contiguous walls are effective in granular soils, cohesive soils, soft rocks. Soft clays, weak organic soils are unsuitable due to wall bulging.
- ✓ They only be used where ground water is not a hazard or where grouting or jet grouting can be used to remedy leakage between the piles.

Liew et al. (2011**)** presented two case studies of collapsed temorary excavation using Contiguous bored pile wall in Klang Valley area, Malaysia. The first project involves the construction of a two-storey basement in an urban area. It consists of a CBP wall propped by taking struts against lower basement slab which was proposed by the contractor to provide peripheral support for 10.5m deep excavation at western boundary of the project site. The designed CBP wall was 16m long and 750mm diameter bored pile with to cut off level at RL 54.6m. In order to facilitate the CBP installation 12m long temporary steel sheet pile were installed at retained ground at RL59.0m with about 0.7m offset from project site boundary to provide sufficient working platform and as the temporary shoring support for the exposed 4.4m temporary excavation.

Inorder to confirm the probable causes of ground distresses and wall movement, Finite Element analysis using "PLAXIS" was performed independently based on surface profile simulating the construction sequences and the following findings were revealed.

a) The distressed ground was located over natural valley where thicker fill was placed over the previous soft deposits without proper engineering treatment to form building platform. Soil deposits at the lower part of the valley and potential concetrated underground seepage were common in hilly terrain and should not be overlooked. Desk study of pre-development ground contours to identify potential geotechnical problems is highly recommended.

b) Filling over valleys without proper site clearing, removal of unsuitable soft deposits and compaction could result in highly unstable backfill for any open excavation. It is important to thoroughly investigate the subsoil condition beneath the fill. Otherwise, proper treatment to the low-lying ground beore the development earthworks shall always be assumed.

c) Occurance of tension cracks during initial open excavation and installation of sheet piles suggested that the underlying subsoil and at the valley area inherently vulreable to ground disturbance and hence are prompted to distressing.

d) The existence of soft compressible material at the valley area was further confirmed during additional subsurface investigation and localized deep cap excavation when reaching the final eacavation level.

e) Original topographical features were the important design consideration for excavation stability and remedial strategy. In these case studies, natural valley with soft deposits was not detected during design stage causing cost escalation as a result of costly remedial work.

f) Purched ground water regime can occure in backfilling over natural valley leading to unfavourable behaviour of backfill.

g) Excessive removal of assive berm with localized pile cap excavation without installing the planned strutting resulted in loss of wall support and led to excessive ground movement.

Using back analysis Liew et al.(2011**)** found that the maximum sheet pile wall displacement as 917mm and for the CBP wall as 609mm which exceeds the allowable 0.002H.

The second project involves the construction of two-level basement in city area using CBP wall with temporary strutting. About 40m stretch of CBP wall collapsed, after the water pipe burst incident at the back lane reported 3 hours ago. The installed walls in this project were 1000mm diameter CBP wall installed at 1075mm centre-to-center and unreinforced CBP wall of 1200mm diameter perimeter CBP wall. Another row of CBP was installed for localized core pit excavation.

An analysis using FE was performed by Liew et al.(2011) and revealed the following findings.

a) Design of unreinforced CBP wall for all cases of the section is adequate for moment resistance. However, the moment capacity of unreinforced CBP wall will drop drastically if any cracking was formed when any of the structural thresholds are exceeded and hence the back calculated moment of unreinforced CBP wall can be unreliable.

b) Design of perimeter CBP wall for all cases is adequate except for the bottom soil layer for shear resistance.

c) Design of lift core CBP wall for all cases is adequate except for the bottom soil layer in which the design is inadequate when the actual construction sequences at site was used, which is significantly deviated from the assumed construction sequences in FE model and apparent cohesion for overburden soil is reduced from 10kPa to 4kPa as justified from the interpreted strength parameters.

d) Design of strutting members is adequate based on extreme strut force predicted by the consultant. However, design of strutting members for all cases is either inadequate or unsafe based on extreme strut forces predicted in the independent analysis by the investigator.

e) There are an increase of approximately 24% in strut force and seven times larger in the maximum predicted wall deflection for perimeter CBP when the apparent cohesion for overburden soil is reduced from 10kPa to 4kPa and actual construction sequences are deviated from site execution. These findings revealed the apparent cohesion is a very sensitive factor on the performance of CBP wall.
f) Adoption of high apparent cohesion in FE analysis be the consultant had caused the underestimation of strut force and virtually led to insufficient provision of strutting members.

Wanchai Teparaksa (2015) studied the analysis, design and performance of contiguous pile wall using Finite Element Method (FEM) based on Mohr- Coulomb failure theory on chao phraya river bank. The contiguous pile wall was applied to be the temporary wall for basement construction of the excellent medical center in Asia, Siriraj Hospital. Three basement floors with 10.85 m depth were excavated next to the Chao Phraya River closed to the preserved buildings seated on shallow foundation. Two temporary bracings with one upper layer full cross bracing and one lower raking strut were constructed. Wanchai Teparaksa(2015) also predicted the behavior of contiguous pile wall by Finite Element Method (FEM) with simulation of all construction sequences. Instruments including inclinometer, tilt meter, Piezometer and ground surface settlement were installed in the contiguous pile, preserved building and in the ground, respectively. The performance of the contiguous pile wall was evaluated by instrumentation monitoring compared with FEM analysis and trigger level. The contiguous pile wall for the Siriraj excellent medical center consists of the row of 1.0 m. diameter bored pile with clearance of 100 mm between each bored pile. Each bored pile acted as the individual pile for resisting lateral earth pressure of 1.1 m width.

From results of the analysis it was found that the maximum lateral deflection of the contiguous pile wall was about 49.41 mm. Instrumentations were also designed to check the performance and behavior of the contiguous pile wall as well as the status of the surrounding buildings.

2.3 Numerical and Analytical studies of deep excavations.

Tung G. and Kung C.(2015) used a simplified soil model, the Modified Pseudo-Plasticity model by conduction a series of small strain triaxial tests on undisturbed Taipei silty clay to analyze the deflection and ground movements caused by braced excavations using Finite element analysis. Two sites having a diaphragm wall 25.6 m deep and 0.9 m thick, 35 m deep, and 0.9m thick were selected to conduct the numerical analyses of excavation. From the results found they concluded that the capability of the soil model adopted in describing the stress-strain-strength of characteristics of soils at a wide range of strain, especially at small strain ranging from 10^{-5} to 10^{2}, plays the crucial role in accurately predicting the excavation-induced ground movements.

Maria A. et al (2011) studied the performance of the deep excavation support system for 20m diaphragm wall with a single row of prestressed anchors in Berlin using finite element program. Generalized effective stress soil model was employed. The effective stress-strain-strength properties for the three sandy till units were modeled under the assumption that all three units had similar material properties but differed principally in their in situ state (i.e. stress conditions, void ratio, and stress history). Parameters for the soil model were derived from an extensive program of laboratory tests on the local Berlin sands. The study showed that the predictions for excavation performance were strongly affected by the vertical profiles of two key state parameters: the initial earth pressure ratio, K0; and the in situ void ratio, e_0. The results showed good agreement between computed and measured wall deflections and tieback forces.

Popa et al (2007). Presented "Numerical modeling and experimental measurements for a retaining wall of a deep excavation in Bucharest, Romania." They summarized a case history of a diaphragm wall for a deep basement of a new building in the center of Bucharest. The excavation impacted a number of historic structures, leading to the use of "top-down" techniques to support the excavation. The numerical results obtained by plane strain FE simulation were compared with measurements recorded during construction. For the soil, a perfect elasto-plastic constitutive law has been used, with Mohr – Coulomb criteria, using the geotechnical parameters issued from laboratory and in situ tests. From the results obtained they concluded that the computed lateral displacements were 15% and 75% of the observed values, depending on if the comparisons were made in an area with or without a grouted wall – not explicitly modeled in the FE simulations – adjacent to the diaphragm wall. The main factors leading to these differences were the soil parameters.

H.F. Schweiger (2005) studied the analysis of a deep excavation project in clayey silt in Salzburg. The excavation was supported by a diaphragm wall, a jet grout panel and three levels of struts. Hardening-Soil model was used as a constitutive model. Because of insufficient information available at the time of design on the material properties of the jet grout panel, the authors varied its stiffness in a parametric study. The effect of taking into account the stiffness of a cracked diaphragm wall on the deformations was also investigated. In some of the 3D calculations a non-perfect contact between diaphragm wall and strut was simulated by means of a non-linear behaviour of the strut. The evaluation of the results and comparison with in situ measurements showed that analyses which took into account the reduced stiffness of the diaphragm wall due to cracking achieved the best agreement with the measurements. Furthermore settlements of buildings could be best reproduced by the three-dimensional model.

E. Erbì and F.M. Soccodato(2011) discussed the results of a 3D numerical study of deep excavations in soft clayey soils. The analyses were carried out using non linear, plasticity hardening soil model, an advanced soil model capable to reproduce the significant non-linearity which characterizes soil behaviour. The parametric study involved different lengths of excavation sides, considering square and rectangular excavations, and different excavation heights. The attention was focused on horizontal displacements (wall deflections) as well as on vertical displacements (settlement profiles behind wall). Two-dimensional (2D) plane strain numerical analyses were also carried out in order to compare results and to highlight 3D effects on predicted displacement fields. From the results E. Erbì & F.M. Soccodato(2011) confirmed that, especially for excavations characterized by relatively low length to excavation depth or length to width ratios, 3D effects play a significant role in reducing the displacements obtained from 2D plane strain analyses.

M. Mitew (2005) conducted numerical analysis and parameter study taking into account two calculation methods, based on different constitutive soil models. Numerical back analysis has been divided into two parts. The first part considered the analysis performed using “Geo4-Sheeting analysis” and Rido - software, employing the method of dependent pressures, in which magnitudes of pressures acting upon a structure depend on deformation of the structure. The second part included numerical analysis performed using finite element method software: Geo4-FEM and Plaxis. The results of numerical analysis have been also compared to the results of in-situ measurements. M. Mitew (2005) concluded that Maximum theoretical displacements of the wall estimated in all FEM analysis were very close to the value of maximum real displacement measured during construction and relatively best results have been obtained when the soil parameters were based on the results of Pressuremeter investigations.

2.4 laboratory and field performance measurements

The performance of deep excavations has been studied through both laboratory tests and field measurements by a number of researchers, and the main findings are summarized in this section.

The advantage of laboratory tests is that factors influencing the results may be controlled quantitatively. Small-scale centrifuge model tests have been used in an attempt to gain a coherent view of the soil-structure interaction behaviour of deep excavations (Bolton and Powrie 1987, Bolton and Powrie 1988, Bolton and Stewart 1994, Richards and Powrie 1998, Takemura, Kondoh et al. 1999). Centrifuge modeling provides a correctly scaled physical model to enable the prototype behaviour of excavation so that it can be effectively used to investigate soil deformation mechanisms during the excavation process. The tests can be repeated and continued until failure, which is not possible in the full scale projects. Moreover, the tests are time-efficient and can observe the long-term behaviour of a geotechnical construction in soil of low permeability over a reasonably short period of time. However, it should be noted that centrifuge testing has its limitations and the conditions it can model are relatively simple.

Field measurement is an effective method, but it is also expensive and takes a long time to obtain the data, and this process is not repeatable. A number of case histories of deep excavations have been reported worldwide with well-documented field data, e.g. in the UK (Skempton and Ward 1952, Wood and Perrin 1984, Simpson 1992), in Chicago (Wu and Berman 1953, Finno, Atmatzidis et al. 1989, Finno and Nerby 1989), in Shanghai (Liu, Ng et al. 2005, Xu 2007, Wang, Xu et al. 2010, Liu, Jiang et al. 2011, Ng, Hong et al. 2012), in Singapore (Wong, Poh et al. 1996, Lee, Yong et al. 1998), in Hong Kong (Leung and Ng 2007), and in Taiwan (Ou, Hsieh et al. 1993, Ou, Liao et al. 1998, Ou, Shiau et al. 2000). These case histories vary from one to another in geological conditions, retaining structures, and construction methods, which make the correlation and comparison difficult, but generally they recorded the main excavation behaviour, e.g. wall deformations, ground movements, earth and pore water pressures, strut loads and wall bending moments, and deformation of adjacent infrastructure. Therefore, they provide valuable resources for understanding the more comprehensive behaviour of deep excavations, and also for calibrating the numerical analyses.

2.4.1 Wall deformation

The wall deformation (i.e. lateral deflection and vertical movement) is the major concern in deep excavations and is monitored in most field measurements. The pattern and magnitude of the wall deformation are influenced by a number of factors, e.g. the soil condition (e.g. stiffness, strength, anisotropy, and creep), the support system (e.g. stiffness, connections, and thermal effects), and construction methods (e.g. top-down, bottom-up, and cut and cover) (Yuepeng Dong 2014).

Field measurements of settlement and lateral deformation obtained from three deep excavation sites constructed in mixed ground profiles were presented and analyzed by Seo M.W. et al.(2010). Settlement measurements were obtained throughout the construction process, categorized in three stages as: preexcavation (preliminary site work and support wall installation), main excavation and bracing/anchor installation and post excavation (removal of bracing as basement construction proceeds). From the study the authors concluded that the maximum preexcavation stage settlements of 0.03%Hw to 0.06%Hw where Hw=wall or trench depth were measured at two sites, with the maximum settlements occurring adjacent to the wall during its installation. Maximum ground surface settlements during the main excavation stage ranged from about 0.15%He to 0.30%He where He=final excavation depth and the distribution of ground settlement extended to a distance of 1.5He to 2.0He from the wall. Maximum settlements occurred at distances of about 0.3He to 0.5He from the wall at two sites where the wall consisted of concrete cast in situ, concrete diaphragm and concrete secant pile walls, creating a significant reverse curvature in the settlement distribution. The maximum post excavation stage settlements ranged from 0.07%He to 0.10%He for the three sites, representing roughly 10 to 60% increases in settlement over the main excavation settlements, depending greatly on the specific support removal methods as well as the basement floor construction details employed at an individual site. Lateral deflections during the main excavation stage were consistent with trends reported in the literature, ranging from 0.12%He to 0.23%He, while lateral movement during post excavation stage ranged from 0.03%He to 0.09%He. Finally, the settlements measured during the main and post excavation stages were related to the support system stiffness.

Ong Tan and Mingwen Li (2011) measured and examined the performance of a 26 m deep top-down excavation in downtown Shanghai Via a long-term comprehensive instrumentation program. The measured excavation responses included diaphragm wall deflections, wall settlements, ground settlements, uplifts of interior steel columns, axial forces of propping struts, groundwater table levels, and settlements of adjacent buildings and utility pipelines. Based on the analyses of field data performed, the following major findings were obtained:

- ✓ The concrete struts along with the floor slabs effectively suppressed lateral wall movements and consequently reduced the chance that the maximum wall deflections would occur above the excavation surfaces,
- ✓ With the progress of excavation to a lower depth, the diaphragm walls underwent a serrated settlement pattern over time,
- ✓ No significant post-excavation wall deflection occurred,
- ✓ The relationship between the interior column uplifts and the maximum wall deflections can be described by a linear equation, and
- ✓ Most system loads due to soil removal were carried by the concrete struts along with the floor slabs. The struts sustained mainly the released earth pressures due to the exposure of the adjacent portions of diaphragm walls, and the soil removal distant from the struts imposed limited effects on the strut axial forces.

Yu Ou C.Y et al.(2012) studied the characteristics of ground surface settlement during excavation. Ten excavation cases in Taipei with good-quality construction and field observation data were selected to study the characteristics of excavation behavior. The location of maximum lateral wall deflection, magnitude of maximum lateral wall deflection, relationship of maximum lateral wall deflection and maximum ground surface settlement, location of maximum ground surface settlement, and apparent influence range were thus established based on the actual excavation cases. Finally, an empirical formula was proposed to predict the ground surface settlement profile at the center section of an excavation, where the behavior may be characterized by plane-strain conditions.

G.B. Liu et al. (2005) Presented and compared the observed response of diaphragm wall and the surface settlement of a deep excavation for a metro station in Shanghai soft clays with similar excavations (retained by a diaphragm wall) in soft clay areas in Asia and five metro station excavations (similar depth) in Shanghai. From the analysis made results showed that the maximum lateral wall deflection (δhm) and ground settlement (δvm) were 0.32% and 0.1% of final excavation depth (He), respectively. Lateral wall deflections were near the average magnitude value in Shanghai, smaller than those in Singapore. The largest lateral wall deflection was near the excavation center and the ratio of $\delta_{hmcor}/\delta_{hmcen}$ of the maximum wall deflection is 0.39–0.74. The ground settlement was relatively small and falls in the Zone I limit described by Peck (1969). The adoption of prestressed steel struts, short excavation sections, fast workmanship sequences and compaction grouting may contribute to the deformation characteristics of deep excavations for metro stations in Shanghai.

Tan and Wei (2011) investigated the performance of a 16–18 m deep excavation for a metro station with in-plane dimensions of approximately 20 m wide by 290 m long which was constructed by using the cut-and-cover technique in soft clay in the Shanghai metropolitan area, in which many high-rise buildings and utilities exist. A long-term comprehensive instrumentation program was conducted during construction. Field observations included deflections of diaphragm walls, vertical movements at wall tops, ground settlements, and settlements of surrounding buildings and utilities were conducted. Analyses of field data indicated that overexcavation and a long construction duration caused the diaphragm walls to develop substantial deflections. The base and middle floor slabs played dominant roles in suppressing post excavation wall deflections and ground settlements. This excavation in general exhibited different behaviors than other excavation projects because of its relatively long shape. Behaviors of deep excavations in Shanghai soft clay were affected not only by construction duration (i.e., time effects), but also by their geometries (i.e., space effects).

2.4.2 Ground movement

Ground movement is inevitable in deep excavations, and its magnitude depends on various factors such as soil properties, type of the retaining systems, excavation geometry, construction sequence, and workmanship. Excessive ground movement will cause damage to adjacent infrastructure. Therefore, understanding the characteristics of ground movement is essential in the design of deep excavations, and to take measures to mitigate the adverse impact on adjacent infrastructure.

Wang J. H.et al (1995) collected and analyzed an extensive database of 300 case histories of wall displacements and ground settlements due to deep excavations in Shanghai soft soils. They concluded that the mean values of the maximum lateral displacements of walls constructed by the top-down method, walls constructed by the bottom-up method including diaphragm walls, contiguous pile walls, and compound deep soil mixing walls, sheet pile walls, compound soil nail walls, and deep soil mixing walls were 0.27%*H*, 0.4%*H*, 1.5%*H*, 0.55%*H*, and 0.91%*H*, respectively, where *H* is the excavation depth. And the mean value of the maximum ground surface settlement was 0.42%*H*. The settlement influence zone reaches to a distance of about 1.5*H* to 3.5*H* from the excavation. The ratio between the maximum ground surface settlement and the maximum lateral displacement of a wall generally ranges from 0.4 to 2.0, with an average value of 0.9. The factors affecting the deformation of the wall were analyzed. The analysis shows that there is a slight evidence of a trend for decreasing wall displacement with increasing system stiffness and the factor of safety against basal heave.

Korff M. and Mair R.J.(2013) Studied and discussed ground displacements related to deep excavation in Amsterdam. The settlement measurements for the Amsterdam deep excavations have been compared to several, mostly empirical, relationships to determine the green field surface displacements and displacements at depth. It is concluded that the surface displacement behind the wall was 0.3-1.0% of the excavation depth, if all construction works were included. Surface displacements behind the wall can be much larger than the wall deflections and become negligible at 2-3 times the excavated depth away from the wall. The shape of the displacement fits the profile of Hshieh and Ou (1998) best. In all three of the Amsterdam cases, the largest effect on the ground surface displacement can be attributed to the preliminary activities. The actual excavation stage caused only about 25%-45% of the surface displacements, with 55%-75% attributed to the preliminary activities. At larger excavation depths the influence zone was significantly smaller than 2 times the excavation depth.

Jill Roboski and Richard J. Finno (2005) Predicted the distributions of ground movements parallel to deep excavations in clay using an empirical procedure for fitting a complementary error function (erfc) to settlement and lateral ground movement data in a direction parallel to an excavation support wall which was proposed based on extensive optical survey data obtained around a 12.8 m excavation in Chicago. The maximum ground movement and the height and length of an excavation wall define the erfc fitting function. The erfc fit was shown to apply to three other excavation projects where substantial ground movement data was reported.

Ou C.Y. et al.(1998) presented the performance of an excavation using the top-down construction method. Strut loads, wall displacement, wall bending moment, ground surface settlement, pore-water pressure and bottom heave were measured. Results obtained from those observations were correlated with the construction activities. The supported wall and the soil near the wall had a deep inward movement, which accounts for the magnitude of the lateral earth pressure acting on the wall. Ou C.Y. et al.(1998) concluded that the maximum horizontal displacement of an inclinometer casing 2 m away from the wall was close to that of the wall. Deep inward movements developed for the wall as well as the soil near the wall. This behavior became less pronounced with increasing horizontal distance from the wall. The maximum lateral wall displacement occurred near the excavation surface. The ratio of maximum lateral wall displacement to excavation depth ranged from 0.51% to 0.57%, except for the initial excavation stages.

2.4.3 Earth and pore water pressure

The understanding of the performance of deep excavations can be improved if more knowledge is known of the original in-situ stresses within the soil, and the changes of earth and pore water pressure during the construction.

Boone S.J. and Westland J.(2005) summarized the basis of apparent earth pressure distribution diagrams, their failings, proposed a new semi-empirical method for determining appropriate design pressures, and proposed an alternative approach to contract specification. They introduced a trial relative wall stiffness, Sr , to estimate the pressure distribution. But the maximum support loads and bending moments can be determined using common indeterminate structural analysis methods.

Tedd, Chart et al.(1984) conducted an extensive instrumentation of a propped embedded retaining wall at Bell Common Tunnel in London, and presented the variation of earth and pore water pressure during the construction period. The total horizontal stress in the ground close to the wall decreased during the wall installation, and the net reduction in total horizontal stress 0.6m behind the wall in London clay was 3 to 4 times greater than the reductions measured 3m and 6m from the wall. The horizontal total and effective stress slightly recovered after the wall installation but continued to decrease at the back of the wall in the subsequent excavation process, and these reductions were greater near the surface and close to the wall. Excavation also caused significant reductions in total stress in front of the wall, which was entirely due to a drop in pore water pressure, and there was a slight increase in effective horizontal stress, which may be expected from the lateral movement of the wall. When the roof structure was being constructed, the total horizontal stresses on both sides of the wall were virtually constant, but there was a gradual increase in pore water pressure in front of the wall and to a smaller extent at the back of the wall.

Powrie and Kantartzi(1996) observed in centrifuge model tests that the pore water pressure reduced during slurry trenching and increased during concreting in the diaphragm wall installation process. However, the net change of pore water pressure during these two processes is small, indicating that the initial ground water conditions may reasonably be taken for the subsequent excavation analysis in which the wished-in-place wall installation method was used.

2.4.4 Prop loads and wall bending moments

The prop loads can be computed from strain gauge measurements prior to installation and changes from the initial values, but corrections are needed to account for the difference of the thermal expansion/contraction of the structural member and gauge wire (Finno, Atmatzidis et al. 1989, Stroud, Hutchinson et al. 1994).

The bending moment (M) of the diaphragm wall can be calculated through the measurements from the reinforcement bar strain gauges, assuming that the variation of stresses over a cross section of the wall is linear and the neutral axis lies along the centre of the wall. Alternatively, the bending moment can be computed from the curvature of the wall deflection curve using the equation $M = EI/r$, where EI is flexural rigidity and r is the radius of curvature. But the bending moments computed from the rebar strain gauges are generally smaller than those from the wall deflection curve, particularly for the location where the maximum lateral wall deflection occurred and its neighboring location. This is because the bending moment from the wall deflection curve is computed without considering cracking concrete so that the moment of inertia (I) is not reduced. As a matter of fact, some cracks actually exist in the concrete because of the deformation of the concrete wall, subsequently thereby reducing the moment of inertia. The reduction factor for the moment of inertia (R) is introduced and then defined as the ratio of the moment obtained from the rebar strain gauge to the moment obtained from the inclinometer measurement. The reduction factor decreases with excavation depth OU, Liao et al.(1998).

2.4.5 Deformation and damage of adjacent infrastructure

A major concern when making deep excavations in urban areas is the impact of construction-related ground movements on adjacent buildings, tunnels, buried pipelines, pile foundations, highways, and bridges. Structures will deform and possibly sustain damage in response to these ground movements. In many cases, strict deformation control is required to minimize damage to adjacent structures when excavating in urban areas. This requirement dictates the use of stiff excavation support systems, particularly when soft clays underlie a site. The required stiffness of an excavation support system is determined by the magnitude and distribution of the deformations expected during the project and their impact on adjacent structures before, during, and after construction. Finno, Sabatini (2002).

Finno R. J., Lawrence S.A. et al(1991) conducted analyses and evaluated the performance of groups of step-tapered piles located adjacent to a 50-ft-deep tieback excavation. The excavation was made through primarily granular soils within an existing framed structure. The main columns were supported by groups of 70-ft-long, unreinforced or lightly reinforced concrete piles. The temporary tieback sheet-pile wall was located as close as 2 ft to the pile caps. They concluded that the field observations, including lateral deformations of the sheet pile and lateral and vertical deformations of the main columns, revealed movements of several of the pile caps was as large as 3in. towards the excavation. This movement was twice as large as normally expected for excavations made under similar conditions. An analysis of the existing foundation conditions and a finite element computation of the bending moments induced in the piles during construction of the cut indicated that the resulting moments were not large enough to cause cracking in the piles. Sheet-pile extraction as close as 2 ft to the main-column pile caps caused the pile caps to translate toward the excavation by an amount no larger than one-half the displaced width of the sheet pile; it did not significantly alter the magnitude or distribution of computed, excavation-induced bending moments in the piles.

Finno and Sabatini (2002) presented the damage caused by an adjacent 12.2-m-deep excavation in soft clay in which the excavation support system was a 0.9-m-wide secant pile wall braced by both cross-lot struts and tiebacks on a three-story school supported by shallow foundations. The school was a reinforced concrete frame structure with exterior reinforced concrete foundation walls. The lateral ground movements associated with the excavation were monitored with four inclinometers placed around the school. The building movements were monitored with optical survey points established on interior columns, exterior walls and on the roof, and with tiltmeters installed on the exterior foundation walls. From the study it was found that the damage to the school mainly consisted of 300 to 500-mm-long hairline cracks in nonload bearing walls. Only a few cracks had widths greater than 6 mm. The school deformed such that the portion closest to the excavation sagged and the remainder hogged. Damage was first observed in the area of sagging when angular distortions reached 1/940 and the excavation was approximately 5.5m deep. Angular distortions as large as 1/300 were observed at the end of the project. The authors concluded that the angular distortions had to be less than 1/1000 to preclude any damage to the school.

Goh A.T.C. et al(2003) applied a simplified numerical procedure based on the finite-element method to analyze the pile response to nearby excavation activities resulting from the construction of a 16 m deep cut-and-cover tunnel. The pile was located 3 m behind a 0.8 m thick diaphragm wall. They concluded that excavation to the formation level that was 16 m below the ground surface resulted in a maximum lateral pile movement of 28 mm. Generally, the theoretical predictions were in reasonable agreement with the measured results.

2.5 Constitutive Soil Models

The accuracy of numerical solutions in deep excavation analysis largely depends on the ability of the constitutive model to describe soil behaviour in generalized stress conditions. However, considering the complexity of soil behaviour, it is not realistic to develop a completely generalized effective stress model for all soils. For a given boundary problem, the complexity of the constitutive model should be closely tied to the major aspects of the problem (e.g., stiffness, strength, deformation, dilation, and anisotropy) to be tackled and/or the accuracy of solution which is required (Whittle 1987). Once the soil model is identified, its application in the finite element analysis requires appropriate procedures to derive the model parameters and calibrate the model through laboratory and/or field tests. A number of advanced soil models have been used in the analysis of deep excavations with certain kinds of success, and their characteristics are discussed briefly in this section.

Yang C. et al. (2008) developed a constitutive model, Plastic Bounding Surface Model for unsaturated cemented and loessic soils under cyclic loading. The developed model was based on the damage theory for structured soils and unsaturated soil mechanics and an elastoplastic model for unsaturated loessic soils under cyclic loading. The description of bond degradation in a damage framework was given, linking the damage of soil's structure to the accumulated strain. The Barcelona Basic Model (BBM) was considered for the suction effects. The elastoplastic model was then integrated into a bounding surface plasticity framework in order to model strain accumulation along cyclic loading, even under small stress levels. The validation of the proposed model was conducted by comparing its predictions with the experimental results from multi-level cyclic triaxial tests performed on a natural loess sampled beside the Northern French railway for high speed train and about 140 km far from Paris. The comparisons showed the capabilities of the model to describe the behaviour of unsaturated cemented soils under cyclic loading.

Bolton M.D. et al (1994) studied the non linear stress-strain behaviour of overconsolidated clays at small strains prior to gross plastic yielding and derived a general form of power function for shear modulus and its implementation inside the yield surface of the Modified Cam Clay model within CRISP finite element program. Simulation of triaxial tests, and ground movements due to tunneling were compared with appropriate data and contracted with constant stifnness analysis. Results from triaxial tests showed that the shear modulus was under estimated by the MCC model for small strains and over estimated for intermediate large strains. From the obsereved behaviour of ground movements in centrifuge tests on tunnels in clay the authors conluded that the magnitude and shape of surface subsidence above the tunnel could not simultaneously be predicted by the MCC model. However the SDMCC model fitted observed behaviour much better, especially when the critical state ratio (M) was permitted to reflect the local strain path (extension or compression) appropriate to tunnel pressure reduction.

A constitutive model with a single yield surface has been developed for the behavior of frictional materials, such as clay, sand, concrete, and rock by Poul V. L.(1990). The model is based on concepts from elasticity and plasticity theories. In addition to Hooke's law for the elastic behavior, the framework for the plastic behavior consists of a failure criterion, a nonassociated flow rule, a yield criterion that described contours of equal plastic work, and a work-hardening/softening law. The functions that describe these components were all expressed in terms of stress invariants. The model incorporates eleven parameters for normally consolidated clay that can be determined from simple experiments, such as isotropic compression and consolidated-undrained triaxial compression tests. A study of the three-dimensional behavior of remolded, normally consolidated clay has served as a basis for evaluating the capabilities of the model. In particular, the variations of stress-strain and pore pressure behavior, relation between principal strains, and normalized undrained shear strength with the relative magnitude of the intermediate principal stress were studied. Overall acceptable and accurate predictions were produced for the normally consolidated clay.

Poul V. L. et al.(2008) developed a Rotational Kinematic Hardening Model for three-dimensional stress reversals in sand. It incorporated rotation and intersection of yield surfaces to achieve a consistent and physically rational fit with experimentally observed soil behavior during large three-dimensional stress reversals. An existing elasto-plastic model with isotropic hardening was used as the basic framework to which the rotational kinematic hardening mechanism has been added. The new combined model preserved the behavior of the isotropic hardening model under monotonic loading conditions, and the extension from isotropic to rotational kinematic hardening under three-dimensional conditions has been accomplished without introducing new material parameters. Predictions of plastic strain increment vector directions from the proposed Rotational Kinematic Model were made by the authors to compare with experimental results from triaxial compression and extension tests in the triaxial plane. Predictions of stress–strain behavior during large stress reversals were also shown to fit well with experimental data. The model was extended to the principal stress space and theoretical plastic strain increment vector directions were compared with experimental data. Within the scatter of the test results, the model was shown to capture the behavior of soil during large stress reversals with reasonable accuracy.

Cecconi M. et al.(2002) developed a constitutive model for granular materials within the framework of strain–hardening elastoplasticity, aiming at describing some of the macroscopic effects of the degradation processes associated with grain crushing. The central assumption of the paper was that, upon loading, the frictional properties of the material were modified as a consequence of the changes in grain size distribution. The effects of these irreversible microscopic processes were described macroscopically as accumulated plastic strain. Plastic strain drives the evolution of internal variables which model phenomenologically the changes of mechanical properties induced by grain crushing by controlling the geometry of the yield locus and the direction of plastic flow. The model was applied at Pozzolana Nera to obsereve the stress–dilatancy relationship to use as guidance for the formulation of hardening laws, and it was concluded that the minimum value of dilatancy always follows the maximum stress ratio experienced by the material.

2.6 Field Studies

2.6.1 Finite Element Analysis of a Deep Excavation A Case Study from the Bangkok MRT

Surarak, C. et al.(2010) conducted a finite element study on the Bangkok Mass Rapid Transit (MRT) Underground Railway project on Sukhumvit station, Thailand. The numerical study focused on initial input of ground condition and the constitutive soil models. The geotechnical conditions were carried out based on soil investigation report. The project was constructed along highly congested roads in the heart of Bangkok city. The tunnel alignment, which is 22 km in length, included 18 underground cut-and-cover underground stations. The station perimeter was constructed of diaphragm walls (D-walls), 1.0 – 1.2 m thick and 20 m to 46 m deep used for earth-retaining and permanent structures. The parameters of constitutive models were determined and calibrated against the laboratory testing results. Finally, all finite element analysis results were compared with the real field investigations.

Geological Conditions

The Bangkok subsoil consists of 7 alternate layers of sand, gravel and clay. The soil profile consists of 2 to 3 m of made ground (MG), underlain by approximately 9 m of normally consolidated Bangkok Soft Clay (BSC). Beneath the BSC layer, there is 2 m of Medium Clay (MC),. A thin, but continuous, medium dense Clayey Sand (CS) of 1.5 m is sandwiched between the First and Second Stiff Clays (1st SC and 2nd SC), with thicknesses of 6 m and 4 m, respectively. At the depth of 23 to 40 m, the Hard Clay (HC) layer (SPT *N* values of 30 to 40), with some sand lenses, is found. This HC layer is then underlain by the Dense Sand (DS) layer, up to 60 m deep. The ground water level was found at 1.5m below the ground surface.

Soil parameters

The following soil parameters were used for base model during analysis.

Table 2.1: Parameters for Hardening Soil Model (HSM) Analysis. Surarak, C. et al.(2010)

Layer	Soil type	Depth (m)	γ_b (kN/m^3)	c' (kPa)	ϕ' (°)	ψ (°)	E_{50}^{ref} (MPa)	E_{oed}^{ref} (MPa)	E_{ur}^{ref} (MPa)	ν_{ur}	m	K_o^{nc}	R_f	Analysis type
1	MG	0 – 2.5	18	1	25	0	45.6	45.6	136.8	0.2	1	0.58	0.9	Drained
2	BSC	2.5 – 12	16.5	1	23	0	0.8	0.85	8.0	0.2	1	0.7	0.9	Undrained
3	MC	12 – 14	17.5	10	25	0	1.65	1.65	5.4	0.2	1	0.6	0.9	Undrained
4	1^{st}SC	14 – 20	19.5	25	26	0	8.5	9.0	30.0	0.2	1	0.5	0.9	Undrained
5	CS	20 – 21.5	19	1	27	0	38.0	38.0	115.0	0.2	0.5	0.55	0.9	Drained
6	2^{nd}SC	21.5 – 26	20	25	26	0	8.5	9.0	30.0	0.2	1	0.5	0.9	Undrained
7	HC	26 – 45	20	40	24	0	30.0	30.0	120.0	0.2	1	0.5	0.9	Undrained

Table 2.2: Parameters for Hardening Soil Model with Small Strain Stiffness (HSS 1 and 2) Analysis. Surarak, C. et al.(2010)

Layer	Soil type	Depth (m)	G_{max} (MPa)	$\gamma_{0.7}$ (%) for HSS 1	$\gamma_{0.7}$ (%) for HSS 2
1	MG	0 – 2.5		HSM	
2a	BSC 1	2.5 – 7.5	7	0.056	0.056
2b	BSC 2	7.5 – 12	10	0.08	0.08
3	MC	12 – 14	12	0.09	0.09
4	1^{st}SC	14 – 20	30	0.1	0.002
5	CS	20 – 21.5		HSM	
6	2^{nd}SC	21.5 – 26	50	0.1	0.002
7	HC	26 – 45		HSM	

Remarks: 1. Strength parameters (ϕ' and c'), dilatancy angle (Ψ) and bulk unit weight for SSM analysis are the same as those of HSM analysis.

2. HSM is adopted for Made Ground (MG), Clayey Sand (CS) and Hard Clay (HC) layers

Finite Element Modeling

The 2D plane strain finite analysis approach, using Plaxis2D v.9 2009 software was adopted in this study. As the ratio of the length (L) to width (B) of Sukhumvit Station box was high (L/B = 8.7), the 3D effect along the long sides of the station was small, thus the 2D plane strain approach was considered appropriate. A seven-layer soil profile was adopted. Importantly, four soil models (i.e., Mohr-Column Model (MCM), Soft Soil Model (SSM), Hardening Soil Model (HSM) and Hardening Soil Model with Small-Strain Stiffness (HSS) were used to evaluate their performances in deep excavation modeling.

To investigate the effect of the initial pore water pressure condition in the finite element modeling, two analyses were conducted. The first applied a drawdown pore water pressure profile, while the second assumed a hydrostatic pore water pressure. For both the maximum lateral wall movement and the maximum surface settlement, the hydrostatic case prediction was two times higher than the corresponding field measurements. The drawdown case seems to give a reasonable agreement, especially for the peak values. More importantly, at the toe of diaphragm wall, the lateral wall movement from the hydrostatic case was nearly three times the measured values. This outcome showed a high degree of instability for the diaphragm wall, which did not occur on site. It is, therefore, concluded that a realistic drawdown pore water pressure was necessary for a finite element analysis in the Bangkok area.

Results and discussion

Four stages of the Finite Element Analysis results, where the excavation depths were at 1.5, 7.5, 12.5 and 21 m, were compared with the monitoring data and conclusions for each model results were withdrawn.

The results from MCM analysis showed that the lateral wall movements at all stages of the excavation were under predicted. The maximum lateral movement of the wall at the final excavation stage was about 15% lower than the measured value. Contrary to the lateral movement, the MCM analysis showed a much shallower and wider surface settlement profile, when compared to the field measurement and empirical prediction.

Analysis results SSM were fairly close to the field measurements at excavation stage 1 to 3 but the maximum lateral wall movement at the final stage slightly under predicted, the measured values by approximately 15 % (similar to MCM predictions). In terms of the ground surface settlement predictions, the SSM gave better trends for the settlement envelope compared to the MCM.

The predicted lateral wall movements at all excavation stages using HSM within the BSC layer (2.5 to 12 m depth) were slightly higher than the field measurements. This overestimation extends further into the deeper layers for the excavation stages 1 to 3. The maximum lateral movement in the last excavation stage (located in 1st and 2nd SC layers) agreed well with the measured values. In the case of the ground surface settlement comparison, the HSM predicted better settlement envelopes compared to those predicted by the MCM and SSM.

The HSS1 analysis improved the lateral wall movement prediction, when compared to those predicted by the HSM for all excavation stages in the BSC and MC layers. The predictions about the deeper layers (1st SC, CS and 2nd SC) were, however, much smaller than in the HSM analysis. Indeed, the predicted maximum lateral wall movement was only one half of the measured magnitudes. The corresponding surface settlements were also under predicted by the HSS 1 analysis.

2.6.2 Modeling of Deep excavation with multi anchored diaphragm wall in Tirana, Albania

Josifovski J. et al. (2011) conducted an analysis and design of a project of eight storey administrative-residential building located in the city centre of Tirana, Albania using finite element software, PLAXIS. The project anticipated a 20.5m deep excavation with six underground storeys. The site was surrounded with six and eight storey buildings with basements. The ground profile was comprised of 10 horizontal soil layers with thickness of 0.7m, 2.4m, 2.0 to 2.5m, 0.5m to 0.7m and 4.5m up to 9m depth. The underground water is present on 4 to 5m below ground surface. In this section the numerical modelling of the 20.5m deep excavation is presented with some conclusive discussions.

Lateral support system

The excavation was secured by a retaining system with a task to ensure the soil stability. The diaphragm wall with thickness *d* = 0.8m total length of *L* = 129.2m and height *H* = 25m had only a temporal character. The diaphragm wall had been comprised out of 2.7m reinforced concrete segments. The supporting structure represented a multi anchored diaphragm wall with height of 20.5m plus additional 4.5m depth bellow the pit. The supports were pre-stressed anchors which introduced additional stabilizing forces into the system. The horizontal anchor spacing was set to *Ls* = 2.7m while the vertical was *hs* = 3m. The anchors were positioned with inclination of $\alpha=15^0$ and they varied in total length.

Soil and anchor properties

The following soil parameters were used as input during analysis.

Table 2.3: Soil and anchor properties. Josifovski J. et al. (2011)

Cohesion	*C*	150	Psi
Internal friction	ϕ	30	degrees
Unit weight	ɣ	19.2	KN/m3
Height	H	11.5	m
Distance	*X*	10	m
Bond length	Lb	15	m
Angle to horizontal	α	15	degrees
Width	B	1.3	m
Start depth	Z1	14.18	m
End depth	Z2	18.06	m
Pressure	P*v*	309.52	kPa
Resistance force	R*k*	2323.44	KN
Partial factor	ɣ*r*	1.35	
Design resistant force	R*d*	1721.06	KN

According to calculated characteristic forces *Rk* which correspond to the required stabilizing force the following anchor types were chosen.

Table 2.4: Anchor type in wall section. Josifovski J. et al. (2011)

level (m)	Anchor type	Po KN	EA KN	L= Lf + Lb (m)
-4	4TTS15	831.6	109952.5	24.5+15
-8	7TTS15	1455.3	109952.5	12.5+15
-11.5	6TTS15	1247	109952.5	10.5+15
-14.5	7TTS15	1455.3	164850	8.5+15

-17.5	6TTS15	1247.4	192325	7+15

Finite Element Modeling

In order to obtain a realistic simulation of the excavation, the problem was analyzed using the finite element method on two and three dimensional models using Plaxis. The ground stress-strain state with the occurring soil effect during the excavation process had been simulated on a two-dimensional plane strain finite element model. The soil material is discretized using the Mohr-Coulomb model while the concrete diaphragm wall with linear material law.

Results and discussion

Beside the soil stresses and displacement, the finite element analysis determined the deformation and internal forces of the diaphragm wall. The maximal calculated horizontal displacement of the wall was 41.9mm at the depth of around 14m. The measured displacements during the excavation had not excided the calculated ones.

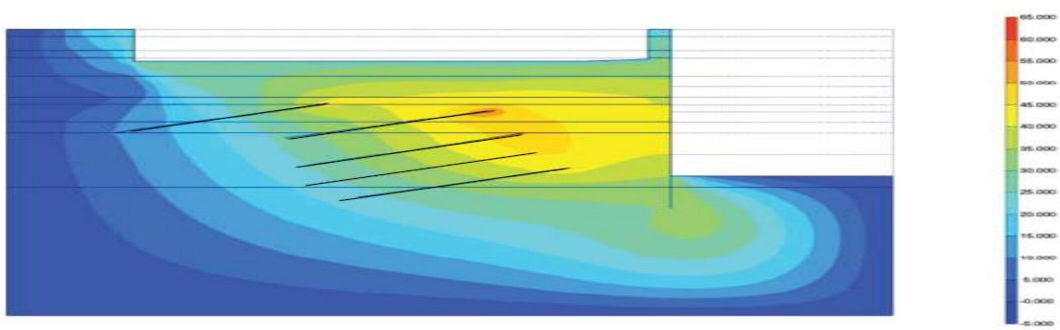

Figure 2.5: Horizontal displacements Josifovski J. et al. (2011)

CHAPTER 3
STUDY AREA DESCRIPTION AND BASE MODEL PARAMETRES

3.1 Description of the study area

Adama also known as Nazret or Nazreth is a city in central Ethiopia and the previous capital of the Oromia Region. Adama forms a Special Zone of Oromia and is surrounded by Misraq Shewa Zone. It is located at 8.54°N 39.27°E at an elevation of 1712 meters, 99 km southeast of Addis Ababa. The city sits between the base of an escarpment to the west, and the Great Rift Valley to the east. Based on the 2007 Census conducted by the Central Statistical Agency of Ethiopia (CSA), this city has a total population of 220,212, an increase of 72.25% over the population recorded in the 1994 census, of whom 108,872 are men and 111,340 women. With an area of 29.86 square kilometers, Adama has a population density of 7,374.82; all are urban inhabitants.

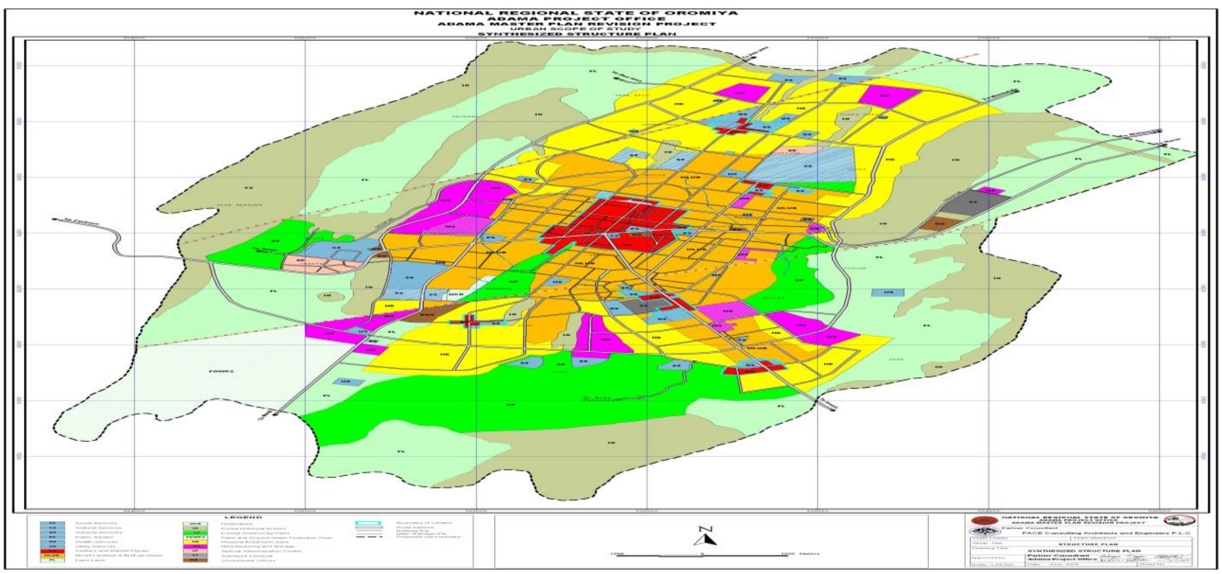

Figure 3.1: Map of Adama town

3.2 Parameter Identification for Base Model

During analysis of deep excavation support system, a number of parameters, which has an effect in the performance of contiguous wall, have to be considered. Therefore based on the investigations made by ADDIS GEOSYSTEMS P.L.C. a representative value of SPT test data are chosen and required soil parameter correlations are used and selected based on data quality, soil profile, consistency and availability. Some relevant parameters for the soil are taken from literatures (Abu gemechu, 2011). German institute for standardization June 2002 and 2003

(Normenausschuss Bauwesen (NaBau) im DIN Deutsches institut fur Normung e.v 2002 and 2003) was used to determine the strength parameters of the soil. The soil types considered for this study are silty soils from Adama town. Ground water level is at deep depth from ground surface hence it has no effect in analysis and during excavation and construction.

The following engineering design parameters are extracted from SPT N values which are conducted by ADDIS GEOSYSTEMS P.L.C and considered to represent the soil in Adama town based on availability.

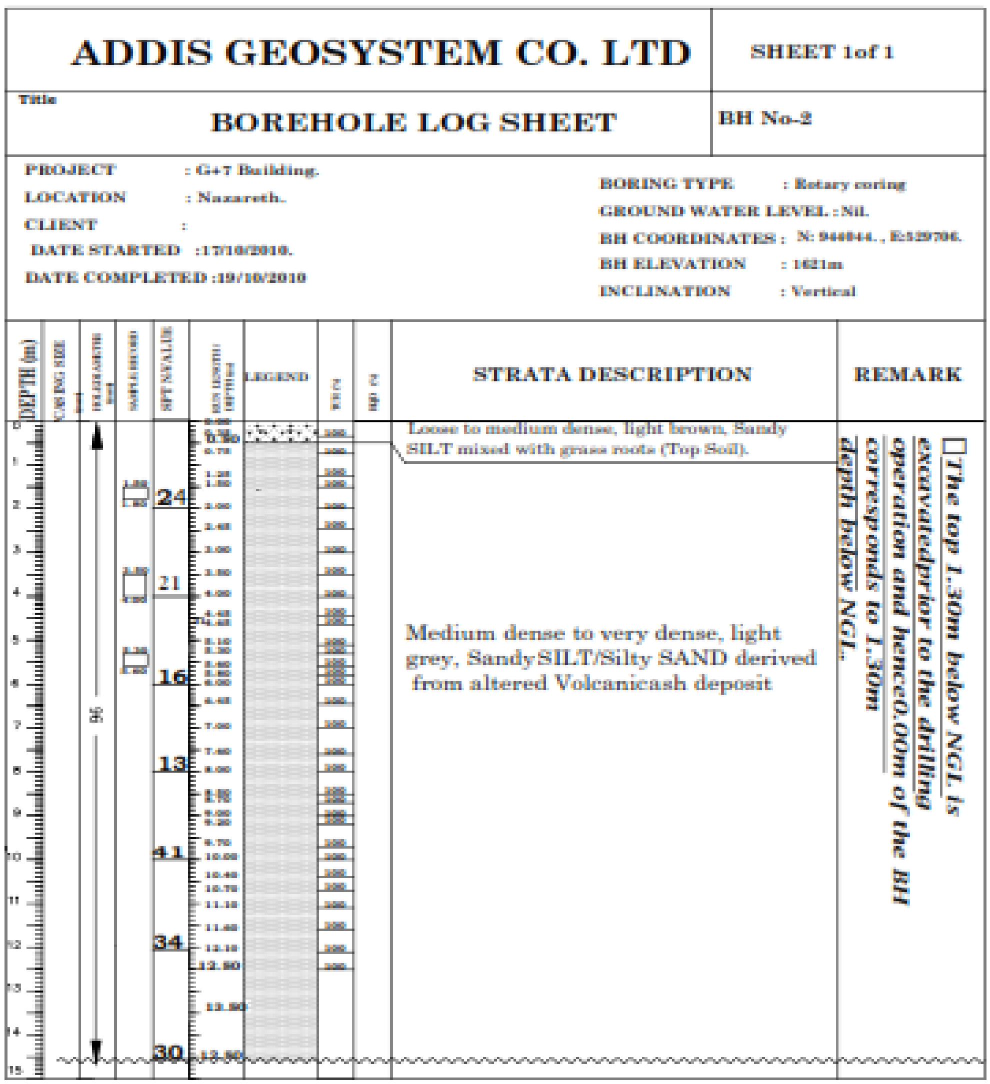

Figure3.2: Representative borehole log sheet.

3.3 Lateral Earth Pressure

Incorrect implementation of design earth pressure may lead to uneconomical or even unsafe designs. Traditionally, apparent earth pressure diagrams are used for designing excavation support systems. These diagrams are semi-empirical approaches back-calculated from field measurements of strut loads which do not represent the actual earth pressure or its distribution with depth. Therefore, apparent earth pressure diagrams are only appropriate for sizing the struts. As previously mentioned, the use of these diagrams yield support systems that are adequate with regards to preventing structural failure, but may result in excessive wall deformations and ground movements. In this study Coulomb's Earth Pressure theory is assumed and wall is assumed as frictional with δ=2ϕ/3, where δ is wall friction and ϕ is soil friction angle. Anchor loads are determined by tributary area methods from apparent earth pressure diagrams proposed by Peck (1969).

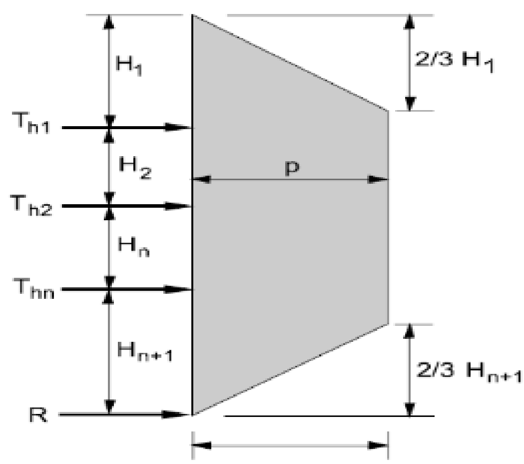

Figure 3.3: Recommended Earth Pressure Diagram for Sands :Walls with multiple levels of ground anchors.Peck(1969)

$$Pe= \frac{0.65\tan^2\left(45-\frac{\phi}{2}\right)\gamma H^2}{H-\frac{H1}{3}-\frac{Hn+1}{3}} \text{ -- eqn 4.4}$$

H_1= Distance from ground surface to upper most ground anchor.

H_{n+1}=Distance from base of excavation to lowermost ground anchor.

T_{hi}=Horizontal load in ground anchor i.

R=Reaction force to be resisted by subgrade (i.e., below base of excavation).

P=Maximum ordinate of diagram.

ɣ= unit weight of soil

H= depth of excavation

H_1= Distance from ground surface to upper most ground anchor.

The trapezoidal diagram is used for anchor load determination for the following reasons:

- ✓ Earth pressures are concentrated at the anchor locations resulting from arching.
- ✓ Earth pressure of zero at the ground surface is appropriate for sands (provided no surcharge loading is present).
- ✓ Earth pressures increase from the ground surface to the upper ground anchor location; and
- ✓ Medium dense to very dense sands, earth pressures reduce below the location of the lowest anchor owing to the passive resistance that is developed below the base of the excavation. (Aiza Malik 2015).

3.4 Earth Pressures due to Surface Load

Uniform surcharge loads are vertical loads applied at the ground surface which are assumed to result in uniform increase in lateral stress over the entire height of the wall. The increase in lateral stress for uniform surcharge loading can be written as

$\Delta\sigma_h = K*q_s$-- eqn 4.5

Where:

$\Delta\sigma_h$ =the increase in lateral earth pressure due to the vertical surcharge load(KPa)

q_s =the vertical surcharge stress applied at the ground surface(KPa)

K =an appropriate earth pressure coefficient.

3.5 Calculation of Ground Anchor Loads from Apparent Earth Pressure Diagrams

Ground anchor loads for flexible anchored wall applications can be estimated from apparent earth pressure envelopes. Methods commonly used include the tributary area method and the hinge method. Both methods, when used with appropriate apparent earth pressure diagrams, provide reasonable estimates of ground anchor loads and wall bending moments for anchored systems constructed in competent soils. Tributary area method is used for ground anchor load calculation.

T_1 = Load over length $H_1 + H_2/2$

T_2 = Load over length $H_2/2 + H_n/2$

T_n= Load over length $H_n /2 + H_{n+1}/2$

R = Load over length $H_{n+1}/2$

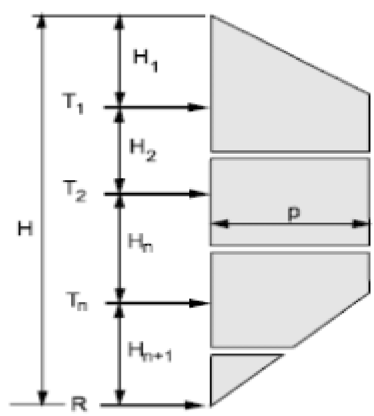

Figure 3.4: Calculation of Anchor Loads for Multi - Level anchored Wall

3.6. Soil, Pile, Diaphragm Wall and Anchor Parameters for base model

The following soil parameters are used as input for base model generation during analysis of 8, 10, 12 and 14m excavation depth**.**

Table 3.1: Soil parameters for base model

depth(m	N30 (corrected)	Consistency	ϕ(deg)	Cu (Kpa)	Es (Mpa)	ɣ bulk (KN/m3)
1						
2	24	Medium Dense	32.8	173.5436	50.62815	18.2

3						
4	21	Medium Dense	32.2	163.0049	52.93048	18.95
5						
6	16	Medium Dense	31.2	129.6053	53.78629	18.35
7						
8	13	Medium Dense	30.6	117.725	55.38996	17.75
9						
10	41	Very Dense	43	259.6545	86.57688	22
11						
12	34	Very Dense	40	223.0084	88.40779	22
13						
14	30	Dense	33	203.7904	90.78347	21.25

Notes: MC – Mohr-Coulomb
-Stiffness parameters assumed to be at reference pressure, Pref=100KPa

During selection of wall parameters for base model, adopted pile diameter is changed to equivalent wall thickness, compared with adopted wall thickness and the less thick is selected for analysis.

Table 3.2: Diaphragm Wall parameters for base model.

			Depth of excavation			
	Wall parameters	**Units**	**8m**	**10m**	**12m**	**14m**
PLATES	**Wall type**		**DW**	**DW**	**DW**	**DW**
	Material type	**Elastic**	**Elastic**	**Elastic**	**Elastic**	**Elastic**
	Adopted diaphragm wall thickness	**kN/m**	**0.3m**	**0.3m**	**0.3m**	**0.3m**
	Normal stiffness, EA	**kN/m**	**9*10^6**	**9*10^6**	**9*10^6**	**9*10^6**
	Flexural Rigidity, EI	**kN/m**	**6.75*10^4**	**6.75*10^4**	**6.75*10^4**	**6.75*10^4**
	Weight, W	**kN/m**	**7.2**	**7.2**	**7.2**	**7.2**
	Poisson's ratio	**-**	**0.15**	**0.15**	**0.15**	**0.15**

Table 3.3: Pile parameters for base model.

			Depth of excavation			
	Wall parameters	**Units**	**8m**	**10m**	**12m**	**14m**
PLATES	**Wall type**		**CW**	**CW**	**CW**	**CW**
	Material type	**Elastic**	**Elastic**	**Elastic**	**Elastic**	**Elastic**
	Adopted pile diameter	**m**	**0.45m**	**0.45m**	**0.45m**	**0.45m**
	Equivalent wall thickness, d	**m**	**0.159m**	**0.159m**	**0.159m**	**0.159m**

	Normal stiffness, EA,	**kN/m**	**4.77*10^6**	**4.77*10^6**	**4.77*10^6**	**4.77*10^6**
	Flexural Rigidity, EI,	**kNm**	**1*10^4**	**1*10^4**	**1*10^4**	**1*10^4**
	Weight, w	**KN/m**	**3.82**	**3.82**	**3.82**	**3.82**
	Poisson's ratio		**0.15**	**0.15**	**0.15**	**0.15**
	Pile spacing		**100mm**	**100mm**	**100mm**	**100mm**

Notes: CW – Contuguous Wall
EA and EI are per unit length of the wall
EA = Et, t = equivalent thickness of the pile or wall
$EI = Et^3/12$

Anchor load calculation (sample calculation for H=8m)

The tributary area method is used to calculate the horizontal anchor loads, T1 andT2 and the reaction force to be resisted by the sub grade, Rc.

The horizontal anchor loads were calculated using the tributary area method, as follows

$T_1=\left(\frac{2H1}{3}+\frac{H2}{2}\right)Pe+\left(H1+\frac{H}{2}\right)Ps$ = 199.69kN/m--------------------------- eqn 4.6a

$T_2=\left(\frac{H2}{2}+\frac{23H3}{48}\right)Pe+\left(\frac{H2}{2}+\frac{H3}{2}\right)Ps$ = 188.18kN/m-------------------------- eqn 4.6b

$Rc=\left(\frac{3H3}{16}\right)Pe+\left(\frac{H3}{2}\right)Ps$ = 63.79kN/m-- eqn 4.6c

Anchor design load

The inclination of all anchors is assumed to be 15º and center-to-center spacing is taken as 3 m.

1. Upper anchor: The anchor design load (DL) was calculated as follows:

$$DL_1=T1*\frac{Lc}{cos\Theta} = 516.8 \text{ kN}$$

2. Lower anchor: The anchor design load (DL) was calculated as follows

$$DL_2=T2*\frac{Lc}{cos\Theta} = 487.01 \text{ kN}$$

The maximum calculated anchor design load is 516.8 kN.

The anchor bond zones will be formed in the medium dense silty sand layer therefore the load transfer rate is controlled by the medium dense silty sand layer, a load transfer rate of 100 kN/m was selected.(Sabatini P.J. 1999, "Ground Anchors and Anchored Systems").The design load with a factor of safety of 2.0 should be able to be achieved with a typical soil anchor bond length of 12 m, assuming a small diameter low pressure grouted anchor.

For a length of 12m the bond strength is

=100KN/m*12m/2 = 600kN

The allowable anchor capacity of 600 kN is larger than the maximum design load of 516.8kN. This implies that the design load can be attained at this site for the assumed anchor spacings and inclination. Right of way estimates can be made based on the bond length required for mobilization of the design load, as follows:

Maximum bond length = 516.8*2/100 = 10.34m

Tendon selection

A 64-mm diameter, Grade 150 prestressing bar may be selected, based on an allowable tensile capacity of 60 percent of the specified minimum tensile strength (SMTS) with allowable tensile capacity that exceeds the calculated maximum design load.(From Properties of prestressing steel bars ,ASTM A722.).

Table 3.4: Anchor parameters for the base model

	Depth of excavation	8m	10m	12m	14m
Anchor parameters	Type	Elastic	Elastic	Elastic	Elastic
	EA, kN/m	1*10^5	1*10^5	1*10^5	1*10^5
	Prestressed load kN	150	150	150	150
	No of Anchors	2	3	4	5
	Anchor spacing	Anchor1=3m Anchor 2=3m	Anchor 1=3m Anchor 2= 3m Anchor3=2m	Anchor 1=3m Anchor 2= 3m Anchor3=3m Anchor4=2	Anchor 1=3m Anchor 2= 3m Anchor3=3m Anchor4=3m Anchor 5=1m

Table 3.5: Excavation and embedment depth parameters for the base model

Parameters	Unit	D_{ex1}	D_{ex2}	D_{ex3}	D_{ex}
Depth of excavation	m	8	10	12	14
Depth of embedment	m	4m	5m	8m	10m

CHAPTER 4
ANALYSIS AND PARAMETRIC STUDY

4.1 INTRODUCTION

The problem is modeled with a geometry model of 105 m width and 14 m depth. Parametric study is conducted for excavation depth of 8,10,12 and 14m. In this study the ground anchor is modeled by a combination of a node-to-node anchor and a geotextile. The geotextile simulates the grout body whereas the node-to-node anchor simulates the anchor rod. In reality, there is a complex three-dimensional state of stress around the grout body. Although the precise stress state and interaction with the soil cannot be modeled with this 2D model, it is possible in this way to estimate the stress distribution, the deformations and the stability of the structure on a global level, assuming that the grout body does not slip relative to the soil. With this model it is certainly not possible to evaluate the pull-out force of the ground anchor. The pile wall is modeled as a beam. The interfaces around the beam are used to model soil-structure interaction effects. Interfaces should not be used around the geotextile that represent the grout body. The excavation is constructed in several excavation stages. The separation between the stages is modeled by geometry lines.

Based on scientific verifications and investigations Mohr coulomb model gives precise prediction of ground deformation for the selected deep excavation support system in the chosen area (For details, see Appendix 1). Since the performance of deep excavation support system and lateral wall, movements are influenced by several factors including wall installation, soil conditions, support system stiffness, and methods of support system installation and interaction between the soil and the support, parameters has to be identified accordingly. Finite element software PLAXIS V8.6 2D is used for analysis. Since the support system contains wall and pile, analysis is done for the less thick wall, which governs the design, and the analysis results are presented.

4.2 Base model generation

Finite element simulation is conducted to overcome the deficiencies of the actual methods used to predict maximum wall movements for deep excavations in cohesive soils. Figure 4.1 shows a

PLAXIS 2D schematic of one of the finite element models used in the analyses. In the simulations, soil elements were modeled with 15-node wedge elements that are generated from the projection of two-dimensional 6-node triangular elements between work planes with a width of 105 meters and depth of 30 meters. A surface load of 107.9 kN/m^2, 125kN/m^2, 150kN/m^2 and 175kN/m^2 are used during analysis. For this purpose, modeling of wall and pile, building and the soil is made using medium mesh size. Horizontal displacement is computed at the most vulnerable location.

The supporting walls were modeled as “wished into place,” which means that the installation of the wall caused no stress changes or displacements in the surrounding soil. Excavations in silty soils with depth of 8m, 10m, 12m and 14m were considered in this study.

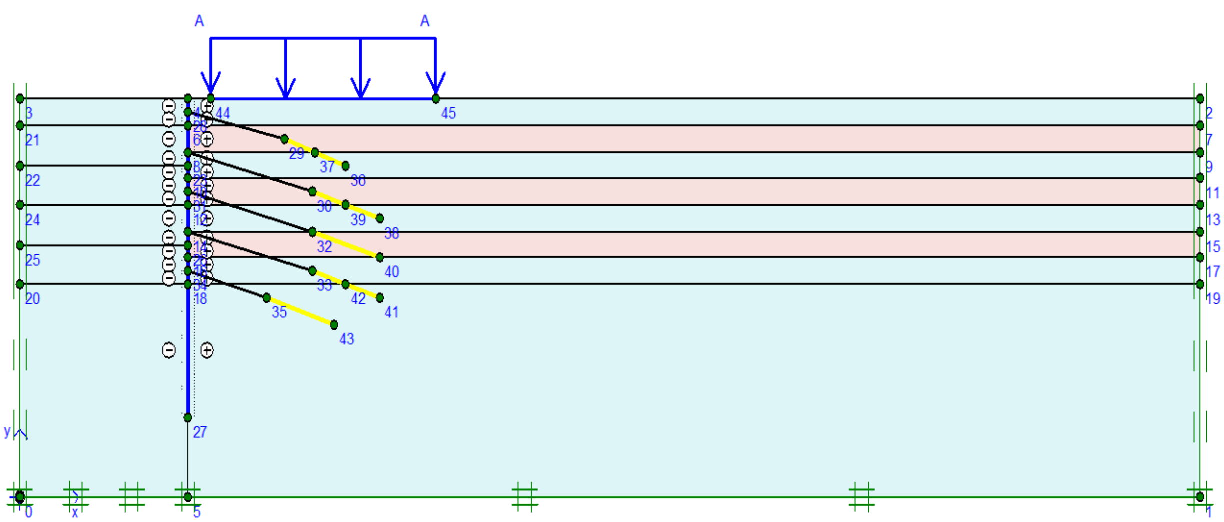

Figure 4.1: Finite element model used in PLAXIS for deep excavation.

4.3 Parametric study and discussion

In this section, the details of the effects of surcharge location, increase in surcharge and change in pile diameter in horizontal displacement of the pile $\delta hmax_p$, ground settlement behind the pile $\delta vmax_p$ and bending moment of pile $Mmax_p$ are presented and discussed for excavation depth of

8m, 10m, 12m and 14m including their construction stages. A G+20 building with dimensions of (20*15) m is assumed having dead load and live load of 60,740.12kN.

The typical construction phases are summarized below.

Table 4.1: Typical construction phases.

	8m	10m	12m	14m
	Initial phase	Initial phase	Initial phase	Initial phase
Phase 1	Pile and wall installation	Pile and wall installation	Pile and wall installation	Pile and wall installation
Phase 2	Excavation to first level RL-3.00m	Excavation to first level RL-3.00m	Excavation to first level RL-3.00m	Excavation to first level RL-2.00m
Phase 3	Installation of anchor at RL-2.00m	Installation of anchor at RL-2.00m	Installation of anchor at RL-2.00m	Installation of anchor at RL-1.00m
Phase 4	Excavation to second level RL-6.00m	Excavation to second level RL-6.00m	Excavation to second level RL-6.00m	Excavation to second level RL-5.00m
Phase 5	Installation of anchor at RL-5.00m	Installation of anchor at RL-5.00m	Installation of anchor at RL-5.00m	Installation of anchor at RL-4.00m
Phase 6	Excavation to final level RL-8.00m	Excavation to final level RL-10m	Installation of anchor at RL-5.00m	Excavation to third level RL-8.00m
Phase 7		Installation of anchor at RL-8.00m	Installation of anchor at RL-8.00m	Installation of anchor at RL-7.00m
Phase 8			Excavation to final level RL-12.00m	Excavation to fourth level RL-11.00m
Phase 9			Installation of anchor at RL-11.00m	Installation of anchor at RL-10.00m
Phase 10				Excavation to final level RL-14.00m
Phase 11				Installation of anchor at RL-13.00m

4.3.1 Effect of Change in location of surcharge.

In this section a surcharge of 107.9 kN/m^2 is placed at a distance of 1.5m, 5m, 10m and 15m and the horizontal displacement ratio, settlement ratio and bending moment ratio results behind the pile wall are presented and discussed. For analysis the soil, pile and anchor parameters listed from table 3.1 to table 3.5 are used.

4.3.1.1 Horizontal Displacement

The horizontal displacement ratio occurred in the pile for excavation depth of 8m, 10m, 12m and 14m are presented in the figure below.

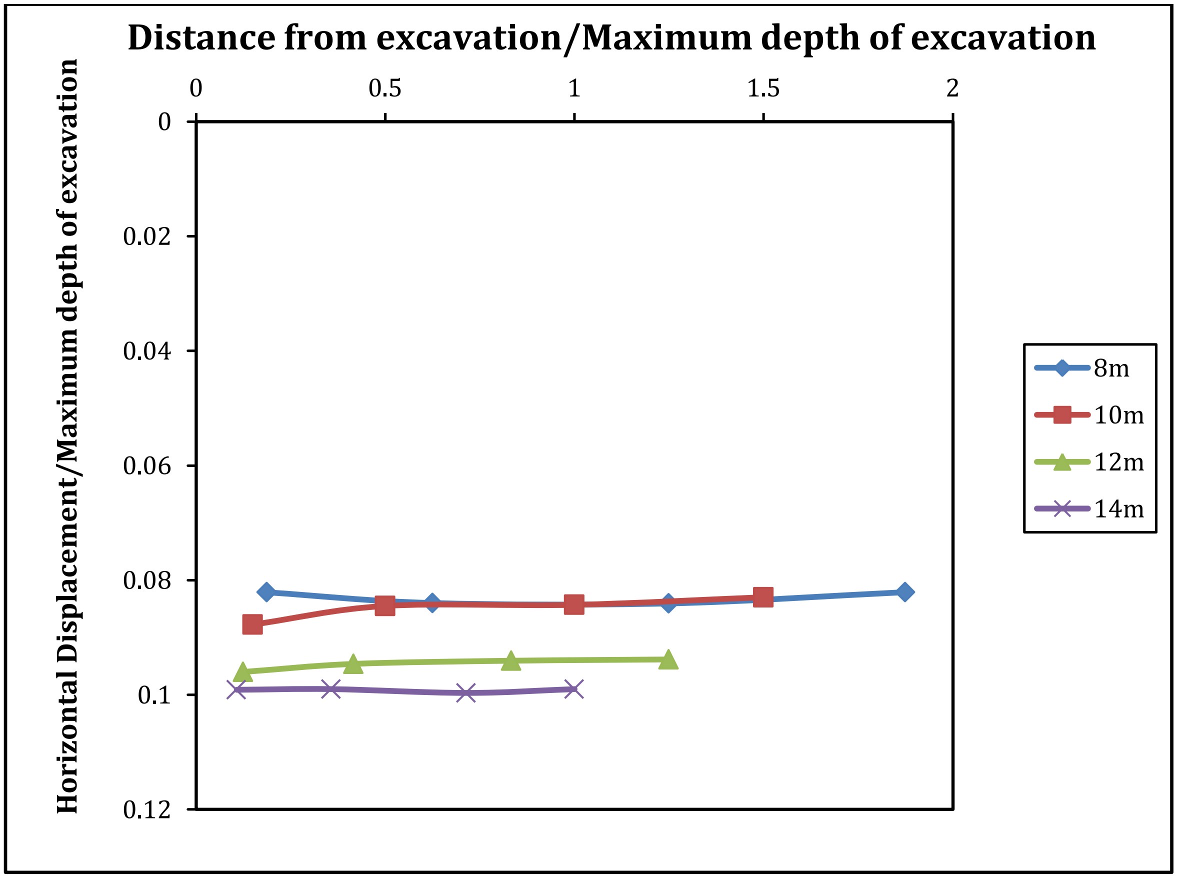

Figure 4.2a: Horizontal displacement ratio behind the pile wall.

The ratio of horizontal displacement to maximum depth of excavation increases by 0.00537% as the depth of excavation increases by 2m but remains almost constant as the ratio of distance from excavation to maximum depth of excavation increases.

4.3.1.2 Vertical Displacement.

The vertical displacement ratio occurred in the pile for excavation depth of 8m, 10m, 12m and 14m are presented in the figure below.

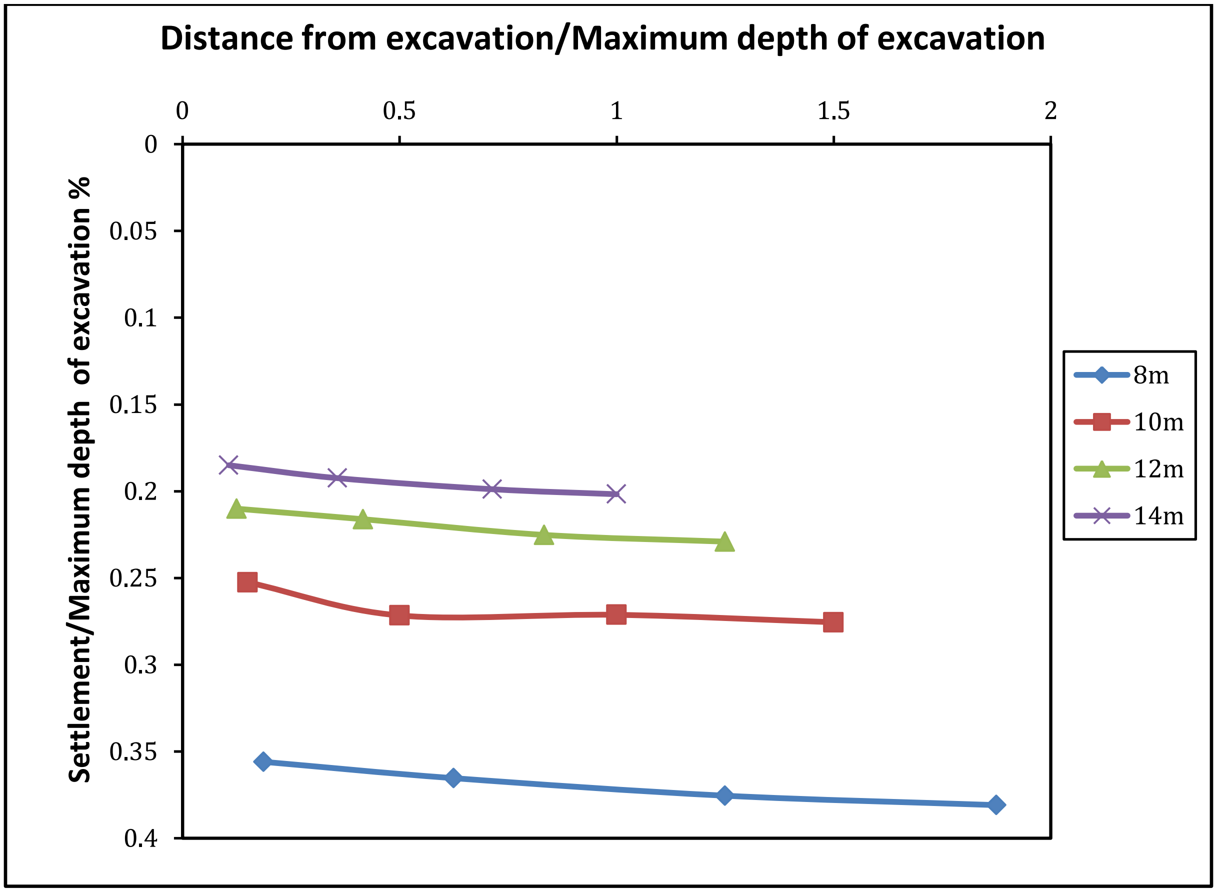

Figure 4.2b: Settlement ratio behind the pile wall

The ratio of settlement to maximum depth of excavation increases slightly as the ratio of distance from excavation to maximum depth of excavation increases for all excavation depths. The settlement ratio for excavation depth of 8m is greater than all. The ratio of settlement to maximum depth of excavation decreases by 0.0556% as the depth of excavation increases by 2m and increases by 0.0162% as the ratio of distance from excavation to maximum depth of excavation increases by 1%.

4.3.1.3 Bending moment

This section deals with the bending moments occurred in the pile for excavation depth of 8m, 10m, 12m and 14m.

From the figure below it can be concluded that the maximum bending moment to active soil moment ratio remains the same as the ratio of distance from excavation to maximum depth of excavation increases. But decreases by 0.0815% as the depth of excavation increases by 2m.

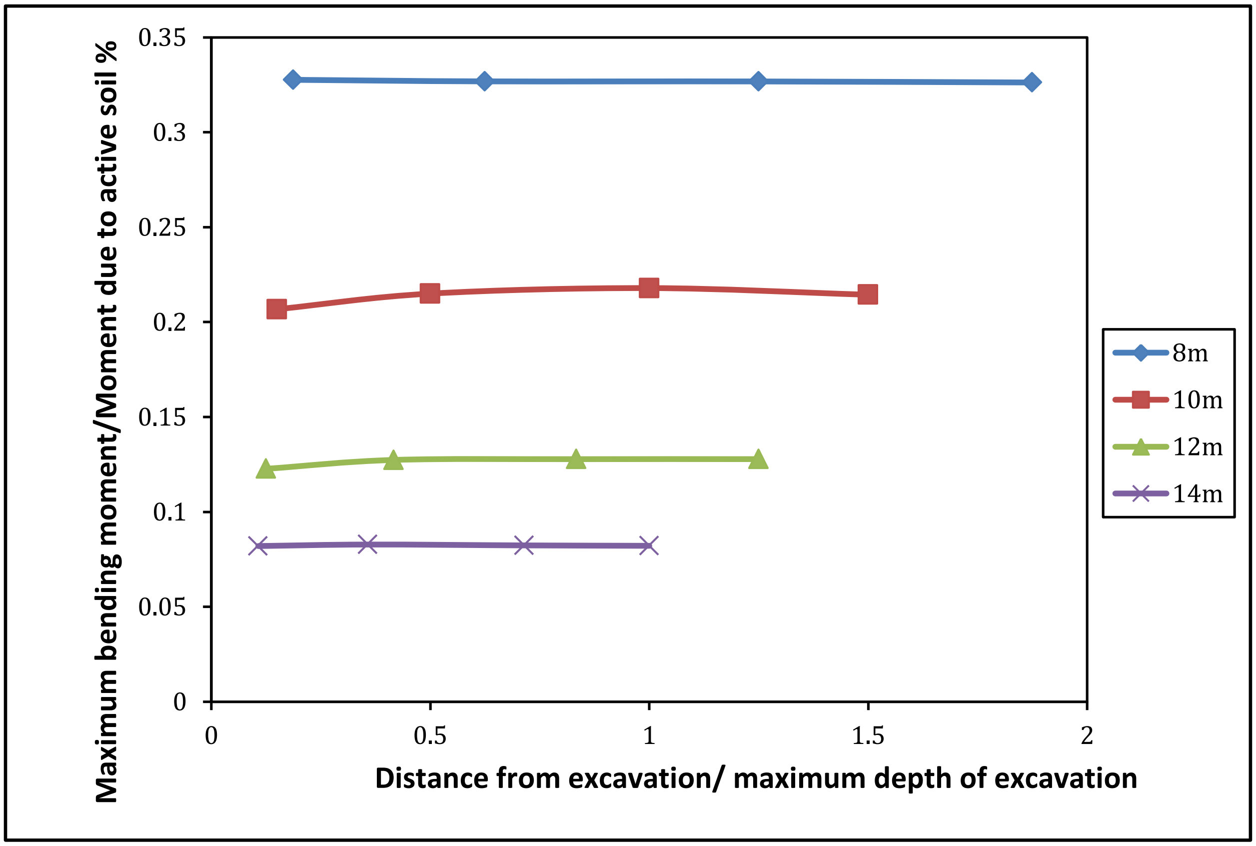

Figure 4.2c: Bending moment behind the pile wall

4.3.2 Effect of Change in magnitude of surcharge

In this section the amount of surcharge is increased from 107.9kN/m^2 to 125kN/m^2, 150kN/m^2 and 175kN/m^2 and are placed at a distance of 1.5m from edge of excavation and the horizontal displacement ratio, settlement ratio and bending moment ratio results behind the pile wall are presented and discussed. For analysis the soil, pile and anchor parameters listed from table 3.1 to table 3.5 are used.

4.3.2.1 Horizontal Displacement

The horizontal displacement ratio occurred in the pile for excavation depth of 8m, 10m, 12m and 14m are presented in the figure below.

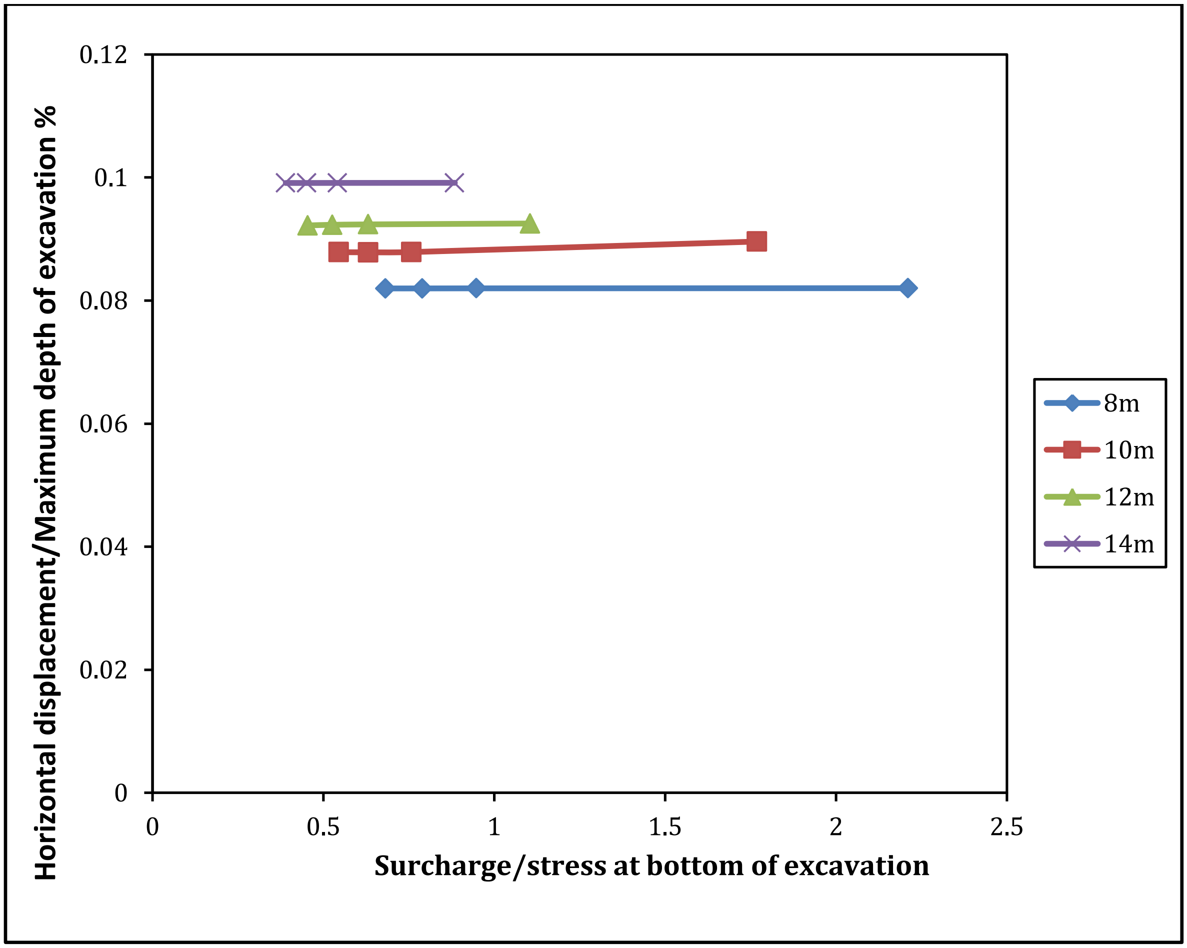

Figure 4.3a: Horizontal displacement ratio behind the pile wall

The horizontal displacement ratio behind the pile wall remains the same as the ratio of surcharge to soil stress at bottom of excavation increases. But it increases by 0.00571% as the depth of excavation increases by 2m.

4.3.2.2 Vertical Displacement

The vertical displacement ratio occurred in the pile for excavation depth of 8m, 10m, 12m and 14m are presented in the figure below.

From the figure below as the ratio of surcharge to stress due to soil increases, the ratio of settlement to maximum depth of excavation remains similar. But it decreases by 0.057% as the depth of excavation increases by 2m.

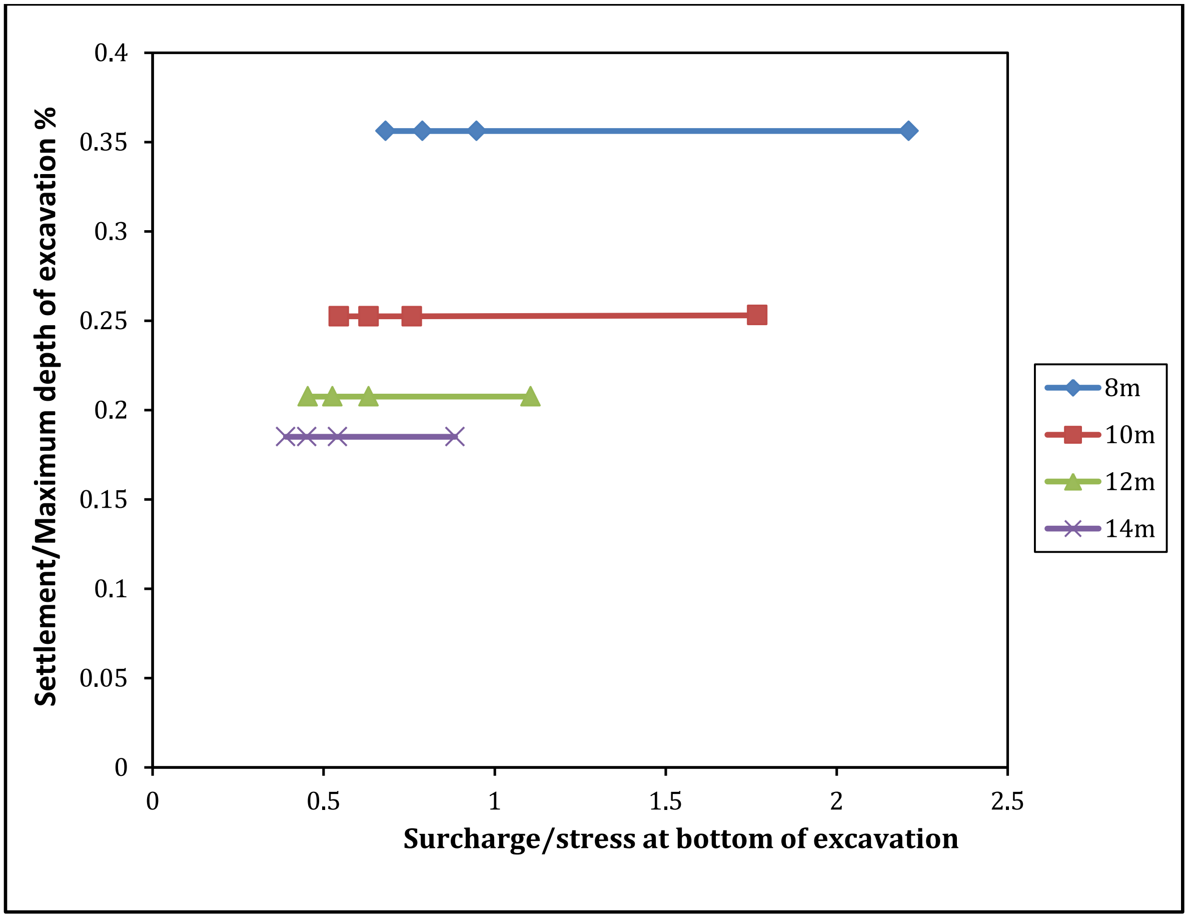

Figure 4.3b: Settlement ratio behind the pile wall

4.3.2.3 Bending moment

This section deals with the bending moments occurred in the pile for excavation depth of 8m, 10m, 12m and 14m and the results are presented in the figure below.

The maximum bending moment to moment due to active soil mass ratio behind the pile wall decreases by 0.085% as the depth of excavation increases by 2m and increases by 0.0176% as the surcharge to stress at bottom of excavation ratio increases by 1%.

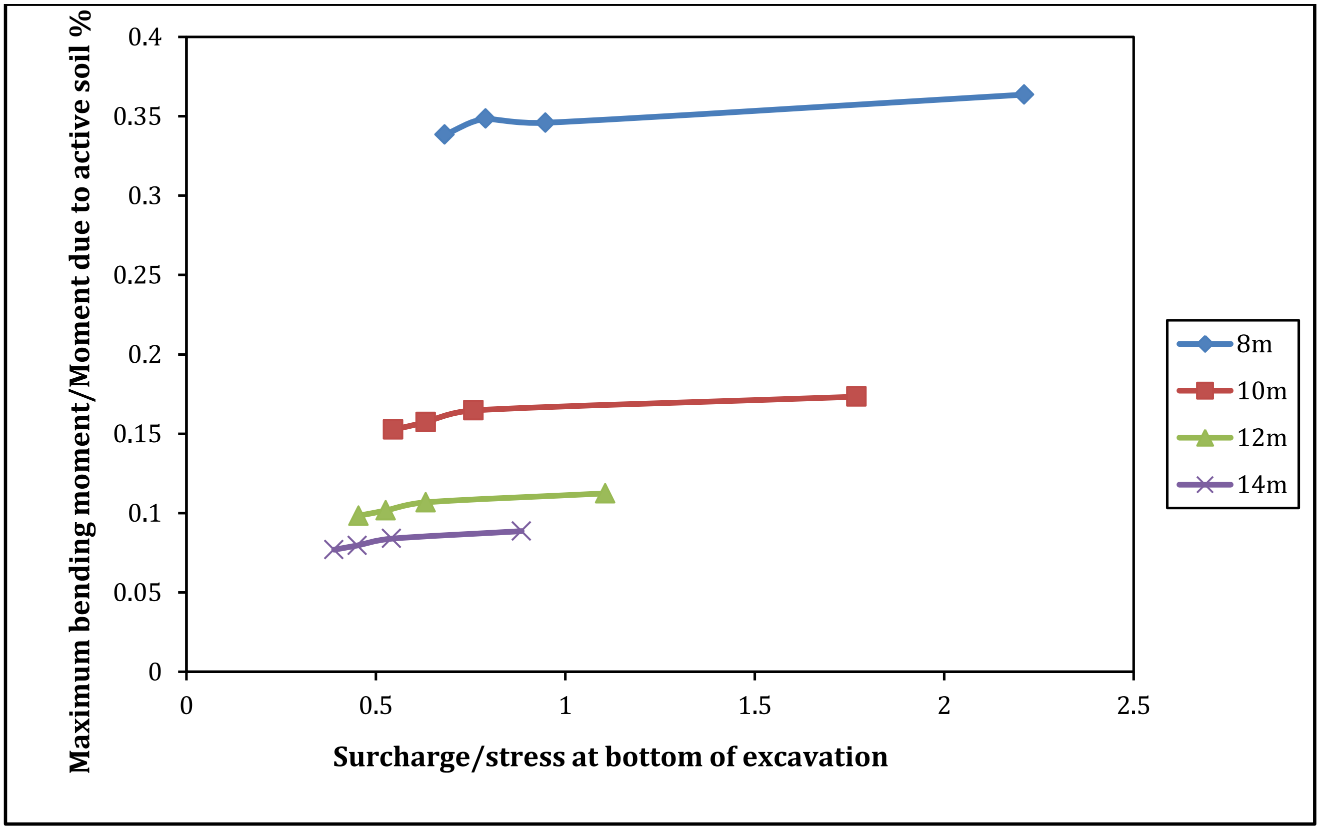

Figure 4.3c: Bending moment behind the pile wall

4.4.2 Effect of Change in pile diameter

In this section, the pile diameter is increased from 45cm to 60cm and 75cm and its effect on the horizontal displacement ratio; settlement ratio and bending moment ratio results behind the pile wall are presented and discussed. For analysis surcharge is kept constant and placed 1.5m away from edge of excavation. The soil and anchor parameters listed from table 3.1 to table 3.5 are used.

4.4.2.1. Horizontal Displacement

The horizontal displacement ratio occurred in the pile for excavation depth of 8m, 10m, 12m and 14m when the pile diameter ratio changes are presented in the figure below. The horizontal displacement to maximum depth of excavation ratio increases by 0.0138% when the depth of excavation increases by 2m but decreases by 0.00175% as the ratio of pile diameter to pile length increases by 1%.

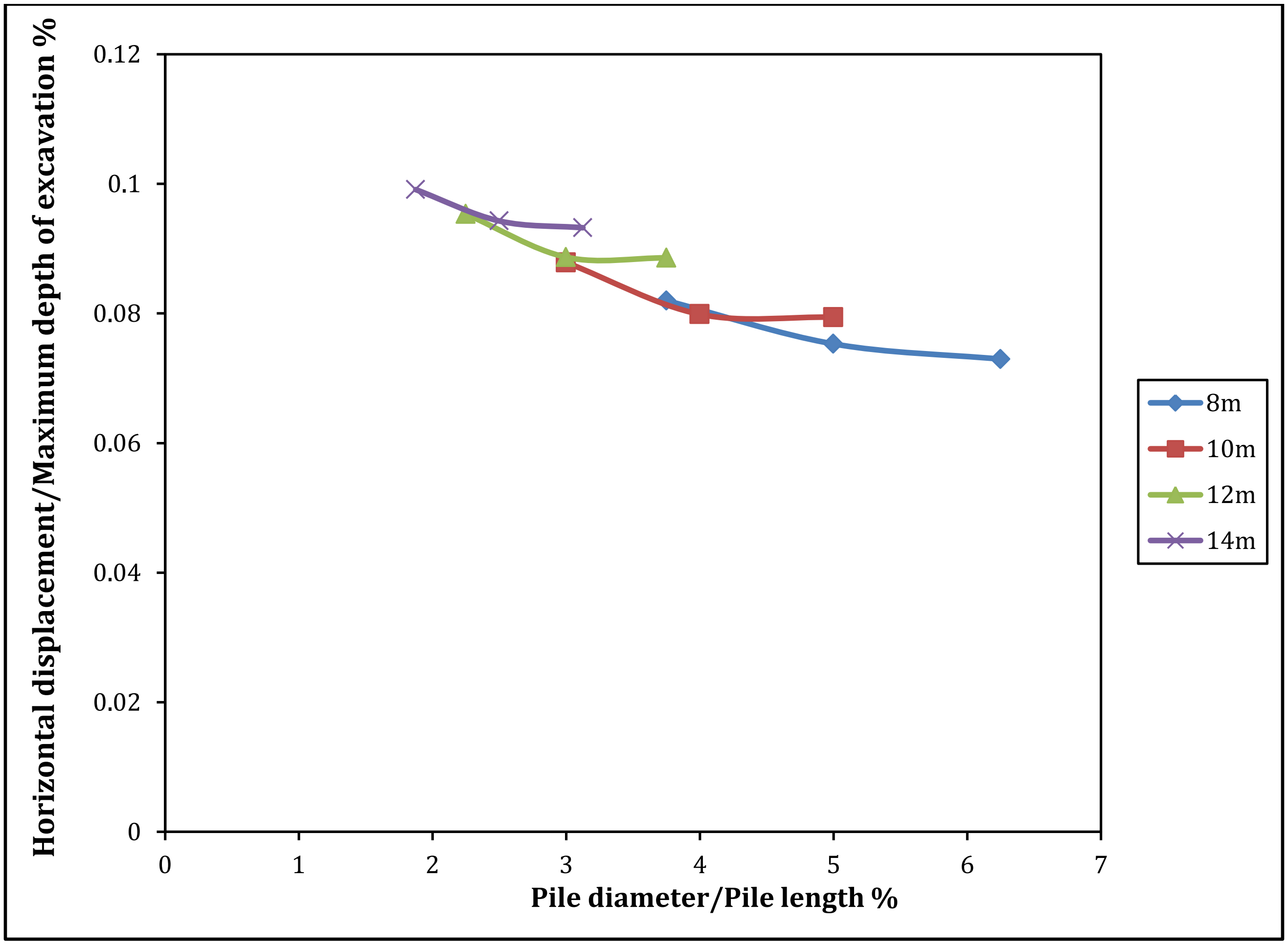

Figure 4.4a: Horizontal displacement ratio behind the pile wall

4.4.2.2. Vertical Displacement

The settlement ratio occurred in the pile for excavation depth of 8m, 10m, 12m and 14m when the pile diameter ratio changes are presented in the figure below.

The settlement to maximum depth of excavation ratio decreases by 0.0447% as the depth of excavation increases by 2m but it remains constant as the ratio of pile diameter to pile length increases.

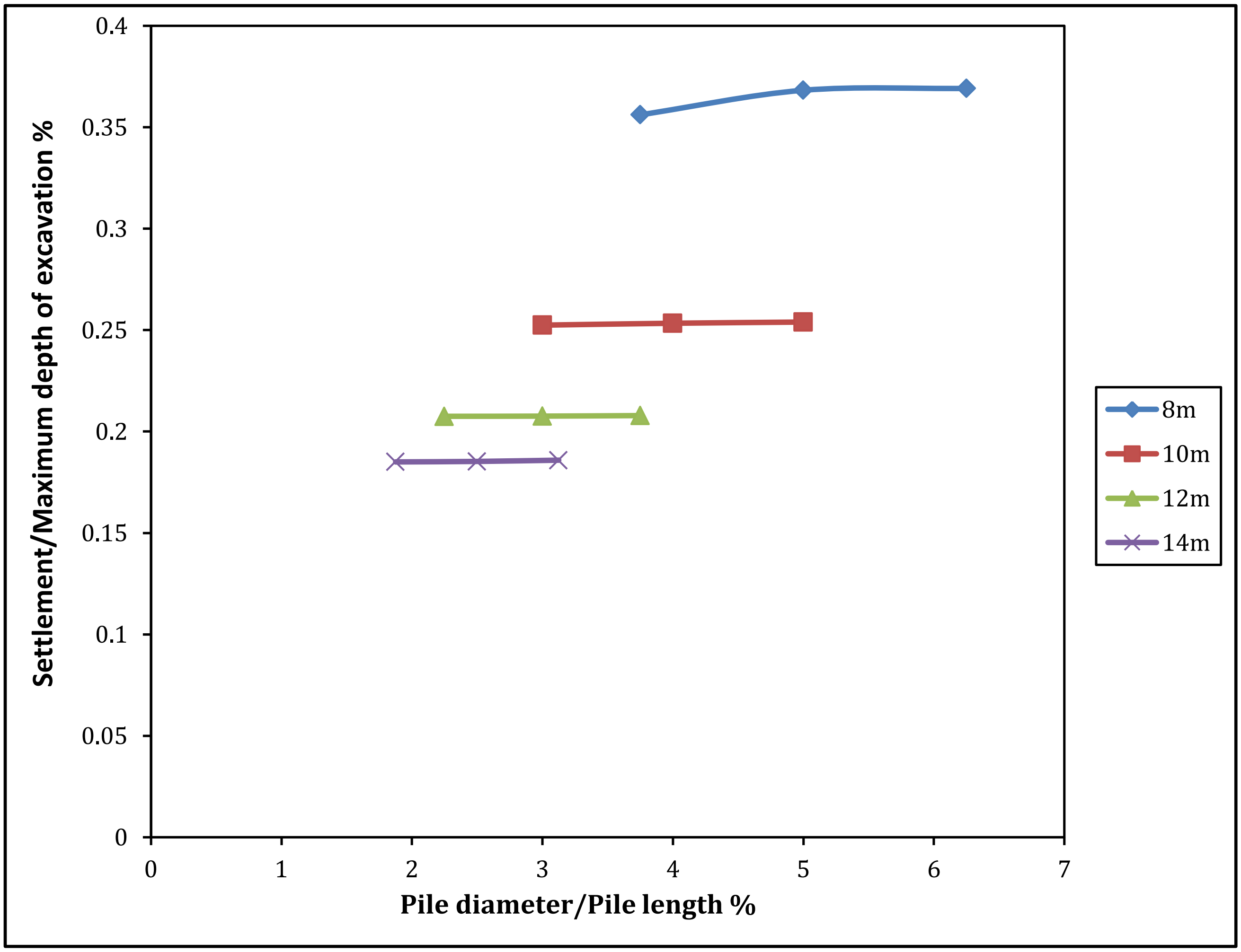

Figure 4.4b: Settlement ratio behind the pile wall

4.4.2.3 Bending moment

This section deals with the bending moments occurred in the pile for excavation depth of 8m, 10m, 12m and 14m and the results are presented in the figure below.

Decrease in the ratio of maximum bending moment to moment due to active soil mass by 0.0304% is observed when the depth of excavation increases by 2m. However, it increases by 0.09% as the ratio of pile diameter to pile length increases by 1%.

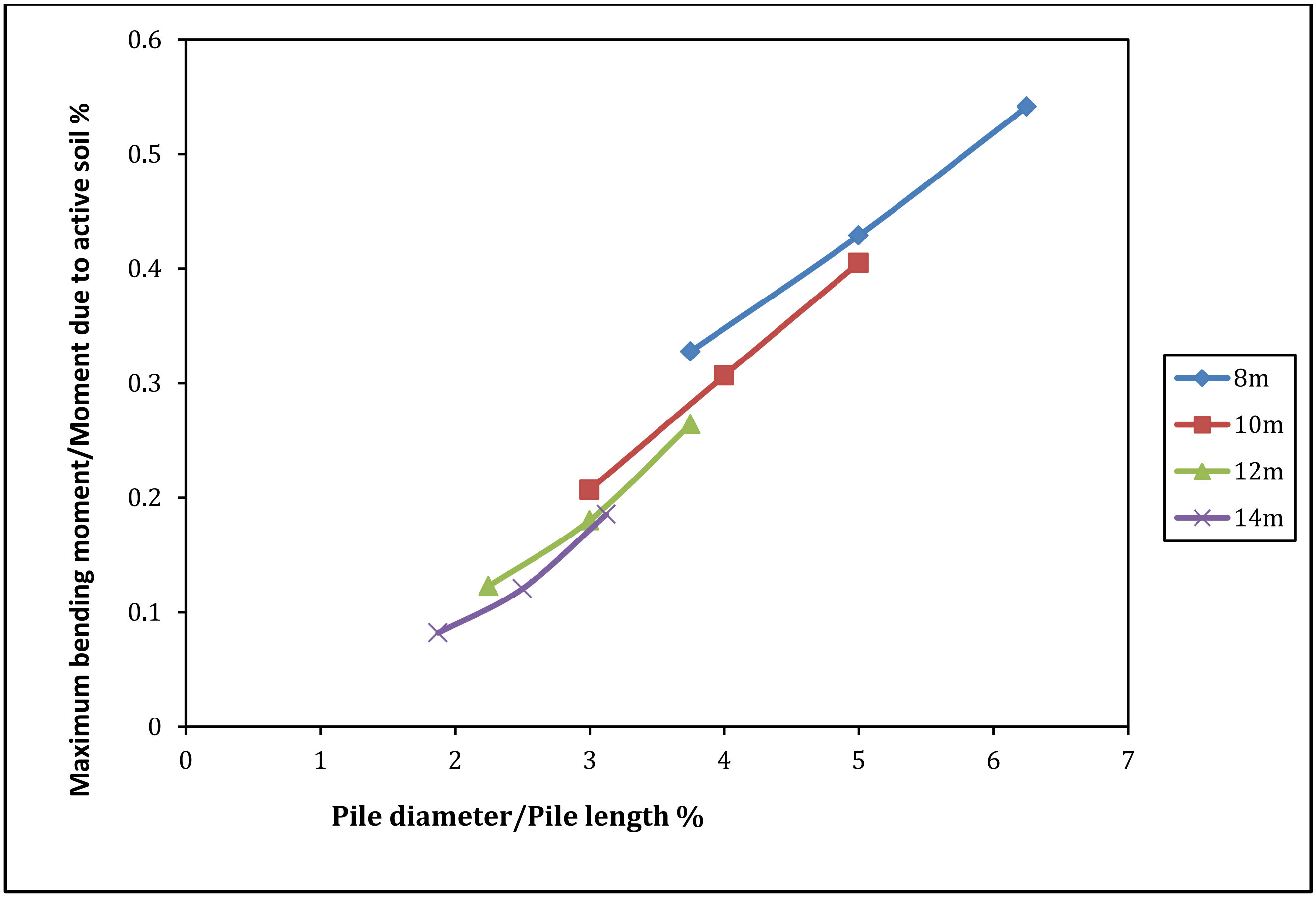

Figure 4.4c: Bending moment behind the pile wall

CHAPTER 5
CONCLUSION AND RECOMMENDATION

5.1 Conclusion

Based on the study and results found during analysis the following conclusions can be withdrawn:

1. Since the performance of deep excavation support system and lateral wall movements are influenced by several factors including wall installation, soil conditions, support system stiffness, and methods of support system installation and interaction between the soil and the support, parameters has to be identified accordingly.

2. An emphasis should be given for damages surrounding excavation area during design for deep excavation support system.

3. Apparent earth pressure diagrams proposed by Peck (1969) are used to calculate strut loads, and are not valid for the calculation of bending moments in the excavation support wall. The trapezoidal pressure diagram is used for anchor load determination for medium dense to very dense sands.

4. A proper understanding of soil-structure interaction is vital to the efficient, accurate and cost effective design of excavation support systems. Mohr coulomb model is used for analysis and simulation of the non-linear, time dependent and anisotropic behavior of soils provided as a special features for the selected area of study and soil type.

5. The performance of contiguous walls is affected by the magnitude and location of surcharge and change in pile diameter.

6. The ratio of horizontal displacement to maximum depth of excavation increases by 0.00537% as the depth of excavation increases by 2m but remains almost constant as the ratio of distance from excavation to maximum depth of excavation increases keeping surcharge constant which is 107.9kPa. In addition, the ratio of settlement to maximum depth of excavation decreases by 0.0556% and maximum bending moment

to active soil moment ratio decreases by 0.0815% as the depth of excavation increases by 2m. However, the moment ratio remains constant and settlement ratio increases by 0.0162% as the ratio of distance from excavation to maximum depth of excavation increases by1%.

7. The horizontal displacement ratio behind the pile wall increases by 0.00571% but the ratio of settlement to maximum depth of excavation and the maximum bending moment to moment due to active soil mass ratio behind the pile wall decreases by 0.057% and 0.085% respectively as the depth of excavation increases by 2m keeping location of surcharge constant which is 1.5m. Moreover, the horizontal deformation and settlement ratio remains almost constant and the moment ratio increases by 0.0176% as the surcharge to stress at bottom of excavation ratio increases by 1%.

8. An increase by 0.0138% in horizontal displacement to maximum depth of excavation ratio is observed when the depth of excavation increases by 2m but decreases by 0.00175% as the ratio of pile diameter to pile length increases by 1%. The settlement to maximum depth of excavation ratio and the ratio of maximum bending moment to moment due to active soil mass decreases by 0.0447% and 0.0304% as the depth of excavation increases by 2m. However, the settlement ratio remains constant and the moment ratio increases by 0.09% as the ratio of pile diameter to pile length increases by 1%.

5.2 Limitations in the analyses and recommendations for future work

A number of issues have been addressed in this thesis and various useful conclusions are drawn above. But there are still some limitations in the analyses and unsolved problems worth further investigation. These limitations are presented here, together with some recommendations for future research.

- The effect of change in anchor spacing, soil stiffness and wall embedment depth on horizontal and vertical displacement and bending moment behind the pile wall has not studied here. Hence, for future research one has to conduct a parametric study.

- The surface load or surcharge is assumed as uniformly distributed. Analysis has not conducted for non-uniform load. This has to be considered for further study.

- Since PLAIXS 2D ignores the corner effects of excavation on deformation and bending moment, its effective to use PLAXIS 3D for further analysis.

- The installation of the wall and pile process causes significant movements in the surrounding ground, which result in appreciable changes in the Insitu soil stress conditions. Therefore, this has to be considered during analysis.

- The assumption of the wall being "wished inplace" overestimates the horizontal stresses at the excavation level and underestimates the lateral deformations. Hence, one has to develop a model that perfectly matches the stress condition.

6. Appendices

Appendix A. Constitutive Soil Model

A.1 Mohr-Coulomb Model

The Mohr-Coulomb model coded in Plaxis version 8.0 is based on an elastic perfectly plastic mode, which is constitutive law with a fixed yield surface, i.e. a yield surface that is fully defined by model parameters and not affected by (plastic) straining. For stress state represented by points within the yield surface, the behavior is purely elastic and all strains are reversible.

In general, stress state, the model's stress-strain behaves linearly in the elastic range, with two defining parameters from Hooke's law (Young's modulus, E and Poisson's ratio, ν). There are two parameters, which define the failure criteria (the friction angle, ϕ and cohesion, c), and a parameter to describe the flow rule (dilatancy angle, ψ which comes from the use of non-associated flow rule which is used to model a realistic irreversible change in volume due to shearing).

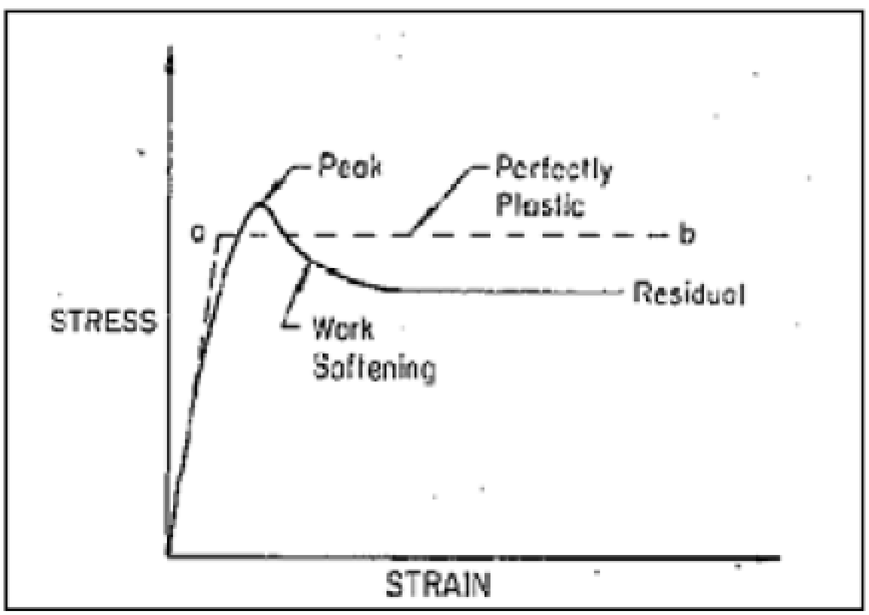

Figure A.1.1 Elastic-perfectly plastic assumption of Mohr-Coulomb model.

Mohr-Coulomb model is a simple and applicable to three-dimensional stress space model (Refer Fig A.1.2) with only two strength parameters to describe the plastic behavior. Regarding its strength behavior, this model performs better. This model is applicable to analyze the stability of dams, slopes, embankments and shallow foundations. Although failure behavior is generally well captured in drained conditions, the effective stress path that is followed in undrained materials may deviate significantly from observations. It is preferable to use undrained shear parameters in an undrained analysis, with friction angle set equal to zero. The stiffness (hence also deformation) behavior before reaching the local shear is poorly modeled. For perfect plasticity, model does not include strain hardening or softening effect of the soil.

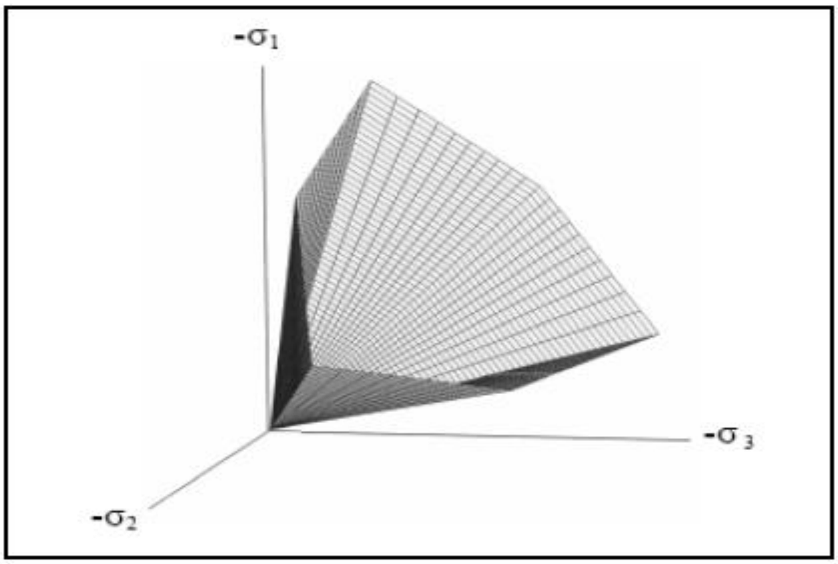

Figure A.1.2: The Mohr-Coulomb yield surface in principal stress space (c = 0)

The simplification of Mohr-Coulomb model where the hexagonal shape of the failure cone was replaced by a simple cone was known as the Drucker-Prager model (Drucker & Prager, 1952).Generally, it shares the same advantages and limitations with the Mohr-Coulomb model but the latter model was preferred over this model.

The strains and strain rates are decomposed into an elastic part and a plastic part in theory of elastoplasticity:

$$\varepsilon = \varepsilon^e + \varepsilon^p \qquad \acute{\varepsilon} = \acute{\varepsilon}^e + \acute{\varepsilon}^p \text{.. eqn A.1.1}$$

The Mohr-Coulomb model requires five parameters. Parameters related to elastic behavior are E and ν, whereas parameters related to plastic behavior are c and ϕ, and ψ, angle of dilatancy. These parameters with their standard units are listed below.

Table A.1.1 Mohr Coulomb parameters

Parameter		Unit
E	Young's Modulus	KN/m2
υ	Poisson's ratio	-
ϕ	Friction angle	Degree
C	Cohesion	KN/m2
ϕ	Dilatancy angle	Degree

PLAXIS uses the Young's modulus as the basic stiffness modulus in the MohrCoulomb model. E_{ur} which tend to increase with the confining pressure is needed for unloading modeling such as in the case of excavations. This behavior in turn results in the deep soil layers tend to have greater stiffness than shallow layers. Hence, when using a constant stiffness modulus to represent soil behavior, a value that is consistent with the stress level and the stress path development should be chosen.

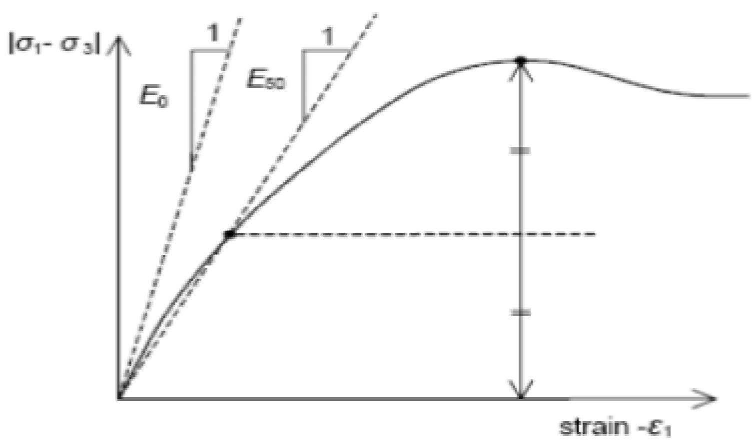

Figure A.1.3: Definition of E_0 and E_{50} for standard drained triaxial test results.

Since standard drained triaxial tests yields a significant rate of volume decrease at the very beginning of axial loading, a low initial value of Poisson's ratio is used. However, when using the Mohr Coulomb model the use of a higher value is recommended. PLAXIS recommends the value of Poisson's ratio between 0.3-0.4 for loading conditions and 0.15-0.25 for unloading condition.

Plaxis can handle Cohesionless sands(c=0), but some options will not perform well. To avoid complications its advised to use a small value of c (c > 0.2 kPa). The friction angle ϕ is entered in degrees. High friction angles, as sometimes obtained for dense sands, will substantially increase plastic computational effort. The dilatancy angle, Ψ ,is specified in degrees. Apart from heavily over consolidated layers, clay soils tend to show little dilatancy (Ψ=0). The dilatancy of sand depends on both the density on the friction angle. A small negative value for Ψ is only realistic for extremely loose sands.

Appendix B. Results from plaxis

B.1 Effect of Change in location of surcharge on pile

B.1.1 For depth of excavation of 8m

Y(from surface)	1.5m			5m			10m			15m		
	Ux	Uy	M	Ux	Uy	M	Ux	Uy	M	Ux	Uy	M
[m]	[mm]	[mm]	[kNm/m]	[mm]	[mm]	[kNm/m]	[mm]	[mm]	[kNm/m]	[mm]	[mm]	[kNm/m]
0	3.306	-0.539	0	6.115	6.622	0	6.115	6.622	0	5.521	8.358	0
0.5	3.132	-0.539	1.152	6.154	6.622	1.156	6.154	6.622	1.1111	5.671	8.358	1.0891
1	2.93	-0.539	5.5724	6.163	6.622	5.748	6.163	6.622	5.604	5.793	8.359	5.5323
1.5	2.581	-0.538	16.702	6.026	6.623	16.95	6.026	6.623	16.772	5.769	8.359	16.668
2	1.806	-0.537	38.097	5.462	6.623	38	5.462	6.623	37.997	5.321	8.359	37.934
2	1.806	-0.537	38.097	5.462	6.623	38	5.462	6.623	37.997	5.321	8.359	37.934
2.25	1.124	-0.534	18.545	4.885	6.626	18.63	4.885	6.626	19.174	4.804	8.362	19.241
2.5	0.329	-0.53	4.0826	4.192	6.628	4.4	4.192	6.628	5.4621	4.168	8.364	5.6507
2.75	-0.49	-0.527	-6.2243	3.465	6.63	-5.561	3.465	6.63	-4.051	3.499	8.366	-3.75
3	-1.27	-0.523	-13.271	2.764	6.632	-12.14	2.764	6.632	-10.27	2.853	8.368	-9.866
3	-1.27	-0.523	-13.271	2.764	6.632	-12.14	2.764	6.632	-10.27	2.853	8.368	-9.866
3.25	-1.97	-0.518	-17.422	2.125	6.635	-15.93	2.125	6.635	-13.79	2.267	8.371	-13.29
3.5	-2.57	-0.514	-19.281	1.571	6.637	-17.49	1.571	6.637	-15.15	1.763	8.373	-14.57
3.75	-3.04	-0.509	-18.973	1.109	6.639	-16.92	1.109	6.639	-14.45	1.348	8.375	-13.79
4	-3.4	-0.503	-16.587	0.736	6.641	-14.3	0.736	6.641	-11.75	1.017	8.377	-11.03
4	-3.4	-0.503	-16.587	0.736	6.641	-14.3	0.736	6.641	-11.75	1.017	8.377	-11.03
4.25	-3.66	-0.497	-11.615	0.434	6.644	-9.254	0.434	6.644	-6.67	0.754	8.38	-5.898
4.5	-3.84	-0.491	-3.4157	0.174	6.646	-1.246	0.174	6.646	1.3274	0.527	8.382	2.1423
4.75	-4.01	-0.485	8.6552	-0.09	6.649	10.45	0.094	6.649	12.963	0.287	8.385	13.808
5	-4.23	-0.477	25.24	-0.44	6.652	26.54	-0.441	6.652	28.959	-0.04	8.387	29.819

5	-4.23	-0.477	25.24	-0.44	6.652	26.54	-0.441	6.652	28.959	-0.04	8.387	29.819
5.25	-4.58	-0.468	8.9356	-0.95	6.657	10.17	-0.949	6.657	12.714	-0.53	8.392	13.665
5.5	-4.99	-0.457	-3.0851	-1.53	6.662	-1.844	-1.533	6.662	0.7773	-1.1	8.397	1.8007
5.75	-5.38	-0.447	-11.588	-2.12	6.667	-10.31	-2.123	6.667	-7.653	-1.68	8.402	-6.575
6	-5.7	-0.435	-17.34	-2.67	6.672	-16.03	-2.665	6.672	-13.38	-2.23	8.407	-12.26
6	-5.7	-0.435	-17.34	-2.67	6.672	-16.03	-2.665	6.672	-13.38	-2.23	8.407	-12.26
6.5	-6.01	-0.411	-22.419	-3.48	6.683	-21.13	-3.485	6.683	-18.66	-3.07	8.417	-17.56
7	-5.77	-0.386	-20.429	-3.85	6.695	-19.67	-3.854	6.695	-18.02	-3.49	8.428	-17.19
7.5	-5.05	-0.357	-7.0937	-3.79	6.708	-8.292	-3.795	6.708	-8.84	-3.5	8.44	-8.82
8	-4.18	-0.327	22.56	-3.54	6.723	17.04	-3.539	6.723	12.085	-3.31	8.453	10.456
8	-4.18	-0.327	22.56	-3.54	6.723	17.04	-3.539	6.723	12.085	-3.31	8.453	10.456
8.5	-3.77	-0.299	22.647	-3.52	6.735	17.76	-3.515	6.735	13.196	-3.32	8.464	11.687
9	-3.89	-0.275	11.187	-3.8	6.744	8.565	-3.799	6.744	6.1546	-3.6	8.472	5.4144
9.5	-4.28	-0.255	0.0003	-4.23	6.75	-0.45	-4.232	6.75	-0.821	-4.01	8.477	-0.836
10	-4.7	-0.238	-2.4757	-4.66	6.754	-2.008	-4.664	6.754	-1.824	-4.42	8.48	-1.668
10	-4.7	-0.238	-2.4757	-4.66	6.754	-2.008	-4.664	6.754	-1.824	-4.42	8.48	-1.668
10.25	-4.89	-0.231	-2.6503	-4.86	6.756	-2.022	-4.862	6.756	-1.749	-4.61	8.481	-1.577
10.5	-5.06	-0.225	-1.9137	-5.05	6.757	-1.628	-5.049	6.757	-1.373	-4.79	8.481	-1.219
10.75	-5.22	-0.22	-0.8335	-5.23	6.758	-0.932	-5.228	6.758	-0.776	-4.96	8.482	-0.676
11	-5.37	-0.215	0	-5.4	6.758	0	-5.402	6.758	0	-5.12	8.482	0

B.1.2 For depth of excavation of 10m

Y(from surface)	1.5m			5m			10m			15m		
	Ux	Uy	M	Ux	Uy	M	Ux	Uy	M	Ux	Uy	M
[m]	[mm]	[mm]	[kNm/m]	[mm]	[mm]	[kNm/m]	[mm]	[mm]	[kNm/m]	[mm]	[mm]	[kNm/m]
0	0.2	-0.647	0	1.86	4.959	0	1.619	4.774	0	1.207	6.306	0
0.5	-0.054	-0.647	0.35	2.02	4.959	0.3956	1.803	4.774	0.426	1.491	6.306	0.392
1	-0.313	-0.647	2.419	2.18	4.959	3.0251	1.979	4.775	3.192	1.766	6.306	2.998
1.5	-0.643	-0.646	12.37	2.25	4.959	13.612	2.065	4.775	13.97	1.957	6.306	13.55
2	-1.301	-0.644	36.49	1.96	4.96	37.943	1.784	4.776	38.46	1.792	6.307	37.84
2	-1.301	-0.644	36.49	1.96	4.96	37.943	1.784	4.776	38.46	1.792	6.307	37.84
2.25	-1.903	-0.642	18.31	1.53	4.962	20.317	1.354	4.778	20.77	1.424	6.309	20.33
2.5	-2.616	-0.638	4.702	0.98	4.964	7.2661	0.796	4.78	7.595	0.932	6.311	7.406
2.75	-3.357	-0.635	-5.09	0.38	4.966	-1.97	0.192	4.781	-1.8	0.396	6.313	-1.71
3	-4.067	-0.631	-11.8	-0.2	4.968	-8.15	-0.4	4.783	-8.14	-0.131	6.314	-7.78
3	-4.067	-0.631	-11.8	-0.2	4.968	-8.15	-0.4	4.783	-8.14	-0.131	6.314	-7.78
3.25	-4.705	-0.627	-15.9	-0.74	4.969	-11.81	-0.94	4.785	-11.9	-0.609	6.316	-11.34
3.5	-5.246	-0.622	-17.9	-1.2	4.971	-13.41	-1.41	4.787	-13.6	-1.018	6.318	-12.86
3.75	-5.677	-0.617	-17.8	-1.58	4.973	-13.01	-1.8	4.789	-13.2	-1.348	6.32	-12.4
4	-5.999	-0.612	-15.7	-1.88	4.975	-10.64	-2.1	4.791	-10.8	-1.603	6.321	-9.979
4	-5.999	-0.612	-15.7	-1.88	4.975	-10.64	-2.1	4.791	-10.8	-1.603	6.321	-9.979
4.25	-6.225	-0.606	-10.7	-2.12	4.977	-5.897	-2.35	4.793	-5.89	-1.796	6.323	-5.202
4.5	-6.385	-0.6	-2.45	-2.32	4.979	1.7751	-2.55	4.795	1.871	-1.958	6.325	2.48
4.75	-6.53	-0.593	9.85	-2.53	4.981	13.106	-2.76	4.797	13.25	-2.134	6.327	13.8
5	-6.735	-0.586	26.85	-2.82	4.983	28.836	-3.06	4.8	28.99	-2.394	6.329	29.48
5	-6.735	-0.586	26.85	-2.82	4.983	28.836	-3.06	4.8	28.99	-2.394	6.329	29.48
5.25	-7.087	-0.576	11.02	-3.27	4.987	12.567	-3.52	4.804	12.73	-2.818	6.333	13.26

5.5	-7.507	-0.566	-0.5	-3.79	4.992	0.6792	-4.05	4.809	0.765	-3.322	6.337	1.388
5.75	-7.923	-0.555	-8.46	-4.32	4.996	-7.608	-4.59	4.813	-7.65	-3.835	6.341	-6.908
6	-8.286	-0.544	-13.6	-4.81	5.001	-13.07	-5.08	4.818	-13.2	-4.306	6.346	-12.4
6	-8.286	-0.544	-13.6	-4.81	5.001	-13.07	-5.08	4.818	-13.2	-4.306	6.346	-12.4
6.5	-8.748	-0.52	-18	-5.52	5.01	-17.34	-5.8	4.828	-17.6	-5.001	6.354	-16.76
7	-8.774	-0.494	-16.5	-5.81	5.021	-14.59	-6.1	4.839	-14.8	-5.294	6.364	-14.12
7.5	-8.409	-0.466	-5.45	-5.76	5.032	-2.056	-6.05	4.85	-2.09	-5.256	6.374	-1.531
8	-7.935	-0.435	19.74	-5.68	5.044	23.717	-5.97	4.863	24.01	-5.202	6.384	24.6
8	-7.935	-0.435	19.74	-5.68	5.044	23.717	-5.97	4.863	24.01	-5.202	6.384	24.6
8.5	-7.722	-0.4	-4.62	-5.96	5.061	-1.565	-6.26	4.88	-1.63	-5.527	6.4	-0.709
9	-7.42	-0.361	-11.1	-6.22	5.08	-10.36	-6.53	4.898	-10.7	-5.857	6.416	-9.717
9.5	-6.872	-0.32	-2.35	-6.26	5.1	-5.478	-6.56	4.918	-6.4	-5.971	6.433	-5.496
10	-6.282	-0.276	20.88	-6.17	5.121	11.884	-6.44	4.939	9.579	-5.962	6.452	10.39
10	-6.282	-0.276	20.88	-6.17	5.121	11.884	-6.44	4.939	9.579	-5.962	6.452	10.39
10.5	-6.123	-0.235	18.42	-6.31	5.14	10.51	-6.51	4.958	10.32	-6.15	6.467	9.004
11	-6.399	-0.199	7.578	-6.7	5.153	3.5962	-6.82	4.972	4.531	-6.551	6.478	2.84
11.5	-6.861	-0.169	-1.9	-7.17	5.163	-2.45	-7.24	4.983	-1.61	-7.02	6.485	-2.482
12	-7.299	-0.144	-4.04	-7.6	5.169	-3.826	-7.63	4.991	-3.78	-7.443	6.488	-3.688
12	-7.299	-0.144	-4.04	-7.6	5.169	-3.826	-7.63	4.991	-3.78	-7.443	6.488	-3.688
12.5	-7.635	-0.122	-5.17	-7.94	5.173	-4.627	-7.93	4.997	-4.08	-7.773	6.49	-4.42
13	-7.851	-0.104	-3.83	-8.16	5.176	-3.407	-8.14	5.001	-2.27	-7.999	6.489	-3.278
13.5	-7.974	-0.09	-1.59	-8.31	5.177	-1.454	-8.29	5.004	-0.27	-8.145	6.488	-1.433
14	-8.056	-0.078	0	-8.41	5.177	0	-8.43	5.006	0	-8.255	6.487	0

B.1.3 For depth of excavation of 12m

Y(from surface)	1.5m			5m			10m			15m		
	Ux	Uy	M	Ux	Uy	M	Ux	Uy	M	Ux	Uy	M
[m]	mm	mm	[kNm/m]	mm	mm	[kNm/m]	mm	mm	[kNm/m]	mm	mm	[kNm/m]
0	-1.932	-0.729	0	-0.05	1.006	0	-0.53	2.888	0	-1.397	3.819	0
0.5	-2.204	-0.729	0.308	-0.1	1.006	0.4546	-0.28	2.888	0.46	-1.003	3.819	0.447
1	-2.48	-0.728	2.401	-0.15	1.007	3.1696	-0.03	2.888	3.21	-0.618	3.819	3.198
1.5	-2.827	-0.727	12.34	-0.29	1.007	13.702	0.121	2.889	13.79	-0.322	3.82	13.78
2	-3.5	-0.726	36.27	-0.79	1.008	37.653	-0.09	2.889	37.78	-0.387	3.82	37.78
2	-3.5	-0.726	36.27	-0.79	1.008	37.653	-0.09	2.889	37.78	-0.387	3.82	37.78
2.25	-4.108	-0.722	18.55	-1.32	1.011	19.885	-0.48	2.891	20.49	-0.706	3.822	20.59
2.5	-4.829	-0.718	5.363	-1.98	1.013	6.5292	-0.99	2.894	7.627	-1.15	3.824	7.842
2.75	-5.583	-0.714	-4.12	-2.68	1.016	-3.08	-1.55	2.896	-1.53	-1.642	3.827	-1.206
3	-6.311	-0.71	-10.7	-3.35	1.019	-9.611	-2.1	2.898	-7.7	-2.126	3.829	-7.28
3	-6.311	-0.71	-10.7	-3.35	1.019	-9.611	-2.1	2.898	-7.7	-2.126	3.829	-7.28
3.25	-6.974	-0.705	-14.7	-3.97	1.021	-13.54	-2.61	2.9	-11.4	-2.565	3.831	-10.85
3.5	-7.546	-0.699	-16.7	-4.5	1.024	-15.33	-3.04	2.903	-13	-2.938	3.833	-12.39
3.75	-8.016	-0.694	-16.5	-4.94	1.027	-15.04	-3.4	2.905	-12.6	-3.235	3.835	-11.93
4	-8.386	-0.688	-14.1	-5.29	1.03	-12.68	-3.67	2.907	-10.2	-3.46	3.837	-9.505
4	-8.386	-0.688	-14.1	-5.29	1.03	-12.68	-3.67	2.907	-10.2	-3.46	3.837	-9.505
4.25	-8.669	-0.681	-8.66	-5.56	1.033	-7.886	-3.89	2.909	-5.43	-3.626	3.839	-4.709
4.5	-8.899	-0.674	0.297	-5.79	1.037	-0.089	-4.07	2.911	2.266	-3.762	3.841	3.006
4.75	-9.13	-0.667	13.49	-6.01	1.04	11.432	-4.27	2.913	13.63	-3.917	3.843	14.36
5	-9.443	-0.659	31.63	-6.3	1.044	27.407	-4.54	2.916	29.38	-4.16	3.845	30.08
5	-9.443	-0.659	31.63	-6.3	1.044	27.407	-4.54	2.916	29.38	-4.16	3.845	30.08
5.25	-9.933	-0.648	16.13	-6.74	1.05	10.992	-4.99	2.92	12.95	-4.57	3.849	13.7
5.5	-	-	5.124	-	1.056	-0.992	-5.51	2.925	0.892	-	3.853	1.656

	10.52	0.637		7.25						5.063		
5.75	-11.14	-0.626	-2.23	-7.76	1.063	-9.326	-6.03	2.929	-7.57	-5.566	3.857	-6.807
6	-11.74	-0.614	-6.8	-8.2	1.069	-14.79	-6.51	2.934	-13.2	-6.027	3.861	-12.45
6	-11.74	-0.614	-6.8	-8.2	1.069	-14.79	-6.51	2.934	-13.2	-6.027	3.861	-12.45
6.5	-12.81	-0.589	-10.8	-8.8	1.084	-18.79	-7.21	2.943	-17.6	-6.703	3.869	-16.92
7	-13.62	-0.562	-12	-8.96	1.099	-15.22	-7.49	2.953	-14.6	-6.973	3.878	-14.2
7.5	-14.14	-0.533	-11.5	-8.75	1.115	-0.655	-7.42	2.963	-0.72	-6.911	3.886	-0.6
8	-14.38	-0.503	-10.2	-8.56	1.133	28.855	-7.36	2.974	28.35	-6.859	3.895	28.21
8	-14.38	-0.503	-10.2	-8.56	1.133	28.855	-7.36	2.974	28.35	-6.859	3.895	28.21
8.25	-14.4	-0.488	-11.6	-8.65	1.145	14.22	-7.53	2.982	13.68	-7.023	3.902	13.59
8.5	-14.35	-0.471	-13	-8.84	1.158	3.8566	-7.77	2.99	3.155	-7.269	3.909	3.136
8.75	-14.23	-0.454	-14.2	-9.04	1.17	-3.347	-8.03	2.998	-4.13	-7.535	3.916	-4.043
9	-14.01	-0.437	-15.1	-9.23	1.183	-8.459	-8.27	3.007	-9.04	-7.775	3.924	-8.839
9	-14.01	-0.437	-15.1	-9.23	1.183	-8.459	-8.27	3.007	-9.04	-7.775	3.924	-8.839
9.25	-13.71	-0.419	-15.7	-9.36	1.197	-11.91	-8.46	3.016	-12.1	-7.962	3.931	-11.8
9.5	-13.3	-0.4	-15.8	-9.42	1.211	-14.26	-8.57	3.025	-13.9	-8.076	3.939	-13.46
9.75	-12.8	-0.38	-15	-9.4	1.226	-15.35	-8.59	3.034	-14.4	-8.108	3.946	-13.85
10	-12.21	-0.36	-12.9	-9.28	1.241	-14.97	-8.53	3.044	-13.6	-8.056	3.954	-12.98
10	-1.932	-0.36	-12.9	-9.28	1.241	-14.97	-8.53	3.044	-13.6	-8.056	3.954	-12.98
10.25	-1.932	-0.36	-8.74	-9.07	1.256	-12.22	-8.38	3.054	-10.8	-7.924	3.962	-10.09
10.5	-1.932	-0.36	-1.34	-8.78	1.272	-6.22	-8.17	3.065	-4.99	-7.73	3.971	-4.228
10.75	-1.932	-0.36	10.49	-8.46	1.289	4.2137	-7.92	3.075	5.122	-7.51	3.98	5.91
11	-1.932	-0.36	27.91	-8.16	1.307	20.275	-7.71	3.087	20.9	-7.325	3.989	21.66
11	-1.932	-0.36	27.91	-8.16	1.307	20.275	-7.71	3.087	20.9	-7.325	3.989	21.66
11.25	-1.932	-0.36	15.16	-7.97	1.327	7.1383	-7.61	3.101	7.452	-7.257	4.001	8.083
11.5	-1.932	-0.36	8.883	-7.82	1.348	1.1632	-7.55	3.115	0.968	-7.237	4.012	1.312

11.75	-1.932	-0.36	9.975	-7.68	1.369	2.6152	-7.5	3.13	1.518	-7.226	4.025	1.327
12	-1.932	-0.36	19.39	-7.55	1.391	11.802	-7.45	3.145	9.215	-7.221	4.037	8.147
12	-1.932	-0.36	19.39	-7.55	1.391	11.802	-7.45	3.145	9.215	-7.221	4.037	8.147
12.5	-1.932	-0.36	14.27	-7.51	1.431	9.1726	-7.53	3.172	6.628	-7.356	4.059	5.395
13	-1.932	-0.36	3.706	-7.69	1.466	1.4129	-7.77	3.193	0.003	-7.616	4.075	-0.648
13.5	-1.932	-0.36	-4.55	-7.9	1.497	-4.938	-8	3.21	-5.16	-7.862	4.086	-5.181
14	-1.932	-0.36	-5.32	-8	1.523	-5.397	-8.12	3.223	-5.2	-7.994	4.093	-5.053
14	-1.932	-0.36	-5.32	-8	1.523	-5.397	-8.12	3.223	-5.2	-7.994	4.093	-5.053
15	-1.932	-0.36	-4.48	-7.81	1.566	-4.49	-7.98	3.24	-4.31	-7.884	4.1	-4.13
16	-1.932	-0.36	-1.21	-7.21	1.601	-1.612	-7.44	3.251	-1.92	-7.384	4.1	-2.021
17	-1.932	-0.36	1.38	-6.44	1.63	0.7576	-6.7	3.257	0.136	-6.685	4.096	-0.172
18	-1.932	-0.36	0	-5.71	1.652	0	-5.96	3.26	0	-5.951	4.091	0

B.1.4 For depth of excavation of 14m

Y(from surface)	1.5m			5m			10m			15m		
	Ux	Uy	M	Ux	Uy	M	Ux	Uy	M	Ux	Uy	M
[m]	[mm]	[mm]	[kNm/m]	[mm]	[mm]	[kNm/m]	[mm]	[mm]	[kNm/m]	[mm]	[mm]	[kNm/m]
0	1.88	0.105	0	2.91	2.289	0	2.556	4.287	0	2.004	5.471	0
0.25	1.334	0.105	2.157	2.51	2.288	2.2015	2.335	4.287	2.171	1.857	5.471	2.173
0.5	0.774	0.105	8.2	2.1	2.288	8.2767	2.101	4.287	8.239	1.697	5.471	8.23
0.75	0.165	0.105	18.44	1.64	2.288	18.588	1.817	4.287	18.52	1.487	5.471	18.48
1	-0.556	0.105	33.2	1.07	2.288	33.521	1.42	4.286	33.33	1.164	5.47	33.25
1	-0.556	0.105	33.2	1.07	2.288	33.521	1.42	4.286	33.33	1.164	5.47	33.25
1.25	-1.464	0.106	15.76	0.3	2.289	16.889	0.836	4.287	16.68	0.655	5.471	16.63
1.5	-2.468	0.108	2.608	-0.56	2.291	4.3783	0.15	4.289	4.44	0.044	5.472	4.454
1.75	-3.488	0.11	-6.91	-1.45	2.292	-4.637	-0.56	4.29	-4.14	-0.594	5.474	-4.05
2	-4.465	0.112	-13.5	-2.32	2.293	-10.78	-1.25	4.291	-9.8	-1.207	5.474	-9.633
2	-4.465	0.112	-13.5	-2.32	2.293	-10.78	-1.25	4.291	-9.8	-1.207	5.474	-9.633
2.5	-6.149	0.117	-19.2	-3.83	2.296	-15.86	-2.43	4.292	-14.1	-2.239	5.476	-13.71
3	-7.372	0.123	-16.8	-4.96	2.298	-13.18	-3.27	4.294	-10.9	-2.944	5.478	-10.41
3.5	-8.2	0.13	-2.97	-5.78	2.301	0.2515	-3.86	4.295	2.672	-3.409	5.479	3.236
4	-8.979	0.139	26.32	-6.64	2.305	28.021	-4.54	4.297	30.21	-3.975	5.48	30.78
4	-8.979	0.139	26.32	-6.64	2.305	28.021	-4.54	4.297	30.21	-3.975	5.48	30.78
4.25	-9.54	0.146	10.26	-7.25	2.309	11.383	-5.09	4.3	13.69	-4.474	5.483	14.36
4.5	-10.16	0.154	-1.55	-7.94	2.313	-0.778	-5.72	4.303	1.573	-5.061	5.485	2.31
4.75	-10.78	0.162	-9.82	-8.62	2.318	-9.239	-6.36	4.306	-6.91	-5.661	5.488	-6.124
5	-11.33	0.17	-15.3	-9.24	2.322	-14.77	-6.96	4.308	-12.5	-6.224	5.491	-11.71
5	-11.33	0.17	-15.3	-9.24	2.322	-14.77	-6.96	4.308	-12.5	-6.224	5.491	-11.71
5.25	-11.79	0.179	-18.4	-9.77	2.327	-17.83	-7.48	4.311	-15.7	-6.715	5.493	-14.91
5.5	-12.14	0.189	-19.8	-10.2	2.333	-18.9	-7.91	4.314	-17	-7.115	5.496	-16.19
5.75	-12.36	0.198	-19.2	-10.5	2.338	-18	-8.23	4.318	-16.3	-7.416	5.499	-15.56

6	-12.47	0.209	-16.5	-10.7	2.344	-15.1	-8.46	4.321	-13.7	-7.621	5.501	-13.01
6	-12.47	0.209	-16.5	-10.7	2.344	-15.1	-8.46	4.321	-13.7	-7.621	5.501	-13.01
6.25	-12.48	0.22	-10.9	-10.8	2.35	-9.794	-8.6	4.324	-8.75	-7.748	5.504	-8.098
6.5	-12.42	0.231	-1.9	-10.9	2.356	-1.407	-8.68	4.328	-0.77	-7.824	5.507	-0.213
6.75	-12.35	0.243	11.17	-10.9	2.363	10.923	-8.76	4.331	11.05	-7.899	5.51	11.48
7	-12.35	0.255	28.96	-11	2.37	28.06	-8.91	4.335	27.56	-8.043	5.513	27.81
7	-12.35	0.255	28.96	-11	2.37	28.06	-8.91	4.335	27.56	-8.043	5.513	27.81
7.25	-12.51	0.27	13.42	-11.3	2.38	12.208	-9.21	4.341	11.39	-8.341	5.518	11.55
7.5	-12.74	0.286	2.632	-11.6	2.39	1.3331	-9.58	4.347	0.149	-8.709	5.524	0.165
7.75	-13	0.302	-4.32	-11.9	2.4	-5.378	-9.94	4.354	-6.79	-9.077	5.529	-6.912
8	-13.23	0.319	-8.38	-12.2	2.411	-8.741	-10.3	4.36	-10	-9.403	5.535	-10.25
8	-13.23	0.319	-8.38	-12.2	2.411	-8.741	-10.3	4.36	-10	-9.403	5.535	-10.25
8.5	-13.51	0.353	-12.5	-12.7	2.434	-11.54	-10.7	4.374	-11.3	-9.865	5.546	-11.19
9	-13.5	0.391	-11.2	-12.8	2.459	-9.703	-10.9	4.389	-8.75	-10.05	5.559	-8.503
9.5	-13.23	0.431	1.305	-12.8	2.486	2.7164	-10.9	4.406	2.766	-10.05	5.572	3.053
10	-13.01	0.474	31.15	-12.8	2.515	32.179	-11	4.424	29.09	-10.14	5.587	29.21
10	-13.01	0.474	31.15	-12.8	2.515	32.179	-11	4.424	29.09	-10.14	5.587	29.21
10.25	-13.12	0.498	15.01	-13.1	2.533	15.987	-11.2	4.435	12.36	-10.39	5.596	12.51
10.5	-13.32	0.523	3.342	-13.4	2.551	4.7569	-11.6	4.447	0.768	-10.71	5.606	0.955
10.75	-13.54	0.549	-4.92	-13.8	2.57	-2.744	-11.9	4.459	-6.96	-11.05	5.616	-6.725
11	-13.73	0.575	-10.8	-14.1	2.589	-7.759	-12.2	4.472	-12.1	-11.33	5.627	-11.78
11	-13.73	0.575	-10.8	-14.1	2.589	-7.759	-12.2	4.472	-12.1	-11.33	5.627	-11.78
11.25	-13.85	0.602	-15.4	-14.4	2.609	-11.48	-12.4	4.485	-15.5	-11.55	5.637	-15.05
11.5	-13.88	0.63	-19	-14.7	2.629	-14.56	-12.5	4.498	-17.9	-11.68	5.648	-17.38
11.75	-13.79	0.658	-21.3	-14.8	2.65	-17.16	-12.5	4.512	-19.4	-11.7	5.66	-18.68
12	-13.57	0.688	-21.9	-14.8	2.672	-19.39	-12.4	4.526	-19.7	-11.6	5.672	-18.79

12	-13.57	0.688	-21.9	-14.8	2.672	-19.39	-12.4	4.526	-19.7	-11.6	5.672	-18.79
12.25	-13.22	0.717	-19.9	-14.8	2.694	-21.01	-12.1	4.541	-17.8	-11.39	5.684	-16.91
12.5	-12.74	0.748	-14.3	-14.6	2.717	-21.89	-11.8	4.557	-12.7	-11.08	5.697	-11.92
12.75	-12.18	0.78	-3.89	-14.2	2.741	-21.8	-11.4	4.573	-2.91	-10.69	5.71	-2.215
13	-11.59	0.812	12.74	-13.7	2.765	-20.48	-10.9	4.59	13.19	-10.29	5.724	13.83
13	-11.59	0.812	12.74	-13.7	2.765	-20.48	-10.9	4.59	13.19	-10.29	5.724	13.83
13.25	-11.07	0.847	1.345	-13.1	2.791	-16.43	-10.5	4.609	1.321	-9.957	5.74	1.827
13.5	-10.55	0.884	-0.87	-12.4	2.817	-8.079	-10.2	4.629	-1.64	-9.635	5.757	-1.437
13.75	-10.03	0.921	7.638	-11.7	2.845	7.2641	-9.79	4.65	5.5	-9.303	5.775	5.127
14	-9.548	0.959	28.48	-11	2.873	32.375	-9.44	4.672	24.02	-9.002	5.793	22.68
14	-9.548	0.959	28.48	-11	2.873	32.375	-9.44	4.672	24.02	-9.002	5.793	22.68
14.625	-9.118	1.046	22.57	-10.1	2.936	27.559	-9.21	4.719	18.79	-8.855	5.831	17.44
15.25	-9.519	1.12	6.317	-10.2	2.988	9.4699	-9.68	4.753	4.663	-9.349	5.857	4.042
15.875	-10.17	1.184	-5.46	-10.7	3.029	-4.351	-10.3	4.777	-5.46	-10.01	5.872	-5.446
16.5	-10.67	1.238	-4.25	-11.1	3.061	-3.607	-10.8	4.793	-4.2	-10.51	5.879	-4.168
16.5	-10.67	1.238	-4.25	-11.1	3.061	-3.607	-10.8	4.793	-4.2	-10.51	5.879	-4.168
17.125	-11.01	1.284	-3.57	-11.4	3.086	-3.152	-11.1	4.801	-3.51	-10.84	5.878	-3.469
17.75	-11.2	1.323	-2.94	-11.5	3.105	-2.629	-11.3	4.803	-2.9	-11.04	5.872	-2.866
18.375	-11.29	1.355	-2.44	-11.6	3.118	-2.198	-11.4	4.8	-2.44	-11.13	5.86	-2.416
19	-11.28	1.382	-2.15	-11.5	3.127	-1.962	-11.4	4.793	-2.16	-11.13	5.845	-2.142
19	-11.28	1.382	-2.15	-11.5	3.127	-1.962	-11.4	4.793	-2.16	-11.13	5.845	-2.142
19.625	-11.19	1.404	-1.98	-11.4	3.131	-1.835	-11.3	4.783	-1.99	-11.05	5.826	-1.975
20.25	-11.02	1.422	-1.9	-11.2	3.133	-1.785	-11.2	4.769	-1.91	-10.89	5.805	-1.899
20.875	-10.78	1.436	-1.92	-10.9	3.131	-1.843	-10.9	4.754	-1.95	-10.66	5.782	-1.934
21.5	-10.47	1.447	-2.09	-10.6	3.128	-2.028	-10.6	4.738	-2.11	-10.35	5.759	-2.084
21.5	-10.47	1.447	-2.09	-10.6	3.128	-2.028	-10.6	4.738	-2.11	-10.35	5.759	-2.084

22.125	-10.08	1.455	-1.62	-10.2	3.123	-1.551	-10.2	4.722	-1.6	-9.967	5.736	-1.574
22.75	-9.625	1.461	-1.09	-9.74	3.117	-1.211	-9.74	4.706	-1.41	-9.522	5.714	-1.495
23.375	-9.131	1.465	-0.58	-9.23	3.112	-0.844	-9.22	4.691	-1.15	-9.02	5.694	-1.301
24	-8.614	1.468	0	-8.68	3.106	0	-8.67	4.677	0	-8.471	5.675	0

B.2 Effect of Change in surcharge on pile

B.2.1 For depth of excavation of 8m

Y(from surface)	107.9 kN/m2			125 kN/m2			150 kN/m2			175 kN/m2		
	Ux	Uy	M	Ux	Uy	M	Ux	Uy	M	Ux	Uy	M
	[mm]	[mm]	[kNm/m]	[mm]	[mm]	[kNm/m]	[mm]	[mm]	[kNm/m]	[mm]	[mm]	[kNm/m]
0	3.306	-0.539	0	2.853	-0.244	0	3.865	-0.249	0	3.788	-0.251	0
0.5	3.132	-0.539	1.152	2.814	-0.244	1.347	3.59	-0.249	1.046	3.531	-0.25	1.0689
1	2.93	-0.539	5.5724	2.739	-0.244	6.29	3.289	-0.249	5.213	3.246	-0.25	5.3017
1.5	2.581	-0.538	16.702	2.502	-0.243	17.9	2.851	-0.248	16.09	2.822	-0.249	16.234
2	1.806	-0.537	38.097	1.809	-0.242	39.35	2.001	-0.247	37.38	1.983	-0.248	37.522
2	1.806	-0.537	38.097	1.809	-0.242	39.35	2.001	-0.247	37.38	1.983	-0.248	37.522
2.25	1.124	-0.534	18.545	1.157	-0.239	19.79	1.289	-0.243	17.79	1.275	-0.245	17.936
2.5	0.329	-0.53	4.0826	0.384	-0.236	5.248	0.468	-0.24	3.341	0.457	-0.241	3.4726
2.75	-0.49	-0.527	-6.2243	-0.421	-0.232	-5.21	-0.374	-0.236	-6.904	-0.38	-0.237	-6.791
3	-1.27	-0.523	-13.271	-1.194	-0.228	-12.5	-1.172	-0.232	-13.83	-1.18	-0.233	-13.74
3	-1.27	-0.523	-13.271	-1.194	-0.228	-12.5	-1.172	-0.232	-13.83	-1.18	-0.233	-13.74
3.25	-1.97	-0.518	-17.422	-1.891	-0.224	-16.8	-1.887	-0.228	-17.86	-1.89	-0.229	-17.8
3.5	-2.57	-0.514	-19.281	-2.484	-0.219	-18.8	-2.491	-0.223	-19.62	-2.5	-0.224	-19.57
3.75	-3.04	-0.509	-18.973	-2.963	-0.214	-18.7	-2.976	-0.218	-19.22	-2.98	-0.219	-19.19
4	-3.4	-0.503	-16.587	-3.327	-0.208	-16.4	-3.344	-0.212	-16.75	-3.35	-0.214	-16.73
4	-3.4	-0.503	-16.587	-3.327	-0.208	-16.4	-3.344	-0.212	-16.75	-3.35	-0.214	-16.73
4.25	-3.66	-0.497	-11.615	-3.591	-0.203	-11.5	-3.609	-0.206	-11.72	-3.61	-0.208	-11.71
4.5	-3.84	-0.491	-3.4157	-3.785	-0.196	-3.34	-3.802	-0.2	-3.475	-3.81	-0.201	-3.469
4.75	-4.01	-0.485	8.6552	-3.958	-0.189	8.686	-3.973	-0.193	8.626	-3.98	-0.194	8.6273
5	-4.23	-0.477	25.24	-4.184	-0.182	25.24	-4.197	-0.186	25.23	-4.2	-0.187	25.232
5	-4.23	-0.477	25.24	-4.184	-0.182	25.24	-4.197	-0.186	25.23	-4.2	-0.187	25.232

5.25	-4.58	-0.468	8.9356	-4.547	-0.172	8.925	-4.558	-0.176	8.95	-4.56	-0.177	8.9462
5.5	-4.99	-0.457	-3.0851	-4.965	-0.162	-3.09	-4.974	-0.165	-3.053	-4.98	-0.167	-3.057
5.75	-5.38	-0.447	-11.588	-5.363	-0.151	-11.6	-5.37	-0.154	-11.54	-5.37	-0.156	-11.54
6	-5.7	-0.435	-17.34	-5.69	-0.139	-17.3	-5.696	-0.143	-17.28	-5.7	-0.144	-17.28
6	-5.7	-0.435	-17.34	-5.69	-0.139	-17.3	-5.696	-0.143	-17.28	-5.7	-0.144	-17.28
6.5	-6.01	-0.411	-22.419	-6.008	-0.115	-22.4	-6.012	-0.118	-22.35	-6.02	-0.12	-22.36
7	-5.77	-0.386	-20.429	-5.785	-0.089	-20.4	-5.788	-0.092	-20.34	-5.79	-0.093	-20.35
7.5	-5.05	-0.357	-7.0937	-5.081	-0.06	-7.05	-5.083	-0.063	-7.043	-5.09	-0.064	-7.044
8	-4.18	-0.327	22.56	-4.23	-0.029	22.43	-4.232	-0.032	22.43	-4.24	-0.033	22.438
8	-4.18	-0.327	22.56	-4.23	-0.029	22.43	-4.232	-0.032	22.43	-4.24	-0.033	22.438
8.5	-3.77	-0.299	22.647	-3.835	0.0008	22.56	-3.837	-0.002	22.56	-3.84	-0.004	22.565
9	-3.89	-0.275	11.187	-3.971	0.026	11.31	-3.972	0.023	11.31	-3.97	0.021	11.311
9.5	-4.28	-0.255	0.0003	-4.382	0.0476	0.249	-4.383	0.044	0.25	-4.39	0.043	0.2503
10	-4.7	-0.238	-2.4757	-4.824	0.066	-2.44	-4.825	0.063	-2.444	-4.83	0.061	-2.444
10	-4.7	-0.238	-2.4757	-4.824	0.066	-2.44	-4.825	0.063	-2.444	-4.83	0.061	-2.444
10.25	-4.89	-0.231	-2.6503	-5.023	0.0741	-3.15	-5.024	0.071	-3.148	-5.03	0.07	-3.148
10.5	-5.06	-0.225	-1.9137	-5.204	0.0815	-3.31	-5.205	0.078	-3.314	-5.21	0.077	-3.315
10.75	-5.22	-0.22	-0.8335	-5.364	0.0882	-3.12	-5.365	0.085	-3.124	-5.37	0.084	-3.125
11	-5.37	-0.215	0	-5.505	0.0942	-2.74	-5.506	0.091	-2.745	-5.51	0.09	-2.746
11	-5.505	0.094	-2.743	-5.505	0.0942	-2.74	-5.506	0.091	-2.745	-5.51	0.09	-2.746
11.25	-5.629	0.1	-2.013	-5.629	0.0997	-2.01	-5.63	0.097	-2.016	-5.63	0.095	-2.017
11.5	-5.741	0.105	-1.324	-5.741	0.1045	-1.32	-5.742	0.101	-1.326	-5.74	0.1	-1.327
11.75	-5.845	0.109	-0.667	-5.845	0.1089	-0.67	-5.846	0.106	-0.668	-5.85	0.104	-0.668
12	-5.945	0.113	0	-5.945	0.1128	0	-5.946	0.11	0	-5.95	0.108	0

B.2.2 For depth of excavation of 10m

Y(from surface)	107.9 kN/m2			125 kN/m2			150 kN/m2			175 kN/m2		
	Ux	Uy	M	Ux	Uy	M	Ux	Uy	M	Ux	Uy	M
	[mm]	[mm]	[kNm/m]	[mm]	[mm]	[kNm/m]	[mm]	[mm]	[kNm/m]	[mm]	[mm]	[kNm/m]
0	0.2	-0.647	0	0.912	-0.376	0	0.033	-0.371	0	-0.68	-0.472	0
0.5	-0.054	-0.647	0.35	0.526	-0.376	0.3	-0.162	-0.371	0.363	-0.76	-0.472	0.405
1	-0.313	-0.647	2.419	0.136	-0.376	2.074	-0.362	-0.371	2.668	-0.85	-0.472	3.047
1.5	-0.643	-0.646	12.37	-0.316	-0.375	11.62	-0.64	-0.37	12.89	-1.03	-0.471	13.68
2	-1.301	-0.644	36.49	-1.077	-0.373	35.36	-1.258	-0.368	37.09	-1.56	-0.47	38.09
2	-1.301	-0.644	36.49	-1.077	-0.373	35.36	-1.258	-0.368	37.09	-1.56	-0.47	38.09
2.25	-1.903	-0.642	18.31	-1.72	-0.37	17.08	-1.845	-0.366	18.92	-2.11	-0.467	19.89
2.5	-2.616	-0.638	4.702	-2.468	-0.367	3.498	-2.547	-0.363	5.304	-2.79	-0.464	6.171
2.75	-3.357	-0.635	-5.09	-3.237	-0.363	-6.16	-3.282	-0.359	-4.545	-3.5	-0.461	-3.828
3	-4.067	-0.631	-11.8	-3.967	-0.359	-12.7	-3.988	-0.355	-11.37	-4.19	-0.457	-10.85
3	-4.067	-0.631	-11.8	-3.967	-0.359	-12.7	-3.988	-0.355	-11.37	-4.19	-0.457	-10.85
3.25	-4.705	-0.627	-15.9	-4.62	-0.355	-16.5	-4.625	-0.351	-15.54	-4.81	-0.453	-15.15
3.5	-5.246	-0.622	-17.9	-5.172	-0.35	-18.4	-5.167	-0.347	-17.64	-5.34	-0.448	-17.24
3.75	-5.677	-0.617	-17.8	-5.612	-0.345	-18.2	-5.601	-0.342	-17.67	-5.77	-0.443	-17.19
4	-5.999	-0.612	-15.7	-5.941	-0.34	-15.9	-5.927	-0.336	-15.56	-6.09	-0.438	-15.02
4	-5.999	-0.612	-15.7	-5.941	-0.34	-15.9	-5.927	-0.336	-15.56	-6.09	-0.438	-15.02
4.25	-6.225	-0.606	-10.7	-6.172	-0.334	-10.9	-6.158	-0.331	-10.65	-6.32	-0.432	-10.16
4.5	-6.385	-0.6	-2.45	-6.336	-0.327	-2.53	-6.323	-0.324	-2.391	-6.48	-0.426	-1.97
4.75	-6.53	-0.593	9.85	-6.484	-0.321	9.845	-6.474	-0.318	9.904	-6.63	-0.419	10.2
5	-6.735	-0.586	26.85	-6.693	-0.313	26.92	-6.684	-0.31	26.93	-6.85	-0.412	26.99
5	-6.735	-0.586	26.85	-6.693	-0.313	26.92	-6.684	-0.31	26.93	-6.85	-0.412	26.99
5.25	-7.087	-0.576	11.02	-7.049	-0.303	11.14	-7.043	-0.3	11.11	-7.21	-0.402	11.01
5.5	-	-	-0.5	-	-0.293	-0.34	-	-0.29	-0.382	-7.64	-	-0.584

	7.507	0.566		7.472			7.468				0.392	
5.75	-7.923	-0.555	-8.46	-7.894	-0.282	-8.29	-7.892	-0.279	-8.328	-8.07	-0.381	-8.586
6	-8.286	-0.544	-13.6	-8.264	-0.27	-13.5	-8.264	-0.268	-13.5	-8.44	-0.369	-13.78
6	-8.286	-0.544	-13.6	-8.264	-0.27	-13.5	-8.264	-0.268	-13.5	-8.44	-0.369	-13.78
6.5	-8.748	-0.52	-18	-8.742	-0.246	-18	-8.744	-0.243	-18	-8.92	-0.345	-18.09
7	-8.774	-0.494	-16.5	-8.785	-0.22	-16.7	-8.789	-0.217	-16.72	-8.96	-0.319	-16.53
7.5	-8.409	-0.466	-5.45	-8.434	-0.191	-5.68	-8.439	-0.188	-5.713	-8.61	-0.291	-5.397
8	-7.935	-0.435	19.74	-7.969	-0.16	19.63	-7.973	-0.158	19.6	-8.15	-0.261	19.65
8	-7.935	-0.435	19.74	-7.969	-0.16	19.63	-7.973	-0.158	19.6	-8.15	-0.261	19.65
8.5	-7.722	-0.4	-4.62	-7.761	-0.124	-4.73	-7.765	-0.121	-4.741	-7.95	-0.225	-4.991
9	-7.42	-0.361	-11.1	-7.463	-0.085	-11	-7.466	-0.083	-10.95	-7.66	-0.187	-11.3
9.5	-6.872	-0.32	-2.35	-6.92	-0.043	-2.12	-6.922	-0.041	-2.102	-7.11	-0.146	-2.585
10	-6.282	-0.276	20.88	-6.342	0.0014	20.73	-6.343	0.004	20.74	-6.51	-0.102	19.66
10	-6.282	-0.276	20.88	-6.342	0.0014	20.73	-6.343	0.004	20.74	-6.51	-0.102	19.66
10.5	-6.123	-0.235	18.42	-6.19	0.0435	18.19	-6.191	0.046	18.19	-6.32	-0.06	18.13
11	-6.399	-0.199	7.578	-6.469	0.08	7.479	-6.47	0.082	7.48	-6.56	-0.024	8.039
11.5	-6.861	-0.169	-1.9	-6.932	0.1115	-1.81	-6.933	0.114	-1.811	-7	0.008	-1.29
12	-7.299	-0.144	-4.04	-7.373	0.1388	-3.81	-7.373	0.141	-3.813	-7.42	0.036	-3.619
12	-7.299	-0.144	-4.04	-7.373	0.1388	-3.81	-7.373	0.141	-3.813	-7.42	0.036	-3.619
12.5	-7.635	-0.122	-5.17	-7.718	0.1624	-4.9	-7.719	0.164	-4.902	-7.75	0.06	-4.849
13	-7.851	-0.104	-3.83	-7.946	0.1825	-4.61	-7.947	0.185	-4.609	-7.97	0.08	-4.648
13.5	-7.974	-0.09	-1.59	-8.062	0.1995	-3.83	-8.063	0.202	-3.832	-8.07	0.098	-3.948
14	-8.056	-0.078	0	-8.084	0.2136	-3.23	-8.084	0.216	-3.231	-8.08	0.113	-3.475
14	-8.084	0.215	-3.231	-8.084	0.2136	-3.23	-8.084	0.216	-3.231	-8.08	0.113	-3.475
14.25	-8.064	0.221	-2.62	-8.064	0.2196	-2.62	-8.064	0.222	-2.619	-8.05	0.119	-2.996
14.5	-8.028	0.226	-1.981	-8.028	0.2249	-1.98	-8.029	0.227	-1.981	-8	0.125	-2.551

14.75	-7.981	0.231	-1.173	-7.98	0.2297	-1.17	-7.981	0.232	-1.172	-7.94	0.13	-1.715
15	-7.926	0.235	0	-7.925	0.234	0	-7.926	0.236	0	-7.87	0.135	0

B.2.3 For depth of excavation of 12m

Y(from surface)	107.9 kN/m2			125 kN/m2			150 kN/m2			175 kN/m2		
	Ux	Uy	M	Ux	Uy	M	Ux	Uy	M	Ux	Uy	M
	[mm]	[mm]	[kNm/m]	[mm]	[mm]	[kNm/m]	[mm]	[mm]	[kNm/m]	[mm]	[mm]	[kNm/m]
0	-1.932	-0.729	0	-1.108	-0.409	0	-1.941	-0.408	0	-2.47	-0.418	0
0.5	-2.204	-0.729	0.308	-1.379	-0.409	0.341	-2.034	-0.408	0.412	-2.45	-0.418	0.474
1	-2.48	-0.728	2.401	-1.655	-0.409	2.355	-2.134	-0.408	2.92	-2.45	-0.418	3.294
1.5	-2.827	-0.727	12.34	-1.999	-0.408	12.05	-2.318	-0.407	13.21	-2.53	-0.418	13.95
2	-3.5	-0.726	36.27	-2.663	-0.407	35.5	-2.849	-0.406	37.03	-2.98	-0.417	37.99
2	-3.5	-0.726	36.27	-2.663	-0.407	35.5	-2.849	-0.406	37.03	-2.98	-0.417	37.99
2.25	-4.108	-0.722	18.55	-3.26	-0.403	17.83	-3.393	-0.403	19.4	-3.5	-0.414	20.33
2.5	-4.829	-0.718	5.363	-3.966	-0.4	4.683	-4.056	-0.4	6.231	-4.13	-0.41	7.044
2.75	-5.583	-0.714	-4.12	-4.7	-0.396	-4.76	-4.756	-0.396	-3.325	-4.81	-0.407	-2.614
3	-6.311	-0.71	-10.7	-5.405	-0.391	-11.3	-5.436	-0.391	-10.09	-5.48	-0.403	-9.374
3	-6.311	-0.71	-10.7	-5.405	-0.391	-11.3	-5.436	-0.391	-10.09	-5.48	-0.403	-9.374
3.25	-6.974	-0.705	-14.7	-6.041	-0.386	-15.4	-6.054	-0.387	-14.43	-6.08	-0.398	-13.8
3.5	-7.546	-0.699	-16.7	-6.582	-0.381	-17.5	-6.584	-0.382	-16.76	-6.6	-0.393	-16.28
3.75	-8.016	-0.694	-16.5	-7.016	-0.376	-17.6	-7.012	-0.376	-17.02	-7.02	-0.388	-16.69
4	-8.386	-0.688	-14.1	-7.343	-0.37	-15.5	-7.335	-0.371	-15.1	-7.34	-0.382	-14.87
4	-8.386	-0.688	-14.1	-7.343	-0.37	-15.5	-7.335	-0.371	-15.1	-7.34	-0.382	-14.87
4.25	-8.669	-0.681	-8.66	-7.575	-0.364	-10.6	-7.566	-0.364	-10.37	-7.57	-0.376	-10.23
4.5	-8.899	-0.674	0.297	-7.742	-0.357	-2.41	-7.733	-0.358	-2.264	-7.74	-0.37	-2.18
4.75	-9.13	-0.667	13.49	-7.894	-0.35	9.801	-7.886	-0.351	9.872	-7.89	-0.363	9.921
5	-9.443	-0.659	31.63	-8.106	-0.342	26.68	-8.1	-0.343	26.7	-8.11	-0.355	26.73
5	-9.443	-0.659	31.63	-8.106	-0.342	26.68	-8.1	-0.343	26.7	-8.11	-0.355	26.73
5.25	-9.933	-0.648	16.13	-8.463	-0.332	10.68	-8.459	-0.333	10.66	-8.46	-0.345	10.68
5.5	-	-	5.124	-	-0.321	-1.06	-	-	-1.098	-8.89	-	-1.083

	10.52	0.637		8.886			8.883	0.322			0.334	
5.75	-11.14	-0.626	-2.23	-9.302	-0.31	-9.25	-9.3	-0.311	-9.295	-9.31	-0.323	-9.287
6	-11.74	-0.614	-6.8	-9.661	-0.298	-14.6	-9.661	-0.3	-14.65	-9.67	-0.312	-14.65
6	-11.74	-0.614	-6.8	-9.661	-0.298	-14.6	-9.661	-0.3	-14.65	-9.67	-0.312	-14.65
6.5	-12.81	-0.589	-10.8	-10.1	-0.274	-18.5	-10.1	-0.275	-18.57	-10.1	-0.287	-18.58
7	-13.62	-0.562	-12	-10.08	-0.247	-15	-10.08	-0.249	-15.02	-10.1	-0.261	-15.03
7.5	-14.14	-0.533	-11.5	-9.722	-0.218	-0.5	-9.723	-0.22	-0.497	-9.73	-0.232	-0.513
8	-14.38	-0.503	-10.2	-9.372	-0.188	29.09	-9.373	-0.19	29.09	-9.38	-0.202	29.08
8	-14.38	-0.503	-10.2	-9.372	-0.188	29.09	-9.373	-0.19	29.09	-9.38	-0.202	29.08
8.25	-14.4	-0.488	-11.6	-9.393	-0.169	14.69	-9.394	-0.171	14.69	-9.4	-0.184	14.69
8.5	-14.35	-0.471	-13	-9.504	-0.15	4.798	-9.505	-0.152	4.799	-9.51	-0.165	4.803
8.75	-14.23	-0.454	-14.2	-9.644	-0.131	-2.11	-9.646	-0.133	-2.108	-9.65	-0.145	-2.1
9	-14.01	-0.437	-15.1	-9.771	-0.111	-7.44	-9.773	-0.112	-7.444	-9.78	-0.125	-7.438
9	-14.01	-0.437	-15.1	-9.771	-0.111	-7.44	-9.773	-0.112	-7.444	-9.78	-0.125	-7.438
9.25	-13.71	-0.419	-15.7	-9.853	-0.09	-11.4	-9.854	-0.092	-11.36	-9.86	-0.104	-11.36
9.5	-13.3	-0.4	-15.8	-9.865	-0.068	-14.1	-9.866	-0.07	-14.13	-9.87	-0.083	-14.13
9.75	-12.8	-0.38	-15	-9.79	-0.046	-15.5	-9.792	-0.048	-15.52	-9.8	-0.061	-15.53
10	-12.21	-0.36	-12.9	-9.621	-0.023	-15.3	-9.623	-0.025	-15.28	-9.63	-0.038	-15.28
10	-1.932	-0.36	-12.9	-9.621	-0.023	-15.3	-9.623	-0.025	-15.28	-9.63	-0.038	-15.28
10.25	-1.932	-0.36	-8.74	-9.359	-2E-05	-12.6	-9.36	-0.002	-12.63	-9.36	-0.015	-12.63
10.5	-1.932	-0.36	-1.34	-9.019	0.0241	-6.65	-9.02	0.022	-6.65	-9.02	0.009	-6.656
10.75	-1.932	-0.36	10.49	-8.638	0.0489	3.865	-8.639	0.047	3.862	-8.64	0.034	3.857
11	-1.932	-0.36	27.91	-8.28	0.0745	20.14	-8.281	0.072	20.14	-8.28	0.06	20.14
11	-1.932	-0.36	27.91	-8.28	0.0745	20.14	-8.281	0.072	20.14	-8.28	0.06	20.14
11.25	-1.932	-0.36	15.16	-8.029	0.1029	7.226	-8.03	0.101	7.227	-8.03	0.088	7.226
11.5	-1.932	-0.36	8.883	-7.822	0.1321	1.56	-7.823	0.13	1.562	-7.82	0.117	1.565

11.75	-1.932	-0.36	9.975	-7.624	0.1619	3.536	-7.624	0.16	3.539	-7.62	0.147	3.548
12	-1.932	-0.36	19.39	-7.446	0.1923	13.58	-7.447	0.19	13.59	-7.45	0.177	13.61
12	-1.932	-0.36	19.39	-7.446	0.1923	13.58	-7.447	0.19	13.59	-7.45	0.177	13.61
12.5	-1.932	-0.36	14.27	-7.338	0.2502	10.84	-7.339	0.248	10.84	-7.34	0.235	10.86
13	-1.932	-0.36	3.706	-7.484	0.3022	2.208	-7.484	0.3	2.21	-7.48	0.287	2.217
13.5	-1.932	-0.36	-4.55	-7.685	0.3494	-4.86	-7.686	0.347	-4.861	-7.69	0.334	-4.862
14	-1.932	-0.36	-5.32	-7.786	0.3926	-5.28	-7.786	0.39	-5.275	-7.79	0.377	-5.278
14	-1.932	-0.36	-5.32	-7.786	0.3926	-5.28	-7.786	0.39	-5.275	-7.79	0.377	-5.278
15	-1.932	-0.36	-4.48	-7.592	0.4694	-4.37	-7.593	0.467	-4.369	-7.59	0.454	-4.368
16	-1.932	-0.36	-1.21	-6.991	0.5371	-1.74	-6.991	0.535	-1.744	-6.99	0.521	-1.738
17	-1.932	-0.36	1.38	-6.217	0.5963	0.64	-6.218	0.594	0.644	-6.22	0.58	0.659
18	-1.932	-0.36	0	-5.483	0.646	0.913	-5.484	0.643	0.922	-5.49	0.629	0.963
18	-5.483	0.646	0.913	-5.483	0.646	0.913	-5.484	0.643	0.922	-5.49	0.629	0.963
18.5	-5.154	0.667	0.881	-5.154	0.6669	0.881	-5.156	0.664	0.874	-5.16	0.65	0.857
19	-4.848	0.685	1.627	-4.848	0.685	1.627	-4.85	0.682	1.463	-4.86	0.668	0.784
19.5	-4.582	0.701	1.862	-4.582	0.7007	1.862	-4.58	0.698	1.605	-4.57	0.683	0.537
20	-4.357	0.715	0	-4.357	0.7147	0	-4.345	0.712	0	-4.3	0.696	0

B.2.4 For depth of excavation of 14m

Y(from surface)	107.9 kN/m2			125 kN/m2			150 kN/m2			175 kN/m2		
	Ux	Uy	M	Ux	Uy	M	Ux	Uy	M	Ux	Uy	M
	[mm]	[mm]	[kNm/m]	[mm]	[mm]	[kNm/m]	[mm]	[mm]	[kNm/m]	[mm]	[mm]	[kNm/m]
0	1.88	0.105	0	1.648	0.1066	0	1.189	0.109	0	0.728	0.112	0
0.25	1.334	0.105	2.157	1.134	0.1065	2.207	0.732	0.109	2.288	0.327	0.112	2.413
0.5	0.774	0.105	8.2	0.606	0.1063	8.359	0.262	0.109	8.606	-0.09	0.112	8.902
0.75	0.165	0.105	18.44	0.028	0.1061	18.74	-0.261	0.109	19.2	-0.56	0.112	19.68
1	-0.556	0.105	33.2	-0.665	0.1058	33.66	-0.901	0.108	34.33	-1.15	0.111	34.99
1	-0.556	0.105	33.2	-0.665	0.1058	33.66	-0.901	0.108	34.33	-1.15	0.111	34.99
1.25	-1.464	0.106	15.76	-1.547	0.1074	16.34	-1.734	0.11	17.18	-1.93	0.112	17.97
1.5	-2.468	0.108	2.608	-2.528	0.109	3.223	-2.671	0.111	4.112	-2.83	0.114	4.938
1.75	-3.488	0.11	-6.91	-3.529	0.1108	-6.3	-3.634	0.113	-5.385	-3.76	0.115	-4.564
2	-4.465	0.112	-13.5	-4.491	0.1128	-12.9	-4.564	0.115	-11.86	-4.66	0.117	-11.04
2	-4.465	0.112	-13.5	-4.491	0.1128	-12.9	-4.564	0.115	-11.86	-4.66	0.117	-11.04
2.5	-6.149	0.117	-19.2	-6.156	0.1175	-18.8	-6.182	0.119	-17.95	-6.23	0.121	-17.19
3	-7.372	0.123	-16.8	-7.369	0.1234	-16.6	-7.369	0.125	-15.95	-7.39	0.127	-15.35
3.5	-8.2	0.13	-2.97	-8.194	0.1308	-2.85	-8.184	0.132	-2.441	-8.19	0.134	-2.055
4	-8.979	0.139	26.32	-8.975	0.1396	26.36	-8.963	0.141	26.54	-8.96	0.142	26.72
4	-8.979	0.139	26.32	-8.975	0.1396	26.36	-8.963	0.141	26.54	-8.96	0.142	26.72
4.25	-9.54	0.146	10.26	-9.536	0.1468	10.27	-9.527	0.148	10.33	-9.52	0.149	10.41
4.5	-10.16	0.154	-1.55	-10.16	0.1544	-1.56	-10.15	0.156	-1.562	-10.1	0.157	-1.536
4.75	-10.78	0.162	-9.82	-10.77	0.1624	-9.83	-10.77	0.164	-9.867	-10.8	0.165	-9.875
5	-11.33	0.17	-15.3	-11.33	0.1709	-15.3	-11.33	0.172	-15.32	-11.3	0.173	-15.34
5	-11.33	0.17	-15.3	-11.33	0.1709	-15.3	-11.33	0.172	-15.32	-11.3	0.173	-15.34
5.25	-11.79	0.179	-18.4	-11.79	0.1798	-18.4	-11.79	0.181	-18.47	-11.8	0.182	-18.48
5.5	-12.14	0.189	-19.8	-12.14	0.1891	-19.8	-12.14	0.19	-19.86	-12.1	0.191	-19.85
5.75	-	0.198	-19.2	-	0.1989	-19.2	-	0.2	-19.3	-12.4	0.201	-19.25

	12.36			12.36			12.37					
6	-12.47	0.209	-16.5	-12.47	0.2092	-16.5	-12.48	0.21	-16.54	-12.5	0.211	-16.47
6	-12.47	0.209	-16.5	-12.47	0.2092	-16.5	-12.48	0.21	-16.54	-12.5	0.211	-16.47
6.25	-12.48	0.22	-10.9	-12.48	0.22	-10.9	-12.48	0.221	-10.95	-12.5	0.222	-10.89
6.5	-12.42	0.231	-1.9	-12.42	0.2314	-1.91	-12.43	0.232	-1.938	-12.4	0.233	-1.893
6.75	-12.35	0.243	11.17	-12.35	0.2432	11.17	-12.35	0.244	11.15	-12.4	0.245	11.17
7	-12.35	0.255	28.96	-12.35	0.2556	28.95	-12.35	0.257	28.95	-12.4	0.257	28.93
7	-12.35	0.255	28.96	-12.35	0.2556	28.95	-12.35	0.257	28.95	-12.4	0.257	28.93
7.25	-12.51	0.27	13.42	-12.51	0.2707	13.42	-12.51	0.272	13.42	-12.5	0.272	13.39
7.5	-12.74	0.286	2.632	-12.74	0.2863	2.634	-12.75	0.287	2.639	-12.7	0.288	2.608
7.75	-13	0.302	-4.32	-13	0.3024	-4.32	-13	0.303	-4.314	-13	0.304	-4.343
8	-13.23	0.319	-8.38	-13.23	0.319	-8.37	-13.23	0.32	-8.373	-13.2	0.321	-8.401
8	-13.23	0.319	-8.38	-13.23	0.319	-8.37	-13.23	0.32	-8.373	-13.2	0.321	-8.401
8.5	-13.51	0.353	-12.5	-13.51	0.3539	-12.5	-13.52	0.355	-12.52	-13.5	0.355	-12.55
9	-13.5	0.391	-11.2	-13.5	0.3913	-11.2	-13.5	0.392	-11.19	-13.5	0.393	-11.21
9.5	-13.23	0.431	1.305	-13.23	0.4313	1.303	-13.23	0.432	1.298	-13.2	0.433	1.285
10	-13.01	0.474	31.15	-13.02	0.474	31.16	-13.02	0.475	31.16	-13	0.475	31.16
10	-13.01	0.474	31.15	-13.02	0.474	31.16	-13.02	0.475	31.16	-13	0.475	31.16
10.25	-13.12	0.498	15.01	-13.12	0.4984	15.01	-13.12	0.499	15.02	-13.1	0.5	15.03
10.5	-13.32	0.523	3.342	-13.32	0.5235	3.346	-13.32	0.524	3.354	-13.3	0.525	3.367
10.75	-13.54	0.549	-4.92	-13.54	0.5492	-4.91	-13.54	0.55	-4.905	-13.5	0.55	-4.895
11	-13.73	0.575	-10.8	-13.73	0.5756	-10.8	-13.73	0.576	-10.83	-13.7	0.577	-10.82
11	-13.73	0.575	-10.8	-13.73	0.5756	-10.8	-13.73	0.576	-10.83	-13.7	0.577	-10.82
11.25	-13.85	0.602	-15.4	-13.85	0.6027	-15.4	-13.85	0.603	-15.42	-13.9	0.604	-15.42
11.5	-13.88	0.63	-19	-13.88	0.6304	-19	-13.88	0.631	-19.01	-13.9	0.631	-19.01
11.75	-13.79	0.658	-21.3	-13.79	0.6588	-21.3	-13.79	0.659	-21.27	-13.8	0.66	-21.28
12	-13.57	0.688	-21.9	-13.57	0.6879	-21.9	-13.57	0.689	-21.88	-13.6	0.689	-21.89

12	-13.57	0.688	-21.9	-13.57	0.6879	-21.9	-13.57	0.689	-21.88	-13.6	0.689	-21.89
12.25	-13.22	0.717	-19.9	-13.22	0.7177	-19.9	-13.22	0.718	-19.92	-13.2	0.719	-19.93
12.5	-12.74	0.748	-14.3	-12.74	0.7484	-14.3	-12.74	0.749	-14.35	-12.7	0.749	-14.35
12.75	-12.18	0.78	-3.89	-12.18	0.7799	-3.89	-12.18	0.781	-3.895	-12.2	0.781	-3.897
13	-11.59	0.812	12.74	-11.59	0.8123	12.74	-11.59	0.813	12.74	-11.6	0.813	12.74
13	-11.59	0.812	12.74	-11.59	0.8123	12.74	-11.59	0.813	12.74	-11.6	0.813	12.74
13.25	-11.07	0.847	1.345	-11.07	0.8477	1.346	-11.07	0.848	1.348	-11.1	0.849	1.35
13.5	-10.55	0.884	-0.87	-10.55	0.8839	-0.87	-10.55	0.885	-0.866	-10.6	0.885	-0.863
13.75	-10.03	0.921	7.638	-10.03	0.921	7.638	-10.03	0.922	7.64	-10	0.922	7.642
14	-9.548	0.959	28.48	-9.548	0.959	28.48	-9.549	0.96	28.48	-9.55	0.96	28.48
14	-9.548	0.959	28.48	-9.548	0.959	28.48	-9.549	0.96	28.48	-9.55	0.96	28.48
14.625	-9.118	1.046	22.57	-9.118	1.0463	22.57	-9.119	1.047	22.57	-9.12	1.047	22.57
15.25	-9.519	1.12	6.317	-9.519	1.1207	6.317	-9.519	1.121	6.317	-9.52	1.122	6.318
15.875	-10.17	1.184	-5.46	-10.17	1.1842	-5.46	-10.17	1.185	-5.464	-10.2	1.185	-5.464
16.5	-10.67	1.238	-4.25	-10.67	1.2384	-4.25	-10.67	1.239	-4.25	-10.7	1.239	-4.25
16.5	-10.67	1.238	-4.25	-10.67	1.2384	-4.25	-10.67	1.239	-4.25	-10.7	1.239	-4.25
17.125	-11.01	1.284	-3.57	-11.01	1.2844	-3.57	-11.01	1.285	-3.572	-11	1.285	-3.572
17.75	-11.2	1.323	-2.94	-11.21	1.3232	-2.94	-11.21	1.324	-2.937	-11.2	1.324	-2.937
18.375	-11.29	1.355	-2.44	-11.29	1.3557	-2.44	-11.29	1.356	-2.445	-11.3	1.356	-2.445
19	-11.28	1.382	-2.15	-11.28	1.3826	-2.15	-11.28	1.383	-2.15	-11.3	1.383	-2.15
19	-11.28	1.382	-2.15	-11.28	1.3826	-2.15	-11.28	1.383	-2.15	-11.3	1.383	-2.15
19.625	-11.19	1.404	-1.98	-11.19	1.4046	-1.98	-11.19	1.405	-1.984	-11.2	1.405	-1.984
20.25	-11.02	1.422	-1.9	-11.02	1.4223	-1.9	-11.02	1.423	-1.896	-11	1.423	-1.896
20.875	-10.78	1.436	-1.92	-10.78	1.4363	-1.92	-10.78	1.437	-1.921	-10.8	1.437	-1.921
21.5	-10.47	1.447	-2.09	-10.47	1.447	-2.09	-10.47	1.447	-2.089	-10.5	1.448	-2.089
21.5	-10.47	1.447	-2.09	-10.47	1.447	-2.09	-10.47	1.447	-2.089	-10.5	1.448	-2.089

22.125	-10.08	1.455	-1.62	-10.08	1.4551	-1.62	-10.08	1.455	-1.622	-10.1	1.456	-1.622
22.75	-9.625	1.461	-1.09	-9.625	1.4608	-1.09	-9.625	1.461	-1.09	-9.63	1.461	-1.09
23.375	-9.131	1.465	-0.58	-9.131	1.465	-0.58	-9.131	1.465	-0.577	-9.13	1.466	-0.577
24	-8.614	1.468	0	-8.614	1.4683	0	-8.614	1.469	0	-8.61	1.469	0

B.3 Effect of Change in Pile diameter on pile

B.3.1 For depth of excavation of 8m

Y(from surface)	45cm			60cm			75cm		
	Ux	Uy	M	Ux	Uy	M	Ux	Uy	M
	[mm]	[mm]	[kNm/m]	[mm]	[mm]	[kNm/m]	[mm]	[mm]	[kNm/m]
0	3.306	-0.539	0	3.37	-0.48	0	1.005	-1.136	0
0.5	3.132	-0.539	1.152	2.57	-0.48	2.6397	0.456	-1.135	3.624
1	2.93	-0.539	5.572	1.76	-0.48	10.084	-0.1	-1.135	12.71
1.5	2.581	-0.538	16.7	0.91	-0.48	23.472	-0.66	-1.135	26.83
2	1.806	-0.537	38.1	-0.04	-0.48	43.978	-1.26	-1.134	45.63
2	1.806	-0.537	38.1	-0.04	-0.48	43.978	-1.26	-1.134	45.63
2.25	1.124	-0.534	18.54	-0.59	-0.48	21.635	-1.58	-1.133	20.88
2.5	0.329	-0.53	4.083	-1.16	-0.47	2.3456	-1.91	-1.132	-1.97
2.75	-0.49	-0.527	-6.22	-1.73	-0.47	-14.27	-2.23	-1.13	-22.9
3	-1.272	-0.523	-13.3	-2.29	-0.47	-28.57	-2.55	-1.128	-41.9
3	-1.272	-0.523	-13.3	-2.29	-0.47	-28.57	-2.55	-1.128	-41.9
3.25	-1.972	-0.518	-17.4	-2.81	-0.47	-40.87	-2.86	-1.126	-59.2
3.5	-2.565	-0.514	-19.3	-3.29	-0.46	-50.43	-3.15	-1.123	-73.8
3.75	-3.041	-0.509	-19	-3.71	-0.46	-55.78	-3.42	-1.121	-83.5
4	-3.4	-0.503	-16.6	-4.07	-0.45	-55.36	-3.66	-1.118	-86.3
4	-3.4	-0.503	-16.6	-4.07	-0.45	-55.36	-3.66	-1.118	-86.3
4.25	-3.658	-0.497	-11.6	-4.37	-0.45	-48.28	-3.88	-1.114	-81.3
4.5	-3.845	-0.491	-3.42	-4.62	-0.44	-37.2	-4.07	-1.111	-71.8

4.75	-4.01	-0.485	8.655	-4.83	-0.44	-22.2	-4.24	-1.107	-58
5	-4.229	-0.477	25.24	-5.01	-0.43	-3.357	-4.4	-1.104	-40
5	-4.229	-0.477	25.24	-5.01	-0.43	-3.357	-4.4	-1.104	-40
5.25	-4.584	-0.468	8.936	-5.19	-0.43	-17.97	-4.55	-1.099	-54.7
5.5	-4.994	-0.457	-3.09	-5.35	-0.42	-28.85	-4.68	-1.094	-65.3
5.75	-5.385	-0.447	-11.6	-5.48	-0.41	-36.26	-4.79	-1.089	-72
6	-5.704	-0.435	-17.3	-5.57	-0.41	-40.48	-4.89	-1.084	-75
6	-5.704	-0.435	-17.3	-5.57	-0.41	-40.48	-4.89	-1.084	-75
6.5	-6.007	-0.411	-22.4	-5.61	-0.39	-42.17	-5	-1.073	-71.8
7	-5.767	-0.386	-20.4	-5.47	-0.37	-31.8	-5.04	-1.062	-52.7
7.5	-5.045	-0.357	-7.09	-5.2	-0.36	-5.924	-5.01	-1.049	-15.6
8	-4.176	-0.327	22.56	-4.89	-0.34	38.862	-4.97	-1.036	41.36
8	-4.176	-0.327	22.56	-4.89	-0.34	38.862	-4.97	-1.036	41.36
8.5	-3.765	-0.299	22.65	-4.75	-0.32	49.869	-4.97	-1.024	62.95
9	-3.886	-0.275	11.19	-4.83	-0.3	34.594	-5.05	-1.013	50.98
9.5	-4.28	-0.255	3E-04	-5.05	-0.29	10.956	-5.18	-1.003	25.06
10	-4.7	-0.238	-2.48	-5.32	-0.28	-5.961	-5.35	-0.995	2.472
10	-4.7	-0.238	-2.48	-5.32	-0.28	-5.961	-5.35	-0.995	2.472
10.25	-4.887	-0.231	-2.65	-5.45	-0.27	-11.9	-5.43	-0.991	-6.33
10.5	-5.059	-0.225	-1.91	-5.57	-0.27	-15.46	-5.51	-0.987	-12.4
10.75	-5.218	-0.22	-0.83	-5.66	-0.26	-16.92	-5.59	-0.984	-15.8
11	-5.373	-0.215	0	-5.74	-0.26	-16.54	-5.67	-0.981	-16.8
11				-	-	-16.54	-5.67	-	-16.8

				5.74	0.26			0.981	
11.25				-5.81	-0.25	-14.27	-5.73	-0.979	-15.2
11.5				-5.85	-0.25	-10.65	-5.8	-0.977	-11.6
11.75				-5.89	-0.25	-5.844	-5.86	-0.974	-6.37
12				-5.91	-0.25	0	-5.92	-0.972	0

B.3.2 For depth of excavation of 10m

Y(from surface)	45cm			60cm			75cm		
	Ux	Uy	M	Ux	Uy	M	Ux	Uy	M
	[mm]	[mm]	[kNm/m]	[mm]	[mm]	[kNm/m]	[mm]	[mm]	[kNm/m]
0	0.2	-0.647	0	-0.41	-0.742	0	-1.16	-1.245	0
0.5	-0.054	-0.647	0.35	-0.84	-0.742	3.4633	-1.65	-1.245	4.585
1	-0.313	-0.647	2.419	-1.29	-0.742	12.935	-2.15	-1.245	15.86
1.5	-0.643	-0.646	12.37	-1.79	-0.742	29.461	-2.66	-1.244	33.2
2	-1.301	-0.644	36.49	-2.42	-0.741	54.116	-3.21	-1.244	56.05
2	-1.301	-0.644	36.49	-2.42	-0.741	54.116	-3.21	-1.244	56.05
2.25	-1.903	-0.642	18.31	-2.82	-0.739	32.96	-3.51	-1.243	32.6
2.5	-2.616	-0.638	4.702	-3.26	-0.737	14.61	-3.82	-1.241	11.1
2.75	-3.357	-0.635	-5.09	-3.71	-0.735	-0.824	-4.13	-1.24	-8.14
3	-4.067	-0.631	-11.8	-4.16	-0.733	-13.21	-4.44	-1.238	-24.8
3	-4.067	-0.631	-11.8	-4.16	-0.733	-13.21	-4.44	-1.238	-24.8
3.25	-4.705	-0.627	-15.9	-4.59	-0.73	-22.33	-4.75	-1.236	-38.4
3.5	-5.246	-0.622	-17.9	-5	-0.728	-28.18	-5.04	-1.234	-48.6
3.75	-5.677	-0.617	-17.8	-5.37	-0.725	-30.76	-5.32	-1.232	-55.5
4	-5.999	-0.612	-15.7	-5.72	-0.721	-30.04	-5.58	-1.229	-58.8
4	-5.999	-0.612	-15.7	-5.72	-0.721	-30.04	-5.58	-1.229	-58.8
4.25	-6.225	-0.606	-10.7	-6.03	-0.718	-25.94	-5.82	-1.227	-58.3
4.5	-6.385	-0.6	-2.45	-6.31	-0.714	-18.29	-6.05	-1.224	-53.9
4.75	-6.53	-0.593	9.85	-6.57	-0.709	-6.967	-6.26	-1.221	-45.6
5	-6.735	-0.586	26.85	-6.82	-0.705	8.1689	-6.45	-1.218	-33.1
5	-6.735	-0.586	26.85	-6.82	-0.705	8.1689	-6.45	-1.218	-33.1
5.25	-7.087	-0.576	11.02	-7.09	-0.699	-10.17	-6.65	-1.213	-53.6
5.5	-	-	-0.5	-7.34	-	-24.74	-6.82	-	-70

	7.507	0.566			0.693			1.209	
5.75	-7.923	-0.555	-8.46	-7.56	-0.686	-35.74	-6.98	-1.204	-82.2
6	-8.286	-0.544	-13.6	-7.75	-0.679	-43.36	-7.11	-1.199	-90.2
6	-8.286	-0.544	-13.6	-7.75	-0.679	-43.36	-7.11	-1.199	-90.2
6.5	-8.748	-0.52	-18	-7.97	-0.664	-48.89	-7.29	-1.189	-94.1
7	-8.774	-0.494	-16.5	-7.99	-0.648	-41.17	-7.37	-1.178	-80.7
7.5	-8.409	-0.466	-5.45	-7.82	-0.631	-19.33	-7.35	-1.166	-49.8
8	-7.935	-0.435	19.74	-7.57	-0.613	17.502	-7.27	-1.153	-0.78
8	-7.935	-0.435	19.74	-7.57	-0.613	17.502	-7.27	-1.153	-0.78
8.5	-7.722	-0.4	-4.62	-7.37	-0.591	-2.543	-7.19	-1.138	-10.3
9	-7.42	-0.361	-11.1	-7.16	-0.567	-7.395	-7.09	-1.121	-5.27
9.5	-6.872	-0.32	-2.35	-6.92	-0.542	5.2905	-6.99	-1.104	17.38
10	-6.282	-0.276	20.88	-6.7	-0.515	38.427	-6.91	-1.086	60.75
10	-6.282	-0.276	20.88	-6.7	-0.515	38.427	-6.91	-1.086	60.75
10.5	-6.123	-0.235	18.42	-6.64	-0.49	43.434	-6.9	-1.069	71.46
11	-6.399	-0.199	7.578	-6.76	-0.468	28.649	-6.97	-1.053	54.37
11.5	-6.861	-0.169	-1.9	-7.01	-0.449	8.5357	-7.1	-1.04	26.62
12	-7.299	-0.144	-4.04	-7.3	-0.431	-5.243	-7.27	-1.028	2.828
12	-7.299	-0.144	-4.04	-7.3	-0.431	-5.243	-7.27	-1.028	2.828
12.5	-7.635	-0.122	-5.17	-7.57	-0.417	-14.45	-7.44	-1.017	-15.7
13	-7.851	-0.104	-3.83	-7.77	-0.404	-17.93	-7.58	-1.008	-25.4
13.5	-7.974	-0.09	-1.59	-7.9	-0.392	-17.22	-7.7	-1	-27.3
14	-8.056	-0.078	0	-7.95	-0.383	-13.72	-7.79	-0.993	-22.5
14				-7.95	-0.38	-13.72	-7.79	-0.993	-22.5
14.25				-7.95	-0.38	-10.92	-7.82	-0.99	-17.9
14.5				-	-0.37	-7.799	-	-	-12.5

				7.94			7.85	0.987	
14.75				-7.92	-0.37	-4.225	-7.87	-0.985	-6.54
15				-7.9	-0.37	0	-7.9	-0.982	0

B.3.3 For depth of excavation of 12m

Y(from surface)	45cm			60cm			75cm		
	Ux	Uy	M	Ux	Uy	M	Ux	Uy	M
	[mm]	[mm]	[kNm/m]	[mm]	[mm]	[kNm/m]	[mm]	[mm]	[kNm/m]
0	-1.932	-0.729	0	-1.6	-0.319	0	-2.43	-0.527	0
0.5	-2.204	-0.729	0.308	-2.02	-0.319	3.4191	-2.91	-0.527	4.96
1	-2.48	-0.728	2.401	-2.46	-0.319	12.688	-3.39	-0.527	17.05
1.5	-2.827	-0.727	12.34	-2.96	-0.319	28.92	-3.9	-0.527	35.58
2	-3.5	-0.726	36.27	-3.58	-0.318	53.27	-4.44	-0.526	59.97
2	-3.5	-0.726	36.27	-3.58	-0.318	53.27	-4.44	-0.526	59.97
2.25	-4.108	-0.722	18.55	-3.97	-0.316	33.003	-4.75	-0.525	38.37
2.5	-4.829	-0.718	5.363	-4.4	-0.314	15.55	-5.06	-0.523	18.73
2.75	-5.583	-0.714	-4.12	-4.85	-0.312	0.9222	-5.37	-0.522	1.22
3	-6.311	-0.71	-10.7	-5.29	-0.309	-10.86	-5.69	-0.52	-14
3	-6.311	-0.71	-10.7	-5.29	-0.309	-10.86	-5.69	-0.52	-14
3.25	-6.974	-0.705	-14.7	-5.73	-0.306	-19.59	-6	-0.518	-26.7
3.5	-7.546	-0.699	-16.7	-6.14	-0.303	-25.16	-6.31	-0.515	-36.4
3.75	-8.016	-0.694	-16.5	-6.52	-0.3	-27.52	-6.6	-0.513	-42.8
4	-8.386	-0.688	-14.1	-6.87	-0.296	-26.63	-6.88	-0.51	-45.9
4	-8.386	-0.688	-14.1	-6.87	-0.296	-26.63	-6.88	-0.51	-45.9
4.25	-8.669	-0.681	-8.66	-7.19	-0.292	-22.37	-7.15	-0.508	-45.4
4.5	-8.899	-0.674	0.297	-7.49	-0.288	-14.56	-7.4	-0.505	-41.1
4.75	-9.13	-0.667	13.49	-7.77	-0.283	-3.071	-7.64	-0.501	-33.1
5	-9.443	-0.659	31.63	-8.05	-0.279	12.242	-7.87	-0.498	-21
5	-9.443	-0.659	31.63	-8.05	-0.279	12.242	-7.87	-0.498	-21
5.25	-9.933	-0.648	16.13	-8.35	-0.272	-5.9	-8.1	-0.494	-42.3
5.5	-	-	5.124	-8.63	-	-20.26	-8.32	-	-59.5

	10.52	0.637			0.266			0.489	
5.75	-11.14	-0.626	-2.23	-8.9	-0.259	-31.04	-8.52	-0.484	-72.8
6	-11.74	-0.614	-6.8	-9.13	-0.252	-38.43	-8.7	-0.479	-82.3
6	-11.74	-0.614	-6.8	-9.13	-0.252	-38.43	-8.7	-0.479	-82.3
6.5	-12.81	-0.589	-10.8	-9.46	-0.237	-43.51	-8.98	-0.468	-89.7
7	-13.62	-0.562	-12	-9.6	-0.22	-35.51	-9.16	-0.457	-81.4
7.5	-14.14	-0.533	-11.5	-9.58	-0.203	-13.76	-9.25	-0.444	-57.3
8	-14.38	-0.503	-10.2	-9.51	-0.184	22.458	-9.26	-0.431	-17.4
8	-14.38	-0.503	-10.2	-9.51	-0.184	22.458	-9.26	-0.431	-17.4
8.25	-14.4	-0.488	-11.6	-9.51	-0.173	8.0958	-9.27	-0.423	-30.3
8.5	-14.35	-0.471	-13	-9.51	-0.161	-4.127	-9.26	-0.415	-41.3
8.75	-14.23	-0.454	-14.2	-9.51	-0.149	-14.21	-9.24	-0.407	-50
9	-14.01	-0.437	-15.1	-9.49	-0.137	-22.12	-9.21	-0.398	-56
9	-14.01	-0.437	-15.1	-9.49	-0.137	-22.12	-9.21	-0.398	-56
9.25	-13.71	-0.419	-15.7	-9.44	-0.124	-27.65	-9.16	-0.39	-59.2
9.5	-13.3	-0.4	-15.8	-9.37	-0.111	-30.67	-9.1	-0.38	-59.3
9.75	-12.8	-0.38	-15	-9.26	-0.097	-30.95	-9.01	-0.371	-56
10	-12.21	-0.36	-12.9	-9.12	-0.084	-28.28	-8.91	-0.361	-49.2
10	-1.932	-0.36	-12.9	-9.12	-0.084	-28.28	-8.91	-0.361	-49.2
10.25	-1.932	-0.36	-8.74	-8.95	-0.069	-22.05	-8.8	-0.352	-38.3
10.5	-1.932	-0.36	-1.34	-8.75	-0.055	-11.51	-8.67	-0.341	-22.7
10.75	-1.932	-0.36	10.49	-8.54	-0.039	4.0071	-8.54	-0.331	-2.06
11	-1.932	-0.36	27.91	-8.33	-0.024	25.158	-8.4	-0.32	24.08
11	-1.932	-0.36	27.91	-8.33	-0.02	25.158	-8.4	-0.32	24.08
11.25	-1.932	-0.36	15.16	-8.15	-0.01	16.62	-8.28	-0.309	20.12
11.5	-1.932	-0.36	8.883	-	0.011	14.75	-	-	22.29

				7.99			8.16	0.297	
11.75	-1.932	-0.36	9.975	-7.84	0.029	19.89	-8.04	-0.284	30.84
12	-1.932	-0.36	19.39	-7.72	0.047	32.385	-7.94	-0.272	46.03
12	-1.932	-0.36	19.39	-7.72	0.047	32.385	-7.94	-0.272	46.03
12.5	-1.932	-0.36	14.27	-7.57	0.082	29.19	-7.77	-0.248	43.78
13	-1.932	-0.36	3.706	-7.56	0.113	11.889	-7.65	-0.226	20.7
13.5	-1.932	-0.36	-4.55	-7.59	0.142	-6.49	-7.56	-0.206	-7.04
14	-1.932	-0.36	-5.32	-7.6	0.169	-15.43	-7.46	-0.187	-25.6
14	-1.932	-0.36	-5.32	-7.6	0.169	-15.43	-7.46	-0.187	-25.6
15	-1.932	-0.36	-4.48	-7.39	0.217	-19.5	-7.16	-0.153	-41.3
16	-1.932	-0.36	-1.21	-6.87	0.26	-10.9	-6.67	-0.122	-29.5
17	-1.932	-0.36	1.38	-6.16	0.299	0.3692	-6.05	-0.095	-7.81
18	-1.932	-0.36	0	-5.44	0.331	5.2079	-5.39	-0.071	6.546
18				-5.44	0.331	5.2079	-5.39	-0.071	6.546
18.5				-5.11	0.345	6.0148	-5.07	-0.06	9.285
19				-4.81	0.357	6.4981	-4.76	-0.051	8.93
19.5				-4.53	0.368	5.076	-4.46	-0.043	5.707
20				-4.28	0.378	0	-4.17	-0.036	0

B.3.4 For depth of excavation of 14m

Y(from surface)	45cm			60cm			75cm		
	Ux	Uy	M	Ux	Uy	M	Ux	Uy	M
	[mm]	[mm]	[kNm/m]	[mm]	[mm]	[kNm/m]	[mm]	[mm]	[kNm/m]
0	1.88	0.105	0	1.15	0.097	0	-0.3	-0.346	0
0.25	1.334	0.105	2.157	0.51	0.097	2.8378	-0.86	-0.346	2.598
0.5	0.774	0.105	8.2	-0.14	0.097	10.106	-1.42	-0.346	9.172
0.75	0.165	0.105	18.44	-0.79	0.097	21.271	-1.98	-0.346	19.13
1	-0.556	0.105	33.2	-1.47	0.096	35.835	-2.55	-0.346	31.93
1	-0.556	0.105	33.2	-1.47	0.096	35.835	-2.55	-0.346	31.93
1.25	-1.464	0.106	15.76	-2.19	0.097	16.839	-3.13	-0.345	10.56
1.5	-2.468	0.108	2.608	-2.93	0.098	0.6777	-3.72	-0.344	-8.55
1.75	-3.488	0.11	-6.91	-3.67	0.1	-12.65	-4.3	-0.343	-25.3
2	-4.465	0.112	-13.5	-4.39	0.101	-23.18	-4.88	-0.342	-39.6
2	-4.465	0.112	-13.5	-4.39	0.101	-23.18	-4.88	-0.342	-39.6
2.5	-6.149	0.117	-19.2	-5.75	0.104	-35.65	-5.99	-0.34	-60.6
3	-7.372	0.123	-16.8	-6.96	0.108	-35.26	-7.03	-0.337	-68.2
3.5	-8.2	0.13	-2.97	-8.02	0.113	-21.22	-7.99	-0.333	-61.4
4	-8.979	0.139	26.32	-8.98	0.119	7.2977	-8.88	-0.328	-39.1
4	-8.979	0.139	26.32	-8.98	0.119	7.2977	-8.88	-0.328	-39.1
4.25	-9.54	0.146	10.26	-9.47	0.123	-10.64	-9.31	-0.325	-59.9
4.5	-10.16	0.154	-1.55	-9.95	0.128	-24.83	-9.72	-0.322	-76.8
4.75	-10.78	0.162	-9.82	-10.4	0.133	-35.45	-10.1	-0.318	-89.7
5	-11.33	0.17	-15.3	-	0.138	-42.69	-	-	-98.8

				10.8			10.5	0.314	
5	-11.33	0.17	-15.3	-10.8	0.138	-42.69	-10.5	-0.314	-98.8
5.25	-11.79	0.179	-18.4	-11.2	0.144	-46.68	-10.8	-0.31	-104
5.5	-12.14	0.189	-19.8	-11.5	0.15	-47.52	-11.1	-0.306	-106
5.75	-12.36	0.198	-19.2	-11.7	0.156	-45.24	-11.4	-0.301	-103
6	-12.47	0.209	-16.5	-12	0.162	-39.83	-11.6	-0.297	-97.6
6	-12.47	0.209	-16.5	-12	0.162	-39.83	-11.6	-0.297	-97.6
6.25	-12.48	0.22	-10.9	-12.1	0.169	-31.21	-11.9	-0.292	-88
6.5	-12.42	0.231	-1.9	-12.3	0.176	-19.11	-12	-0.286	-74.6
6.75	-12.35	0.243	11.17	-12.4	0.183	-3.311	-12.2	-0.281	-57.4
7	-12.35	0.255	28.96	-12.5	0.191	16.442	-12.4	-0.276	-36.2
7	-12.35	0.255	28.96	-12.5	0.191	16.442	-12.4	-0.276	-36.2
7.25	-12.51	0.27	13.42	-12.6	0.2	1.9817	-12.5	-0.269	-49.3
7.5	-12.74	0.286	2.632	-12.7	0.21	-8.467	-12.6	-0.262	-58.4
7.75	-13	0.302	-4.32	-12.8	0.22	-15.21	-12.8	-0.255	-63.9
8	-13.23	0.319	-8.38	-12.9	0.23	-18.58	-12.9	-0.248	-65.9
8	-13.23	0.319	-8.38	-12.9	0.23	-18.58	-12.9	-0.248	-65.9
8.5	-13.51	0.353	-12.5	-13.1	0.251	-19.96	-13	-0.233	-65.3
9	-13.5	0.391	-11.2	-13.1	0.274	-14.76	-13.1	-0.217	-58.7
9.5	-13.23	0.431	1.305	-13.1	0.299	-0.834	-13	-0.199	-43.6
10	-13.01	0.474	31.15	-13.1	0.325	24.086	-13	-0.181	-17.9
10	-13.01	0.474	31.15	-13.1	0.325	24.086	-13	-0.181	-17.9
10.25	-13.12	0.498	15.01	-13.1	0.34	3.5294	-13	-0.171	-38.3

10.5	-13.32	0.523	3.342	-13.2	0.356	-13.43	-12.9	-0.16	-55
10.75	-13.54	0.549	-4.92	-13.2	0.371	-27.05	-12.8	-0.149	-68.1
11	-13.73	0.575	-10.8	-13.2	0.387	-37.55	-12.8	-0.138	-77.4
11	-13.73	0.575	-10.8	-13.2	0.387	-37.55	-12.8	-0.138	-77.4
11.25	-13.85	0.602	-15.4	-13.1	0.404	-45.05	-12.7	-0.126	-82.7
11.5	-13.88	0.63	-19	-13	0.421	-49.64	-12.5	-0.114	-83.8
11.75	-13.79	0.658	-21.3	-12.9	0.438	-51.17	-12.4	-0.102	-80.6
12	-13.57	0.688	-21.9	-12.7	0.456	-49.46	-12.2	-0.09	-72.7
12	-13.57	0.688	-21.9	-12.7	0.456	-49.46	-12.2	-0.09	-72.7
12.25	-13.22	0.717	-19.9	-12.4	0.475	-43.41	-12	-0.077	-59.1
12.5	-12.74	0.748	-14.3	-12.1	0.493	-31.66	-11.8	-0.064	-38.5
12.75	-12.18	0.78	-3.89	-11.7	0.513	-13.29	-11.6	-0.051	-10.4
13	-11.59	0.812	12.74	-11.3	0.532	12.63	-11.3	-0.037	25.74
13	-11.59	0.812	12.74	-11.3	0.532	12.63	-11.3	-0.037	25.74
13.25	-11.07	0.847	1.345	-11	0.554	11.139	-11.1	-0.023	34.59
13.5	-10.55	0.884	-0.87	-10.6	0.575	19.109	-10.9	-0.008	52.68
13.75	-10.03	0.921	7.638	-10.3	0.598	37.453	-10.7	0.008	80.54
14	-9.548	0.959	28.48	-10	0.62	67.098	-10.5	0.023	118.7
14	-9.548	0.959	28.48	-10	0.62	67.098	-10.5	0.023	118.7
14.625	-9.118	1.046	22.57	-9.67	0.673	69.436	-10.2	0.059	132.6
15.25	-9.519	1.12	6.317	-9.77	0.718	38.259	-10.2	0.09	93.86
15.875	-10.17	1.184	-5.46	-10.1	0.757	4.3535	-10.3	0.117	40.88
16.5	-	1.238	-4.25	-	0.79	-8.904	-	0.141	5.1

	10.67			10.5			10.5		
16.5	-10.67	1.238	-4.25	-10.5	0.79	-8.904	-10.5	0.141	5.1
17.125	-11.01	1.284	-3.57	-10.9	0.819	-15.18	-10.7	0.162	-20.9
17.75	-11.2	1.323	-2.94	-11.1	0.844	-16.55	-10.9	0.18	-36.5
18.375	-11.29	1.355	-2.44	-11.2	0.865	-15.42	-11	0.195	-44.4
19	-11.28	1.382	-2.15	-11.2	0.883	-13.93	-11	0.209	-47.1
19	-11.28	1.382	-2.15	-11.2	0.883	-13.93	-11	0.209	-47.1
19.625	-11.19	1.404	-1.98	-11.1	0.898	-12.56	-11	0.221	-46.6
20.25	-11.02	1.422	-1.9	-11	0.911	-11.61	-10.8	0.23	-44.1
20.875	-10.78	1.436	-1.92	-10.7	0.921	-10.87	-10.6	0.239	-39.9
21.5	-10.47	1.447	-2.09	-10.4	0.929	-10.1	-10.3	0.246	-34.4
21.5	-10.47	1.447	-2.09	-10.4	0.929	-10.1	-10.3	0.246	-34.4
22.125	-10.08	1.455	-1.62	-10	0.936	-8.089	-9.97	0.252	-26.4
22.75	-9.625	1.461	-1.09	-9.6	0.941	-5.33	-9.57	0.257	-16.8
23.375	-9.131	1.465	-0.58	-9.12	0.945	-2.459	-9.15	0.261	-7.45
24	-8.614	1.468	0	-8.63	0.949	0	-8.71	0.265	0

REFERENCES

1. Aiza Malik(2015) "Geotechnical Statistical Evaluation of Lahore Site Data and Deep Excavation Design". Civil and Environmental Engineering Master's Project Reports, Paper 13.
2. A.Siemińska-Lewandowska & M. Mitew-Czajewska (2011) "The study of displacements of diaphragm walls built in Warsaw Quaternary soils" Geotechnical Aspects of Underground Construction in Soft Ground, Taylor & Francis Group, London, ISBN 978-0-415-68367-8.
3. A.S.Osman and M.D. Bolton(2004) "Ground Movement Predictions for Braced Excavation in Undrained Clay" Journal of Geotechnical and Geoenvironmental Engineering, Vol. 132, No. 4.
4. A.T.C. Goh, K.S.Wong, C.I.Teh & D.Wen (2003) " Pile Response Adjacent to Braced Excavation" Journal of Geotechnical and Geoenvironmental Engineering, Vol. 129, No. 4.
5. B.C.B. Hsiung (2008) " A case study on the behaviour of a deep excavation in sand" Computers and Geotechnics Vol. 36, pp. 665–675.
6. Bowles, J.E. (1996). "Foundation Analysis and Design", Fifth Edition, McGraw-Hill, New York. Fourth Edition, 1988.
7. Brinkgreve, R., Broere, W., & Waterman, D. (2004). PLAXIS 2-D Professional Version 8.6 - User's Manual. PLAXIS b.v., The Netherlands.
8. C.Yang, Y.J.Cui, J.M. Pereira, M.S.Huang(2008) "A Constitutive Model For Unsaturated Cemented Soils Under Cyclic Loading" Computers and Geotechnics, Vol. 35, pp. 853-859.
9. C.Y. Ou, J.T. Liao and H.D. Lin(1998) " Performance of Diaphragm Wall Constructed Using Top-Down Method" Journal of Geotechnical and Geoenvironmentol Engineering, Vol. 124, No.9.
10. David G. Zapata-Medina(2007) "Semi-Empirical Method for Designing Excavation Support Systems Based on Deformation Control" University of Kentucky Master's Theses, Paper 468.

11. Dinakar K. N. and S.K. Prasad (2014) "Behaviour of Tie Back Sheet Pile Wall For Deep Excavation Using PLAXIS" International Journal of Research in Engineering and Technology, Volume: 03.
12. E. Erbì & F.M. Soccodato(2011) "A 3D numerical study of deep excavations in clayey soils" Geotechnical Aspects of Underground Construction in Soft Ground – Viggiani (ed) Taylor & Francis Group, London, ISBN 978-0-415-68367-8.
13. E.H.Ramadan, M. Ramadan, M. Khashila & M. Kenawi(2013) " Analysis of Piles Supporting Excavation Adjacent to Existing Buildings" Proceedings of the 18th International Conference on Soil Mechanics and Geotechnical Engineering, Paris.
14. Elkady T. (2013) " Effect of Excavation-induced Movements on Adjacent Piles" Proceedings of the 18th International Conference on Soil Mechanics and Geotechnical Engineering, Paris.
15. G.B. Liu & J. Jiang, C.W.W. Ng(2008) " Performance of a deep excavation in soft clay" Geotechnical Aspects of Underground Construction in Soft Ground Taylor & Francis Group, London, ISBN 978-0-415-48475-6.
16. Grabe J. (2010) "Sheet piling handbook design" Hamburg, German.
17. H.B. Zhang, J.J. Chen, X.S. Zhao, J.H.Wang, and H. Hu (2015) "Displacement Performance and Simple Prediction for Deep Excavations Supported by Contiguous Bored Pile Walls in Soft Clay" Journal of Aerospace Engineering.
18. Helmut F. Schweiger (2005) "Modelling issues for numerical analysis of deep excavations" Computational Geotechnics Group, Institute for Soil Mechanics und Foundation Engineering Graz University of Technology, Austria.
19. H.F. Schweiger, F. Scharinger & R. Lüftenegger (2008) " 3D finite element analysis of a deep excavation and comparison with in situ measurements" Computational Geotechnics Group, Institute for Soil Mechanics and Foundation Engineering, Graz University of Technology, Austria.
20. H.Popa, A. Marcu & L. Batali (2008) "Numerical modelling and experimental measurements for a retaining wall of a deep excavation in Bucharest, Romania" Geotechnical Aspects of Underground Construction in Soft Ground, Taylor & Francis Group, London, ISBN 978-0-415-48475-6.

21. Intsiful & Sekyi K. (2015) "Deformation-based Excavation Support System Design Method" Theses and Dissertations, Civil Engineering, Paper 29.
22. J. H. Wang; Z. H. Xu; and W. D. Wang (2010)"Wall and Ground Movements due to Deep Excavations in Shanghai Soft Soils" journal of geotechnical and geoenvironmental engineering Vol. 136: pp. 985-994.
23. J. Josifovski 1, S. Gjorgjevski and M. Jovanovski (2011) " Deep Excavation with Multi Anchored Diaphragm Wall" Proceedings of the 15th European Conference on Soil Mechanics and Geotechnical Engineering oi:10.3233/978-1-60750-801-4-1485.
24. J.Roboski & R.J. Finno(2005) " Distributions of Ground Movements Parallel to Deep Excavations in Clay" paper submitted to the Canadian Geotechnical Journal.
25. J.T. Blackburn and R.J. Finno (2006) " Three-dimensional effects observed in an internally braced excavation in soft clay" Paper submitted to the Journal of Geotechnical and Geoenvironmental Engineering.
26. K.H. Goh & R.J. Mair(2011) " The response of buildings to movements induced by deep excavations" Geotechnical Aspects of Underground Construction in Soft Ground Taylor & Francis Group, London, ISBN 978-0-415-68367-8.
27. K.H. Yang and C.N.Liu(2007) " Finite Element Analysis Of Earth Pressures for Narrow Retaining Walls" Journal of GeoEngineering, Vol. 2, No. 2, pp. 43-52.
28. K. S. Ti, Bujang B.K. Huat, J.Noorzaei, M.S. Jaafar & G. S.Sew (2009) " Review of Basic Soil Constitutive Models for Geotechnical Application" G&P Geotechnics Sdn Bhd Bandar Tasik Selatan, KL, Malaysia, Vol. 14 Bund. J.
29. Liew, Shaw-Shong & Loh, Yee-Eng (2011) "Two case studies of Temporaray Excavation using Contiguous Bored pile wall" G&P Geotechnics Sdn Bhd, Kuala Lampur.
30. M.A. Nikolinakou, A. J. Whittle, S.Savidis and U.Schran(2011) "Prediction and Interpretation of the Performance of a Deep Excavation in Berlin Sand" Journal of Geotechnical and Geoenvironmental Engineering, Vol. 137, No. 11.
31. M.Cecconi1, A.DeSimone, C.Tamagnini and G.M.B. Viggiani(2002) " A constitutive model for granular materials with grain crushing and its application to a pyroclastic soil"

International Journal for Numerical and Analytical Methods in Geomechanics 6:1531–1560.

32. M. D. Bolton and W. Powrie(1988) " Behaviour of diaphragm walls in clay prior to collapse" Journal of Geotechnique Vol.38, No. 2, pp. 167-189.
33. M.D. Boton, G.R. Dasari & A.M. Britto " Putting small strain non-linearity into Modified Cam Clay Model" Computer methods and Advances in Geotechnics, Siriwardane & Zaman(eds), Balkema, Rotterdam, ISBN 90 5410 380 9.
34. M.D. Bolton, S.Y. Lam and P.J. Vardanega (2010) " Predicting and Controlling Ground Movements Around Deep Excavations" the 11th International Conference of the DFI-EFFC, London.
35. M. Korff & R.J.Mair (2013) " Response of piled buildings to deep excavations in soft soils" Proceedings of the 18th International Conference on Soil Mechanics and Geotechnical Engineering, Paris.
36. M.S. Pakbaz, S. Imanzadeh, K.H. Bagherinia (2013) " Characteristics of diaphragm wall lateral deformations and ground surface settlements: Case study in Iran-Ahwaz metro" Tunnelling and Underground Space Technology Vol. 35, pp.109–121.
37. M.W. Seo, S.M. Olson,K.S. Yang and M.M. Kim (2010) "Sequential Analysis of Ground Movements at Three Deep Excavation Sites with Mixed Ground Profiles" Journal of Geotechnical and Geoenvironmental Engineering, Vol. 136, No. 5.
38. Paul R. Dawson (1979) " Constitutive Models Applied In The Analysis Of Creep Of Rock Sait" Computational Physics & Mechanics Division I - 5531 Sandia Laboratories, Albuquerque, New Mexico 87185.
39. Poul V. Lade, Jerry A. Yamamuro and Suresh K. Gutta (2008) "Rotational kinematic hardening model for three-dimensional stress reversals in sand" International Journal For Numerical And Analytical Methods In Geomechanics 2009; **33**:967–991.
40. Peck R.(1969) "Deep excavations and tunneling in soft ground" Proceedings of the 7th International Conference on Soil Mechanics, pp. 225-290.
41. P.J. Sabatini, D.G. Pass, R.C. Bachus (1999) " Geotechnical Engineering Circular No. 4 Ground Anchors and Anchored Systems" US Dept. of transportation, FHWA-IF-99-015.

42. Poul V. Lade (1989) "Single-Hardening Model With Application to Normally Consolidated Clay" Journal of Geotechnical Engineering, Vol. 116, No. 3.
43. R.Catzenbach,(2003), DIN-4094Bb1;1990-12
44. R.J. Finno (2006) "Analysis and numerical modeling of deep excavations" Geotechnical Aspects of Underground Construction in Soft Ground Taylor & Francis Group, London, ISBN 978-0-415-48475-6.
45. R.J. Finno and L.S. Bryson (2002) " Response of Building Adjacent to Stiff Excavation Support System in Soft Clay" Journal of Performance of Constructed Facilities, Vol. 16, No. 1.
46. R.J. Finno, D.K. Atmatzidis and S.B. Perkins (1989) " Observed Performance of A Deep Excavation in Clay" Journal of Geotechnical Engineering, Vol. 115, No. 8.
47. R.J. Finno, J.T.Blackburn and J. F. Roboski (2006) " Three-dimensional effects for supported excavations in clay" paper submitted to the Journal of Geotechnical and Geoenvironmental Engineering.
48. R.J.Finno, S.A.Lawrence, N.F.Allawh and I.S.Harahap (1991) " Analysis of Performance of Pile Groups Adjacent to Deep Excavation" Journal of Geotechnical Engineering, Vol. 117, No. 6.
49. R.Riker & D. Dailer(1988) "Design, construction and performance of a deep excavation in soft clay" International Conference on Case Histories in Geotechnical Engineering. Paper 22.
50. S.J. Boone & J.Westland(2005) " Design of excavation support using apparent earth pressure diagrams" Taylor & Francis Group plc, London, UK.
51. Surarak, C. (2010). Geotechnical Aspects of the Bangkok MRT Blue Line Project. Ph.D. Thesis, Griffith University, Australia.
52. Teferra, A. (1992). "Foundation Engineering" Addis Ababa: Addis Ababa University Press.
53. Tewodros Fekadu (2010) "Analysis and parametric study of deep excavation with diaphragm wall using finite element based software" Addis Ababa University Master's Theses, Dept. of Civil Engineering. Addis Ababa, Ethiopia.

54. Tianteng Zhou (2015) " 3D FEM Analysis For Sequential Excavation" Delt University of Technology Mastres thesis.
55. V.R.Godavarthi, D.Mallavalli, R.Peddi, N.Katragadda, and P.Mulpuru (2011) " Contiguous Pile Wall as a Deep Excavation Supporting System" Leonardo Electronic Journal of Practices and Technologies ISSN 1583-1078, pp. 144-160.
56. W.Teparaksa(2008) "Behavior and performance of deepest barrette pile along Chao Phraya River on Bangkok‖" Guest speaker, The 2nd Asian Workshop on ATC 18 Mega Foundations, Korean Geotechnical Society, Seoul, Korea.
57. W.Zhang; A.T.C.Goh and Y. Zhang (2015) "Probabilistic Assessment of Serviceability Limit State of Diaphragm Walls for Braced Excavation in Clays" ASCE-ASME Journal of Risk and Uncertainty in Engineering Systems, School of Civil and Environmental Engineering, Nanyang Technological Univ., Singapore 639798.
58. Y.Tan and B.Wei(2012) " Observed Behaviors of a Long and Deep Excavation Constructed by Cut-and-Cover Technique in Shanghai Soft Clay" Journal of Geotechnical and Geoenvironmental Engineering, Vol. 138, No. 1.
59. Yuepeng Dong(2013) " Advanced Finite Element Analysis of Deep Excavation Case Histories" University of Oxford PHD theses, Dept. of engineering science.